High-Pressure Solutions of C_6F_{13}- and C_4F_9- Based Polyfluoroacrylates in CO_2: Synthesis, Solubility, Viscosity, Adsorption, and Sealing of Cement Cracks

by

Peter Charles Kweku Lemaire III

B.S.E in Chemical Engineering, Carnegie Mellon University, 2012

Submitted to the Graduate Faculty of the

Swanson School of Engineering in partial fulfillment

of the requirements for the degree of

Doctor of Philosophy

University of Pittsburgh

2022

UNIVERSITY OF PITTSBURGH

SWANSON SCHOOL OF ENGINEERING

This dissertation was presented

by

Peter Charles Kweku Lemaire III

It was defended on

December 13, 2021

and approved by

Dr. Eric Beckman Ph.D., Professor, Dept. of Chemical and Petroleum Engineering

Dr. Badie Morsi Ph.D., Professor, Dept. of Chemical and Petroleum Engineering

Dr. Andrew Bunger Ph.D., Associate Professor, Dept. of Civil and Environmental Engineering

Dr. Frank Adamsky Ph.D., Regulatory Affairs Manager, Daikin America Inc.

Dr. Dustin Crandall Ph.D., Research Engineer, National Energy Technology Laboratory

Dissertation Director: Dr. Robert Enick Ph.D., Professor, Dept. of Chemical and Petroleum Engineering

High-Pressure Solutions of C_6F_{13}- and C_4F_9- Based Polyfluoroacrylates in CO_2: Synthesis, Solubility, Viscosity, and Sealing of Cement Cracks

Peter Charles Kweku Lemaire III, PhD

University of Pittsburgh, 2022

A thorough literature review and experimental comparison of many purported CO_2-thickeners has demonstrated that polyfluoroacrylate (PFA) is the only high molecular weight homopolymer capable of dissolving in CO_2 at typical petroleum reservoir conditions. PFA is a liquid carbon dioxide (CO_2)-soluble and supercritical CO_2-soluble, amorphous or semi-crystalline, hydrophobic and oleophobic polymer. In this dissertation, several PFAs with -C_6F_{13} and -C_4F_9 based pendant moieties have been synthesized via bulk polymerization. The ability of PFA-CO_2 solutions to dissolve in and thicken CO_2 without the need for additional co-solvents is assessed and compared to the previously reported C_8F_{17}-based PFAs. With the exception of one ultra-high molecular weight sample (M_w = 2.89E6 Da) that could not dissolve in CO_2 up to 62 MPa, all the samples synthesized showed remarkably similar solubility in CO_2 from 1-5 wt% and 25-125 °C as the C_8F_{17}-based PFAs in the literature. In addition, both the C_4F_9 and C_6F_{13} PFA showed the ability to thicken CO_2 like their C_8F_{17} analogs. Although all three versions of PFA exhibited comparable CO_2-solubility and CO_2-thickening, PFA based on the -C_6F_{13} and -C_4F_9 moieties will generate more benign perfluoroalkanoic ultimate degradation products. C_6F_{13}-based PFAs were then tested for their ability to seal dry cracks in Portland cement. In conjunction with researchers at NETL and SINTEF, it was shown that high-pressure PFA-CO_2 solutions can significantly reduce the apparent permeability of dry cracks in split or cracked Portland cement cylinders. For a cracked cement with nanoDarcy apparent permeability, the crack was quickly and completely sealed. For a cracked cement sample with microDarcy apparent permeability, the apparent permeability was reduced by 92% when the experiment was terminated because of excessive pressure drop buildup. For cracks with milliDarcy apparent permeability, reductions in apparent permeability ranged from 22-96%, with the better results generally associated with higher PFA concentration, lower crack apparent permeability, and slower PFA-CO_2 injection rates. After these tests, the cement halves, which were glued together by PFA, were pried apart. Wettability tests demonstrated that PFA coats the entire cement surface area that bounds the crack, rather than just the inlet of the crack.

Table of Contents

List of Tables

List of Figures

Preface

I would like to thank my parents, sister, aunts, and uncles for all their support of me and my education growing up and their encouragement through this difficult Ph.D. process. Thank you to my beautiful wife, Angie, and baby Kiara for laughs and support throughout this whole process and helping me stay on track and motivated. I also would like to thank all the people who directly helped me in the research contained within this thesis: Thank you, Dr. Adamsky of Daikin America Inc. for supplying the monomer, advising us on polymerization, discussing methods of detecting wettability alteration, and engaging in helpful regulatory discussions and serving on my committee. Thank you, Shinsuke (Sunny) Ohshita of Daikin Industries Ltd. in Osaka Japan for providing polymer characterization. Thank you, Dustin Crandall and Johnathan Moore of NETL in Morgantown WV for preparing cement samples and obtaining permeability measurements and conducting CT imaging and for Dustin serving on my committee. Thank you, Deepak Tapriyal of NETL Pittsburgh for contact angle measurements and photos to track wettability alterations. Thank you, Albert Barrabino and Amir Ghaderi, petroleum researchers at SINTEF AS in Trondheim, Norway for discussing methods of assessing this method of sealing cracks using PFA synthesized in our lab at Pitt. Thank you, Richard Kelly of Linde in New York for helpful discussions of CO_2-soluble polymers used in fracturing. Thank you, Robert Taylor and Robert Lestz for providing samples of the crosslinked phosphate esters used to thicken liquid propane for hydraulic fracturing. Thank you Zuhair Yousif and Sunil Kokal of Saudi Aramco for the sample of PSM. Thank you, Barbara Kutchko and Richard Hammack of NETL for their assistance in the development of this project. I would also like to thank UCFER and NETL for the financial support of this work. I would especially like to give my gratitude for my advisor, Dr. Robert Enick for all his support over the past years and Dr. Eric Beckman for essential aid in helping me with my three papers generated from this work. Thank you, Dr. Morsi and Dr. Bunger, for serving on this committee and your support and questions throughout this process.

List of Nomenclature

12-HSA	12-hydroxystearic acid
AIBN	azobisisobutyronitrile
Am	amorphous
AOT	bis (2-ethylhexyl)sulfosuccinate sodium salt
C/O	CO_2-in-oil
C/W	CO_2-in-water or CO_2-in-brine
CO_2	carbon dioxide
CPE	crosslinked phosphate ester
CuO	copper oxide
DSC	differential scanning calorimeter
EG	ethylene glycol
GO	graphene oxide
GPC	gel permeation chromatography
HAD2EH	hydroxy aluminum di-2-ethylhexanoate
HFE	hydrofluoroether
HFIP	hexafluoroisopropanol
K	characteristic constant for the viscometer (mPa cm^4 g^{-1})
LPG	liquefied petroleum gas
MEHQ	monomethyl ether hydroquinone
M_n	number average molecular weight
M_w	weight average molecular weight
NaF_7H_4	sodium pentadecfluoro-5- dodecyl sulphate
NETL	National Energy Technology Laboratory
NGL	natural gas liquid
Ni-diHCF$_4$	nickel bisnonofluoropentane sulphosuccinate
NP	nanoparticle
P1D	poly(1-decene)
PDI	polydispersity index
PDMS	polydimethylsiloxane
PFA	polyfluoroacrylate
PFBA	perfluorobutanoic acid
PFHxA	perfluorhexanoic acid
PFOA	perfluorooctanoic acid
P(HFDA-VAc)	poly(heptadecafluoro decyl acrylate-co-vinyl acetate)
P(HFDA-EAL)	poly(heptadecafluoro decyl acrylate-co-ethyl acrylate)
polyFAST	poly(fluoroacrylate-styrene)
polyFAPA	poly(fluoroacrylate-co-phenyl acrylate)
polyFAVB	poly(fluoroacrylate-vinyl benzene)
PSM	proprietary mixture of polymer, oil, surfactants, and solvents
PVAc	poly(vinyl acetate)
PVEE	poly(vinylethyl ether)

P-x	pressure-composition
SC	semi-crystalline
TBC	4-tert-butyl catechol
TBTF	tributyl tinfluoride
Vc_t	cylinder terminal velocity (cm/s)
μ	viscosity (mPa s)
ρ_c	falling object density (2.7 g/cm^3 for aluminum)
ρ_l	fluid density (g/cm^3)

1.0 Thickening CO_2 with Direct Thickeners, CO_2-in-Oil Emulsions, or Nanoparticle Dispersions: Literature Review and Experimental Validation

1.1 Introduction

Carbon dioxide (CO_2) thickeners could be transformative technologies for improving the performance of CO_2 during petroleum recovery in two ways: by suppressing unfavorable mobility ratios during CO_2 enhanced oil recovery (EOR) [1] and allowing higher loadings of larger proppant particles to be blended with the high-pressure liquid CO_2. The ideal CO_2 thickener would be an affordable, safe, pumpable, environmentally benign additive that could quickly establish a high viscosity, CO_2-rich fluid. Further, the ideal thickener would not require organic co-solvents or prolonged stirring and would thicken CO_2 at typical wellhead, injection wellbore, and reservoir conditions [1]. The thickener would increase the viscosity of CO_2 to the desired value via manipulation of its concentration in CO_2. For example, during CO_2 hydraulic fracturing operations, one could target viscosity values that would facilitate the loadings of proppant particles comparable to that of aqueous fluids, whereas during CO_2 EOR one attempts to increase the viscosity of CO_2 to be comparable with the viscosity of the oil being displaced [2]. Three strategies for thickening CO_2 will be reviewed: direct thickeners that dissolve in CO_2 [3], indirect thickeners that establish high quality CO_2 foams or emulsions [4], and dispersed nanoparticle-based CO_2 thickeners [5].

The largest body of research has focused on “direct thickeners” for CO_2. The term “direct thickener” was coined by John Heller and co-workers at Petroleum Recovery Research Center of

New Mexico Institute of Mining and Technology during their pioneering work in this area in the early 1980's [6]. *"Direct thickener" infers that a compound will dissolve in the* CO_2 *and form a thermodynamically stable, transparent, single-phase solution that is significantly more viscous than pure* CO_2. The attainment of a stable single-phase solution is particularly important for EOR in conventional formations where the fluid must flow through an interconnected network of micron-scale pores. It would be beneficial if the thickener was water-insoluble, in order to prevent it from partitioning into brine. Further, the ideal direct thickener would be unlikely to exhibit significant adsorption onto sandstone or carbonate surfaces. As a rule of thumb, it would be desirable, for technical, economic and logistical reasons, to thicken CO_2 by a factor of 10-100 with as little thickener as possible; preferably 0.01 - 0.1wt%.

The secondary emphasis of this section will focus on indirect thickening via the generation of carbon dioxide-rich foams or emulsions with a high "apparent viscosity". The most notable and common examples of CO_2-based foams are high-pressure CO_2-in-water (C/W) (i.e., CO_2-discontinuous, water-continuous) emulsions or foams that are stabilized by the presence of water-soluble surfactants. The term "emulsion" is typically used if the system contains sub-critical liquid CO_2, while "foam" is used for systems containing supercritical CO_2. There have been numerous reports and reviews of C/W foams [2] and such foams have been tested in the field. Therefore, this section will *not* include C/W foams. However, *it is also possible to generate an indirect* CO_2 *thickener that is a completely anhydrous, high apparent viscosity,* CO_2*-in-oil (C/O) emulsion or foam* (i.e., CO_2-discontinuous, oil-continuous emulsions or foams that are stabilized by the presence of oil-soluble surfactants). C/O emulsions have long been a niche area of interest related to waterless hydraulic fracturing in water-sensitive formations. The literature related to C/O foams and emulsions *will* be included in this section. We recently reported that a novel, mineral oil-soluble surfactant composed of a polydimethyl siloxane (PDMS) backbone with multiple pendant tricontyl groups (-$C_{30}H_{61}$) can stabilize CO_2-in-mineral oil (C/O) foams. The PDMS backbone molecular weight was chosen such that it was more CO_2-philic than oil-philic, while the pendant tricontyl groups were oil-philic and CO_2-insoluble. Our group also replicated numerous earlier attempts to form C/O emulsions and foams with commercially available surfactants [2]. To date, C/O foams have not been suggested for use in EOR because of the lower expense and greater ease in making C/W foams. However, there is a continuing interest in C/O foams for completely waterless fracturing, especially in water-sensitive formations. During hydraulic fracturing, the apertures of the flow paths (the wellbore and the hydraulic fractures) are orders of magnitude greater than the pore sizes in sandstone and carbonates encountered during EOR. Therefore, when CO_2 is being considered as a fracturing fluid [7] either transparent single-phase solutions of direct thickeners dissolved in CO_2, or indirect thickeners that stabilize waterless, opaque, two-phase C/O emulsions may be useful.

The third “thickening” strategy that will be reviewed is related to a handful of attempts to *increase the apparent viscosity of* CO_2 *via the dispersion of nanoparticles (NPs)*. There have been a very small number of reports of dispersing nanoparticles in CO_2 and an even smaller number of studies in which such particles were designed to induce a significant increase in CO_2 viscosity. Typically, the nanoparticles are surface-modified to prevent agglomeration and promote dispersion in CO_2, or the nanoparticles are added in conjunction with a CO_2-soluble polymer.

Table 1 [8] presents a summary of the attributes, advantages and disadvantages of direct thickeners, indirect thickeners, and NP-based thickeners.

Table 1: Summary of thickening technologies discussed in this section

Thickener Type	Working Principle	Thickening potential	Advantages	Disadvantages
Direct thickener: high molecular weight polymers or copolymers	Dissolved polymer coils enhance viscosity, especially if the coils become swollen; specific intermolecular associations are also possible for copolymers	Very high; 1-2 order-of-magnitude increases possible at several weight percent	• Has shown incredible CO_2 thickening potential • Viscosity enhancement has been noted by various groups using different types of viscometers • Fluorinated polymers and copolymers can dissolve and thicken CO_2 without co-solvents • High molecular weight polydimethyl siloxane and high molecular weight polyvinyl acetate are both relatively inexpensive commodity chemicals	• Best thickeners are based on expensive fluoroacrylate monomer • Polymers are either extremely viscous liquids or solids at ambient temperature; making pumping difficult • Polymers can be slow to dissolve in CO_2 at ambient temperature • Silicone and oxygenated hydrocarbon polymers require very large amounts of organic co-solvent to dissolve in CO_2 • Light alkanes extracted into CO_2 act as anti-solvents for fluorinated polymers • Polymers can adsorb onto porous media, altering wettability and permeability
Direct thickener: small associating compounds	Intermolecular association; self-assembly in solution; cross-linking via chelation of trivalent metallic ions	Very high viscosity enhancement has been reported, but only when very large amounts of co-solvent (e.g. 25-50 vol% co-solvent in 50-75% CO_2) are used. Modest thickening has been reported for a few low molecular weight polymers that do not require co-solvent	• There has been commercial success in light alkane thickening with cross-linked phosphate esters (consisting of two low viscosity easy-to-handle and pump liquids that thicken very rapidly when mixed in the solvent); tailoring non-fluorous phosphate esters to remain soluble in CO_2 upon crosslinking has not been studied and is a promising area for future research • Non-fluorous oligomers modified with associating groups are another promising thickener for future studies	• Compounds are typically solid or very viscous liquids at ambient temperature, making pumping difficult • Heating/cooling cycles may be required for dissolution and thickening, but this would be impractical in the field • Lack of consensus concerning the thickening potential of oligomers; some reporting no enhancement, others reporting modest increases • Solubility of these compounds in CO_2 at field conditions can be so low that extremely large amounts of co-solvent are required
Indirect thickeners; waterless emulsion	High apparent viscosity emulsions or foams; small CO_2 droplets separated by oil films	One well-documented oil-soluble surfactant has been identified. A proprietary oil-surfactant mixture has also been identified.	• Can create high apparent viscosity increases • No water • An oil that is not completely miscible with CO_2 (e.g. mineral oil) must be added as the continuous phase • Only specialty surfactants will be able to work • Suitable for waterless fracturing in water-sensitive formations	• The emulsion or foam is thermodynamically unstable • Extensive and/or intense mixing may be required • Although the surfactant does not have to be fluorinated, its synthesis will nonetheless lead to an expensive product • Not suitable for enhanced oil recovery because very large volumes of mineral oil (10-20 vol% of the emulsion) must be injected along with the CO_2
Nanoparticle dispersions	Ligands attached to the surface of nanoparticles promote dispersion and inhibit particle aggregation	Unknown	• High tunability and functionality • It is probable that non-fluorinated ligands can be used for surface functionalization	• This concept is in its infancy • Solubility and thickening have not yet been verified • The ability of the dispersion to flow through porous media has not been well substantiated • A high concentration of nanoparticles will likely be required to attain large viscosity increases

1.1.1 Direct CO_2 Thickeners that Dissolve in CO_2 and Form a High Viscosity, Transparent, Stable, Single-Phase Solution

Two commonly used classes of direct thickener candidates for increasing liquid viscosity (whether water, oil, CO_2, or natural gas liquids (NGLs)) include high molecular weight polymers or associating polymers, and low molecular weight, self-assembling compounds that form supramolecular structures. Although it is possible to identify high molecular weight polymers that readily dissolve in common liquids (e.g. polyacrylamide in water, poly-alpha-olefins in hydrocarbon-based oils) and thicken them, the ability to dissolve high molecular weight polymers in dense CO_2 at wellbore or reservoir conditions is extremely challenging because CO_2 is a poor solvent relative to oils and organic solvents. Heating and/or the addition of a CO_2-soluble organic co-solvent (both of which are undesirable for field-scale operations) may be required to facilitate dissolution of the polymers in the solvent.

The fundamental advantage of the small molecule thickener is that remarkably high increases in viscosity, including the formation of transparent rigid gels, can be attained at mass concentrations in the 0.1 – 1.0 wt% range [9, 10]. The apparent molecular weight of the supramolecular structure formed by these associating small molecules can exceed the molecular weight of conventional polymers. However, many (but not all) small molecule thickeners require heating and mixing when combined with a fluid to attain dissolution, followed by cooling to realize gelation and viscosity enhancement. Further, the viscosity of a fluid that has been thickened with small molecules at low temperature typically diminishes dramatically when the fluid is heated to temperatures great enough to diminish the intermolecular attractive forces that favor self-assembly. Note that small self-assembling compounds may “thicken” a solution via the formation of micron- or nanometer-scale fibers dispersed in the solvent as the liquid-thickener mixture cools. Although such a mixture may appear to be viscous when assessed with a conventional viscometer, these fibers may be retained by the inlet face of a porous medium rather than flowing through the rock with the solvent. These opaque, two-phase mixtures of interlocking solid fibers suspended in a liquid are *not* considered to be direct thickeners for the purposes of this study. Although it is relatively easy to identify small molecule oil thickeners, the ability to dissolve small molecules in CO_2 that form viscosity-enhancing supramolecular networks that remain dissolved in a CO_2-rich solution is extremely challenging.

Therefore, our study was intended to present the first peer-reviewed critical literature review of polymeric, associating polymers, low molecular weight polymers, oligomers, and small molecule associating thickeners, in addition to reviews of indirect thickening with waterless emulsions, and thickening with dispersion of nanoparticles. Further, in an attempt to confirm the thickening capability of some thickeners, or resolve conflicting reports concerning other thickener performance, this section provides an experimental assessment of the solubility and thickening capabilities of many readily obtainable thickeners was conducted [8]

1.1.1.1 Polymeric Direct Thickener Literature Review

There have been a number of polymeric direct thickeners studied throughout the literature. Polyfluoroacrylates (PFA) have garnered much attention in the past after the pioneering work by DeSimone and coworkers [11], showing that they significantly dissolve in and thicken liquid and supercritical CO_2. Various groups have expanded upon this work by creating PFA copolymers with associating groups to improve thickening while hopefully maintaining its CO_2 solubility, including styrene (PolyFAST) [12], vinylbenzene (polyFAVB) [13], phenyl acrylate (polyFAPA)

[14], vinyl acetate (polyHFDA-VAc) [7], and ethyl acrylate (polyHFDA-EAL) [15]. Heller's team showed that poly(vinyl ethyl ether) (PVEE) and poly-1-decene (P1D) were soluble in CO_2 to 5.5 and 10.3 g/L (0.57−1.2 wt %, respectively. However, neither PVEE, nor P1D, nor any other commercial polymer tested by their team thickened CO_2 to the extent desired (ideally a 10- to 100-fold increase) [6]. There have been multiple reports of dissolving PDMS [6, 16-18] and PVAc [19], but they all required to be low molecular weight polymers or a large amount of cosolvent to dissolve significantly in CO_2.

Table 3 presents a summary of the attributes, advantages and disadvantages of many of the polymeric direct thickening candidates.

Table 2: Summary of polymeric direct thickeners [8]

Polymer	Reported Solubility in CO_2	Thickening potential	Advantages	Disadvantages
PFA	Up to ~10 wt%	Up to ~10-fold	• Can dissolve in CO_2 without co-solvents • Easy synthesis • Thickening has been verified in several labs using different viscometers	• Based on very expensive fluoroacrylate monomer • Hydrolysis degradation products can be hazardous, especially for C_8F_{17} based PFA • Can adsorb onto rock • Sticky polymer that requires extensive mixing • Difficult to pump unless heated • Alkanes extracted in CO_2 act as polymer anti-solvent • Thickening is not significant at very low concentrations of ~0.1wt%
Fluoro-acrylate copolymers polyFAST, polyFAPA polyFAVB P(HFDA-VAc) P(HFDA-EAL)	Up to ~10 wt%	Up to 500-fold	• Can dissolve in CO_2 without co-solvents • Easy synthesis • Styrene is very inexpensive co-monomer • Thickening has been verified in several labs using different viscometers • Thickening achieved via both high molecular weight and intermolecular associations	• Based on expensive fluoroacrylate monomer • Hydrolysis degradation products can be hazardous, especially for C_8F_{17} based PFA • Requires even longer mixing than PFA • Can adsorb onto rock • Difficult to pump unless heated • Alkanes extracted in CO_2 act as polymer anti-solvent • Thickening is not significant at very low concentrations of ~0.1wt%
PDMS	High molecular weight PDMS: Up to ~10 wt% in solutions of (CO2 + 25+% toluene)	Up to ~10-fold	• Commercially available in large quantities over a very wide range of molecular weight (up to 10^6) • Most PDMS is inexpensive • Ultra-high molecular weight PDMS is the best thickener but is more difficult to synthesize and is more expensive than lower molecular weight PDMS • Relatively safe and benign polymer	• Very low molecular weight PDMS does not require co-solvent but does not induce significant thickening • High molecular weight PDMS requires co-solvents to dissolve in CO_2 • High molecular weight PDMS is very sticky and difficult to pump unless heated • Requires extensive mixing with CO_2 • Solubility in CO_2 decreases considerably as MW increases, necessitating more co-solvent • Thickening is not significant at very low concentrations of ~0.1wt%
PVEE	Up to ~1wt%	Reports vary from no thickening to ~2-fold	• Can dissolve in CO_2 at low MW • Inexpensive	• Literature lacks explanation of how a non-associating low molecular weight polymer or oligomer can induce significant viscosity increases • Lacks consensus in literature concerning thickening capability; reports vary from no thickening to several 10's of % increase • Even in the best case, it does not thicken CO_2 considerably • Does not have high solubility in CO_2
P1D	Up to ~10wt%	Reports vary: no thickening; up to ~100%; up to 10-fold	• Can dissolve in dilute concentration in CO_2 at low MW without co-solvent • Low molecular weight polymer that is easy to pump	• Literature lacks explanation of how a non-associating low molecular weight polymer or oligomer can induce significant viscosity increases • Lacks consensus in literature concerning thickening capability; reports vary from no thickening to several 10's of % increase, to 10-fold increases • Even in the best case, it does not thicken CO_2 considerably • Thickening is not significant at very low concentrations of ~0.1wt%
PVAc	0-5 wt%	Up to 7%	• Commercial polymer available in large quantities as pellets • Relatively inexpensive • Safe and benign polymer • Most CO_2-philic oxygenated hydrocarbon polymer ever identified	• Although PVAc can dissolve in CO_2 without co-solvent, the pressures are well above oilfield pressures, therefore large amounts of co-solvent are required • Solubility decreases as molecular weight increases • Thickening is not significant at very low concentrations of ~0.1-1.0 wt% • Cannot be pumped unless dissolved in large volumes of co-solvent • Requires extensive mixing

This summary indicates that the only high molecular weight homopolymer capable of dissolving in CO_2 at typical EOR or fracturing pressures and temperatures without the need for a co-solvent is PFA. The most effective CO_2-soluble CO_2-thickener is a random copolymer of fluoroacrylate and styrene, poly FAST, but only if the PFA composition is less than 29 mol% styrene, the optimal polyFAST composition. Higher styrene content quickly leads to CO_2-insolubility of polyFAST and reduced thickening due to increased intramolecular (rather than intermolecular) associations of the pendent benzene groups, while lower styrene content promotes CO_2-solubility but diminishes intermolecular pi-pi interactions between pendent aromatic groups.

It appears that the least expensive, non-fluorous, high molecular weight commodity polymers that can thicken CO_2 are polydimethyl siloxane (PDMS) and poly(vinyl acetate) PVAc, however, both polymers require a very large amounts of co-solvent (e.g. 25 vol% toluene or hexane and 75% CO_2) to attain dissolution at pressures commensurate with oilfield conditions.

1.1.1.2 Small Associating Molecule Direct Thickener Literature Review

Table 4 presents a summary of the attributes, advantages and disadvantages of many of the small molecule direct thickening candidates.

Table 3: Summary of several commonly studied small molecule direct CO_2 thickener candidates [8]

Small associating molecule	Reported Solubility in CO_2	Thickening potential	Advantages	Disadvantages
Tin fluorides, notably TBTF	CO_2-insoluble Low CO_2-solubility observed even when large amounts of co-solvent (e.g. pentane) added	Incredible but only for light alkanes such as ethane, propane and butane	• Effective in light alkanes at very low concentrations of several 1/10th wt% • Capable of thickening ethane, propane, butane, pentane	• Insoluble in CO_2 • Massive amounts of co-solvent required (50+%) for dissolution in CO_2 • Dry powder form • Intensive mixing required • Heating/cooling cycle hastens dissolution but is not practical for field application
Hydroxyaluminum disoaps, notably HAD2EH	CO_2-insoluble Low CO_2-solubility observed even when large amounts of co-solvent added	Incredible but only for light alkane such as propane and butane	• Proven thickener of light hydrocarbons (e.g. Napalm) • Capable of thickening propane, butane, pentane	• Insoluble in CO_2 • Massive amounts of co-solvent required for dissolution in CO_2 • Dry powder form • Intensive mixing required • Heating/cooling cycle hastens dissolution but is not practical for field application
12-hydroxystearic acid (12-HAS)	CO_2-insoluble Up to 3% but only if ~15% ethanol co-solvent added to CO_{2z}	Very modest for the fluid phase Significant if an opaque two-phase solid fiber-liquid gel forms	• Thickens hydrocarbon liquids and chlorinated solvents • Inexpensive and commercially available in large amounts	• Dry powder form • Requires a co-solvent • Requires a heating/cooling cycle • Very modest thickening attained if a single-phase solution is formed • Low temperature 100-fold thickening caused by formation of interlocking solid fibers (not a thickened solution)
Crosslinked phosphate esters (CPE); consists of a phosphate ester solution and an acidic crosslinking solution containing a trivalent metal ion	0-3%	From slight thickening to significant thickening to gelation, with increasing concentration	• Proven thickener for propane, butane, liquified petroleum gas (LPG) • Two low viscosity, easy-to-pump liquids (PE and acidic crosslinker solution) • Very fast chelation leads to rapid thickening • Phosphate esters are very CO_2-soluble	• Although the phosphate esters can easily dissolve in CO_2, upon an attempt to crosslink and thicken, the crosslinked network precipitates • Requires very high alkane co-solvent concentrations to dissolve in CO_2 • Little research has been done of tailoring CPE to remains soluble in CO_2
Fluorosurfactants; Ni-diHCF_4 or NaF_7H_4	Up to 6 wt%	Up to 70% increase	• Dissolves in CO_2 without co-solvent • Only requires a tiny amount of water to stabilize the micelles	• Small viscosity increases are attained using high concentrations of a very expensive fluorosurfactant • Research surfactant; not commercially available
Urea-based thickeners	Up to 5 wt%	Up to 3-fold increase	• Large viscosity increases possible • Intermolecular attractions well understand • Flexible functionality, easy to manipulate the design of the compound	• Requires expensive fluorinated ureas to dissolve in CO_2 • Non-fluorinated ureas are either insoluble or require extremely high-pressures to dissolve • Solid form • Commonly require heating/cooling cycles • CO_2-solube ureas are research chemicals, not commercially available
AOT	Up to 2wt% if ~20 wt% co-solvent added	Up to 3-fold increase	• Soluble in CO_2 with alcohol co-solvent • Commercially available in large amounts • Inexpensive surfactant	• Co-solvent (e.g. ethanol) required for dissolution • Modest viscosity increase at high concentration • Solid form
EG	Up to 3 wt%	Up to 4-fold increase	• Soluble in CO2 • Inexpensive	• The patent does not provide an explanation of how EG self-assembles to become a thickener

Some small molecule thickeners, particularly CPE and TBTF, can thicken organic solvents such as liquid ethane and propane quickly and dramatically at very low concentrations, with little or no heating. However, no small molecule thickener for high-pressure CO_2 has yet been identified in the peer-reviewed literature. Typically, these thickeners require extremely high concentrations of co-solvent (e.g. 25 vol% hexane or toluene and 75% CO_2), oftentimes in conjunction with an extensive heating/cooling cycle and intense mixing to thicken the CO_2-cosolvent mixture. A patent [20] claimed that ethylene glycol (EG), an inexpensive chemical available in bulk quantities, thickens CO_2 although no explanation of how or why this molecule would self-assemble in CO_2 to increase viscosity was provided.

1.1.2 Indirect Thickeners for the Stabilization of Two-Phase Waterless CO_2-in-Oil (C/O) Emulsions and Foams.

Table 5 provides a summary of indirect CO_2-thickening candidates for stabilizing waterless CO_2-in-oil (C/O) emulsions or foams.

Table 4: Summary of indirect CO_2-thickening candidates for stabilizing waterless CO2-in-oil emulsions or foams

Stabilizer	CO_2 Droplet size	Emulsion stability	Apparent viscosity	Advantages	Disadvantages
Commercially available ethoxylated resin acids	coarse foams, multiple mm droplet size	< 1 hr	Up to 10 mPa s	Inexpensive, commercially available surfactants	Coarse, multi-mm sized droplets emulsions Limited stability Low apparent viscosity Requires a substantial amount of oil to form a foam or emulsion
Poly trimethyl hydrosilyl siloxane	not reported	not detailed	not detailed	Commercially available fairly inexpensive	not a significant amount of data reported
Specialty surfactant (PDMS with multiple tricontyl (C_{30}) pendant groups) dissolved in mineral oil	extremely small droplets (0.005-0.100 mm)	~3 days	Up to 5 mPa s	Designed specifically for the CO_2-oil system Multiple-day stability in quiescent conditions Very small CO_2 droplets (5 – 100 microns) Viscosity verified but capillary viscometry and falling object viscometry	Although non-fluorinated, the silicone starting material is expensive Research surfactant, not commercially available Requires a substantial amount of oil to form a foam or emulsion
PSM (proprietary mixture of polymer, oil, surfactants, and solvents)	prolonged mixing(hours) required to generate large CO_2 droplets (0.1-1.0 mm)	< 1 day	Reported to be up to 100 mPa s	A new chemical product designed to thicken CO_2 All components found in a single mixture	Reported to be a CO_2-soluble direct thickener in literature; but our sample was an indirect thickener that yielded a C/O emulsion Required prolonged stirring to establish emulsion in our lab Mm-sized droplets, a few droplets of ~5 mm diameter

Note that the only verifiable high-pressure C/O emulsion was recently reported with the polydimethyl siloxane polymer with 88 repeat units, including 7 pendent tricontyl (C_{30}) groups [4]. These C/O emulsions were composed of 10-100 micron sized bubbles of CO_2 separated by films of mineral oil. The emulsion completely filled the cell were stable for about an hour before any collapse occurred, thereby allowing the measurement of foam viscosity. The apparent viscosity of these emulsions was measured with both falling object viscometry and capillary viscometry. In the supporting information for the same paper, it was shown that stabilizers that were previously reported in conference proceedings did not establish C/O emulsions that were stable for hours or composed of small (sub-mm) bubbles.

1.1.3 Increasing the Viscosity of CO_2 Using Stable, Dilute Suspensions of Nanoparticles (NPs) in CO_2

Although nanocomposites in CO_2 is seen as a promising field of CO_2 viscosification, there were not enough results in the literature for a table of results in this section.

Very recently, it has been reported that ~2-8wt% of a nanocomposite composed primarily of high molecular weight (600,000) P1D and graphene oxide (GO) particles (e.g. 20,000 - 80,000 ppm nanocomposite containing up to 500 ppm GO) thickens CO_2 (e.g. a 23-fold increases at 60000 ppm nanocomposite containing 300 ppm GO)[5]. However, no details of the falling ball were provided, and no explanation of how P1D of such high molecular weight (600,000) was CO_2-soluble when prior researchers indicated that only very low molecular weight P1D could dissolve in CO_2.

In another study, Zhang and co-workers [21] proposed combining a partially sulfonated fluorinated copolymer that contained styrene with a nanocomposite fiber formed by combining nanoparticles in a polyester fiber. The authors reported that the viscosity of CO_2 was increased 100-fold at a 1wt% concentration of these components along with a comparable amount of diesel.

1.1.4 Unspecified Thickener Compositions

There are several literature references, including patents, conference proceedings and journal articles, that describe the thickening of CO_2 with compounds or mixtures that are not fully specified, and hence not reproducible by other investigators. These alleged thickeners include TNJ [22], X [23], new surfactant [24], Chemical B [25], small molecule system [26], System A and System B [27], and fluorinated, dual, twin-tailed surfactant with divalent metal cations [28].

1.2 Materials and Experimental Methods for Assessments of Purported CO_2 Thickeners

It was not feasible to assess every compound that has been proposed as a CO_2-thickener, because many of these novel compounds are not available commercially and must be synthesized, purified and characterized prior to being evaluated, while others are not adequately described in the literature to ascertain their exact composition. However, several of the polymeric and small molecule compounds that have been reported to thicken CO_2, Figure 1, are either commercially available, readily synthesized, or were provided to us as gifts for assessment. The co-solvents required for the dissolution of many of these thickener candidates are also readily available, and co-solvent concentrations above 25% were not considered. The objective of this experimental work was not to optimize the conditions for CO_2 thickening (temperature, pressure, co-solvent concentration, thickener concentration). Rather, the objective of this experimental study was to use a windowed high-pressure falling object viscometer to validate if the purported thickener dissolved completely in CO_2, or established a foam or emulsion) and also had the ability to thicken CO_2 as described in the literature.

1.2.1 Materials

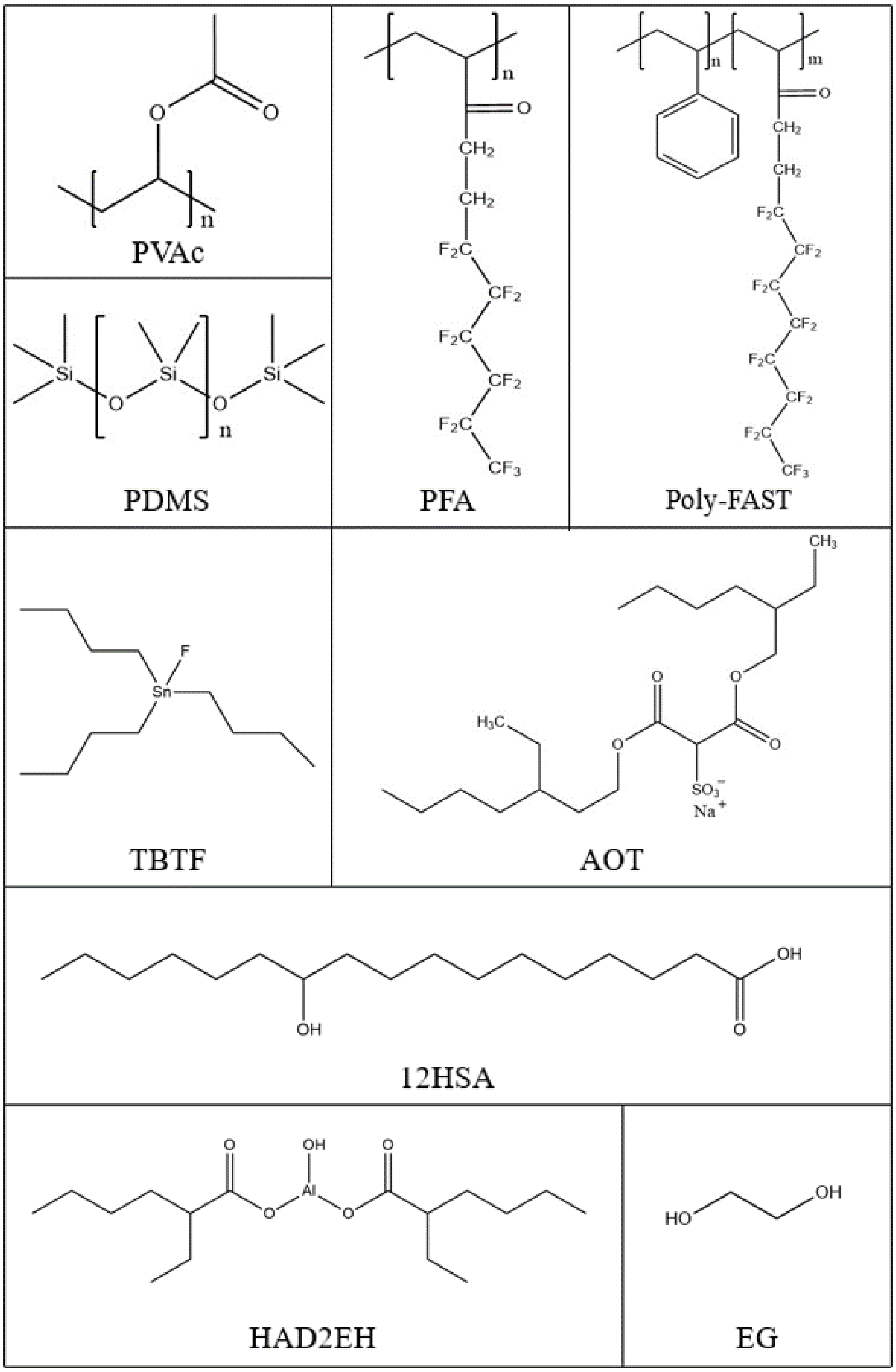

Figure 1: Molecular structures of the purported CO_2 thickeners experimentally assessed in this section

1.2.1.1 High Molecular Weight Polymeric Thickeners.

The following high molecular weight polymers were assessed in this study.

PolyFAST, (Mw ~500,000) based on the –C_6F_{13} moiety in the fluoroacrylate monomer, was synthesized according to our team’s previously published procedure for bulk co-polymerization of a copolymer containing styrene (29 mol%) and fluoroacrylate (71 mol%) monomers [12].

PFA, (Mw ~124,000), based on the –C_6F_{13} moiety in the fluoroacrylate monomer, was synthesized according to our previously published procedures for bulk homopolymerization of the fluoroacrylate monomer [29].

PDMS, polydimethyl siloxane, was obtained from Clearco. Two samples (Mw 500,000+, 20,000,000 cSt, and Mw 308,000, 1,000,000 cSt) were used as received without further purification.

PVAc, polyvinyl acetate (Mw ~500,000) was obtained from Sigma Aldrich and used without further purification.

PSM, a proprietary "Polymer Solvent Mixture" mixture of allyl ethers, acrylate, acrylic long carbon chain esters/benzenes, propylene carbonate/allyl ethyl carbonate, dimethyl carbonate, and white oil/silicon or oil/petroleum ether was obtained from the manufacturer (Beijing AP Polymer Technology Co., Ltd.) in the form of an emulsion with 35% active ingredients.

1.2.1.2 Low Molecular Weight Polymeric or Oligomeric Thickeners.

The following low molecular weight polymers or oligomers were evaluated in this study:

P1D, poly-1-decene (Mw ~910), which can be considered as an oligomer, was obtained from Sigma Aldrich and used without further purification.

PVEE, polyvinyl ethylether (Mw ~3800), was obtained from Sigma Aldrich and used without further purification.

1.2.1.3 Small Molecule Associative Thickeners.

The following small molecules were evaluated in this study.

AOT, bis(2-ethylhexyl) sulfosuccinate sodium salt (97%), was obtained from Sigma Aldrich and used without further purification.

EG, anhydrous ethylene glycol (99.8%), was obtained from Sigma Aldrich and used without further purification.

TBTF, tributyltin fluoride (97%), was obtained from Sigma Aldrich and used without further purification.

12HSA, 12-hydroxystearic acid (99%) was obtained from Sigma Aldrich and used without further purification.

HAD2EH, hydroxyaluminum di(2-ethylhexanoate) (96%), was obtained from TCI and used without further purification.

OG160/XL064, a proprietary two-component mixture; OG160, a phosphate ester blend designed specifically for gelling butane and propane[30]. XL064, a trivalent iron-based acidic crosslinking solution were obtained from the inventors and used as received. A preliminary test verified that 0.5 vol% OG160 + 0.5 vol% XL064 increased the viscosity of liquid propane and butane by 2-3 orders of magnitude at 25 °C and 34.5 MPa. The OG160/XL064 combination was used rather than a phosphate ester – crosslinker blend designed for hexane; that product had longer alkyl groups in the OG components and induced very modest changes in propane viscosity [10].

1.2.1.4 Co-Solvents

Ethanol (99.5%), hexanes (98.5%, ~64% n-hexane) and toluene (99.8%) were obtained from Sigma Aldrich and used without further purification.

1.2.2 Methods

The solubility of polymeric and small molecule direct thickeners was assessed using a non-sampling, visual technique. The relative viscosity of the CO_2-thickener solution was also determined using falling object viscometry.

1.2.2.1 Solubility Measurements

Whether thickener candidates could dissolve in CO_2 was determined using a visual technique that is detailed in our prior publications [1, 10, 12, 29, 31-33]. Known amounts of the thickener and liquid CO_2 are charged to a fully windowed, agitated, invertible, variable-volume (10-100 ml), high-pressure view cell (Schlumberger, 69 MPa (10000 psi) at 180 °C). This phase behavior cell is kept within an isothermal airbath with cooling and heating capabilities (CSZ, -20

°C to 180 °C). The contents are then compressed to pressures up to 69 MPa and mixed with a magnetically driven, slotted fin impeller (2000 rpm) at the top of the sample volume. After mixing, the impeller rotation is stopped and the entire cylindrical sample volume is inspected to verify that a single, transparent fluid phase has been attained. If so, the single-phase is expanded at a very slow rate until a second phase occurs, typically in the form of a cloud of thickener-rich droplets or particles. The pressure at which the second phase begins to appear is the cloud point pressure. Typically, this procedure is repeated five times and the average value of the cloud points is determined. By repeating this procedure for various compositions (i.e. different ratios of CO_2 and thickener), a cloud point locus that represents a small portion of the overall pressure-composition diagram can be constructed.

If a thickener is insoluble in CO_2, as evidenced by the thickener remaining as a second phase (solid or liquid) after extended mixing, then the experiment can be repeated using a co-solvent such as ethanol or toluene.

If, upon mixing, a foam or emulsion is being formed (as evidenced by dispersed bubbles or droplets of CO_2 within a second continuous film phase), then the mixing is continued until the emulsion is formed to its fullest extent. In such a case, the additive is not considered as a direct thickener, but rather as a mixture that promotes the formation of a high quality (i.e. high vol % CO_2) waterless, CO_2-in-oil emulsion.

1.2.2.2 Falling Object Viscometry

The assessment of the CO_2-thickening capability of each candidate was determined using the same apparatus that was employed for solubility measurements and has been detailed in prior publications[10, 12, 29, 31-33]. A close clearance Pyrex sphere (ball diameter = 3.1587 cm) or an aluminum cylinder (diameter = 3.16179 cm, height = 2.54 cm) is placed in the cylindrical sample volume with a 3.1750 cm diameter. The mixture is then stirred and compressed to a pressure several thousand psi greater than the previously measured cloud point to assure the attainment of a single phase. Mixing is then stopped, and the occurrence of a transparent single phase is verified. The entire phase cell (which is mounted on a steel rod and has coiled tubing leading to and from the cell) is then quickly inverted, and the fall of the object observed. The foremost advantage of this visual technique is that it is possible to easily observe undissolved particles or undissolved viscous droplets of a thickener-rich phase that can impede the fall of the ball or cylinder. The complete fall of the ball is observed, and the velocity is determined by measuring the duration of the fall between two locations separated by a known distance. The terminal velocity of the ball or cylinder falling within the confined ~15 cm column of thickened CO_2 is typically attained within the first third (5 cm) of the fall. The viscometer is also calibrated by determining the terminal velocity of the same object in pure CO_2 at the same temperature and pressure.

Because the concentrations of the thickeners in CO_2 is low, it is reasonable to assume that the density of the CO_2-thickener solution is approximately the same as the density of pure CO_2 at the same conditions. Therefore, the driving force for the fall (falling object density - fluid density) is roughly the same for pure CO_2 and thickened CO_2. As a result, relative viscosity (the ratio of solution viscosity to pure CO_2 viscosity) can be estimated simply by determining the ratio of the terminal velocity in CO_2 to the terminal velocity in the CO_2-thickener solution. For example, if the ball falls five times slower, then the thickened CO_2 is about five times more viscous than pure CO_2. Viscosity measurements were repeated five times, and in all cases the five relative viscosity values for each test fell within ±10% of the average value.

This technique can also be used to assess the apparent viscosity of an emulsion of foam, but only if the emulsion or foam is stable enough to fill the entire sample for the duration of the experiment.

1.3 CO_2 Thickener Relative Viscosity Results

Tables 5-8 present a summary of the relative viscosity results obtained in this study. The results are presented within the major groups; polymeric direct thickeners, small molecule direct thickeners, and indirect thickeners. No nanoparticle dispersions were available for evaluation. For the falling object column, “B” means a falling ball was used in the experiment and “C” means a falling cylinder was used.

Table 5: Relative viscosity results for solvents used in this section

Thickener	**T °C**	**P MPa**	**CO_2 Conc. [wt%]**	**Co-solvent**	**Co-solvent Conc [wt%]**	**Falling object**	**Relative visc. (±10%)**
None	23		100	-		C	1.0
None	23	14-28	76	Toluene	24	C	1.1
None	23	21-35	76	Ethanol	24	C	1.7

1.3.1 High Molecular Weight Polymeric Direct Thickeners

polyFAST – PolyFAST exhibited remarkably greater CO_2-thickening (138-fold increase at 4 wt%) than any other compound and did not require co-solvent addition to attain a single phase. However, polyFAST requires a greater pressure to dissolve in CO_2 than PFA (a less effective thickener) because polyFAST contains ~29 mol% of styrene, which is far less CO_2-philic than the fluoroacrylate monomer.

PFA – PFA is capable of thickening CO_2, but not as effectively as polyFAST. The sample of PFA used in this study was not as effective as the PFA used in our prior study, in which the CO_2 viscosity was increased by a factor of ~3 at low shear rate using only 1 wt% PFA [29]. The molecular weight of the PFA in this study was likely less than that of the PFA in our prior study. The results verify that 3-5 fold increases in CO_2 can be attained using several wt% PFA.

PDMS– High molecular weight PDMS is essentially CO_2 insoluble, therefore toluene was used to promote dissolution of enough PDMS in CO_2 to attain viscosity enhancement at pressures below 60 MPa (8700 psi) [6, 16, 34, 35]. 3-6-fold increases in CO_2 viscosity were realized using 2 wt% PDMS (Mw 500,000+) in the presence of 23 wt% toluene and 75 wt% CO_2. When the same mass concentration of a lower molecular weight PDMS (Mw 308,000) was used, the CO_2 viscosity increased by a factor of ~2, representing a 100% increase. Note that the toluene addition alone to the CO_2 (no PDMS) would account for a CO_2-toluene solution relative viscosity of about 1.1.

PVAc – PVAc requires substantial amounts of a co-solvent, such as toluene, to dissolve in CO_2 at pressures below ~30 MPa (4350 psi). A single-phase solution of 23 wt% toluene, 75 wt% CO_2 and 2 wt% of the PVAc was evaluated. At a concentration of ~2 wt% of the highest molecular weight PVAc that was available (Mw 500,000), the viscosity of CO_2 increased by about 70% to a relative viscosity of 1.7. As was the case with PDMS, a portion of this increase was attributable to the presence of the toluene in CO_2, which results in a relative viscosity of 1.1.

Table 6: Relative viscosity results for high molecular weight polymeric thickeners

Thickener	Mw	T °C	P MPa	Thickener Conc. [wt%]	CO_2 Conc. [wt%]	Co-solvent	Co-solvent Conc [wt%]	Is thickener soluble?	Falling object	Relative visc. (±10%)
polyFAST	5.0E5	25	27.6	4	96	-	-	yes	C	138
PFA	1.24E6	25	13.8	4	96	-	-	yes	C	2.8
PFA	1.24E6	25	20.7	4	96	-	-	yes	C	4.2
PFA	1.24E6	25	27.6	4	96	-	-	yes	C	5.4
PDMS	5.0E5	23	10.3	2	75	Toluene	23	yes	B	3.6
PDMS	5.0E5	23	13.8	2	75	Toluene	23	yes	B	4.1
PDMS	5.0E5	23	20.7	2	75	Toluene	23	yes	B	4.7
PDMS	5.0E5	23	27.6	2	75	Toluene	23	yes	B	5.6
PDMS	3.1E5	23	10.3	2	75	Toluene	23	yes	B	1.9
PDMS	3.1E5	23	13.8	2	75	Toluene	23	yes	B	2.1
PDMS	3.1E5	23	20.7	2	75	Toluene	23	yes	B	2.0
PDMS	3.1E5	23	27.6	2	75	Toluene	23	yes	B	2.0
PVAc	5.0E5	23	20.7	2	75	Toluene	23	yes	B	1.7
PVAc	5.0E5	23	27.6	2	75	Toluene	23	yes	B	1.7

1.3.2 Low Molecular Weight Polymeric Thickeners

PVEE – No significant increase in solution viscosity was detected when 2 wt% PVEE was dissolved in CO_2 at 100 °C and 8000 psi. Toluene was then introduced to allow a single phase to be attained at lower temperature and pressure. For mixtures of 2 wt% PVEE, 23 wt% toluene and 75 wt% CO_2, viscosity increase of about 30% (relative to pure CO_2) were measured at 23 °C and 1500 – 4000 psi. The addition of toluene alone yielded a relative viscosity of 1.1.

P1D – The addition of 2 – 4 wt% P1D in CO_2 did not increase the viscosity of CO_2 by more than a 5% percent in any of our measurements.

Table 7: Relative viscosity results for low molecular weight polymeric thickeners

Thickener	Mw	T °C	P MPa	Thickener Conc. [wt%]	CO_2 Conc. [wt%]	Co-solvent	Co-solvent Conc [wt%]	Is thickener soluble?	Falling object	Relative visc. (±10%)
PVEE	3800	100	55.2	2	98	-	-	yes	C	1.0
PVEE	3800	23	10.3	2	75	Toluene	23	yes	B	1.3
PVEE	3800	23	27.6	2	75	Toluene	23	yes	B	1.3
P1D	910	23	34.5	2	98	-	-	yes	B	1.0
P1D	910	100	48.3	4	96	-	-	yes	C	1.0

1.3.3 Small Molecule Direct Thickeners

OG160/XL064 – 0.5 vol% OG160 and 0.5 vol% of XL064 were mixed with hexane at 23 °C. A thick, viscoelastic solution formed. This thickened hexane sample was added to the sample volume of the high-pressure phase behavior cell along with liquid CO_2 such that a 50 vol% thickened hexane: 75 vol% CO_2 mixture formed (0.125 vol% OG160:0.125 vol% XL064: 24.75 vol% hexane: 75% vol CO_2) at 22 °C and 17.2 MPa (2500 psi). Because the density values of CO_2, hexane, OG160 and XL064 at 22 °C and 17.2 MPa (2500 psi) are 0.91, 0.65, 1.01, and 1.30 g/ml, respectively, this corresponds to 80.648 wt% CO_2, 19.010% hexane, 0.150 wt% OG160, and 0.192 wt% XL064. Upon mixing, the crosslinked phosphate ester precipitated and would not re-dissolve in the CO_2-hexane solution despite prolonged mixing at an elevated pressure of 48.3 MPa. Apparently, a greater proportion of co-solvent is needed to attain a stable single-phase, such as the 50 vol% CO_2:50 vol% light alkanes mixture reported by Taylor and workers [36].

EG – No detectable increase in viscosity was detected with the addition of 2 wt% EG to CO_2.

AOT – AOT is insoluble in CO_2. When ethanol was used as a co-solvent, a single phase of 1.5 wt% AOT was attained in a mixture containing 20 wt% ethanol and 78.5 wt% CO_2. The relative viscosity was 2.5 times greater than that of pure CO_2. Note that the addition of ethanol alone resulted in a CO_2-ethanol solution relative viscosity of 1.7.

TBTF - A solution that contained 2 g TBTF and 23 g toluene (8wt% TBTF) was made into a transparent gel by heating the mixture gently to 40 °C while stirring and letting the TBTF completely dissolve. The solution was then cooled to 23 °C and a clear, highly viscous solution formed. This viscous solution was placed in the sample volume of the phase behavior apparatus in a 2:23:75 (TBTF : toluene : CO_2) wt% ratio. The high-pressure CO_2 acted as an anti-solvent at 34.5 MPa (5000 psi) and 23 °C, dissolving the toluene and leaving fibers and flakes of TBTF behind. The solution was then heated to ~75 °C at 34.5 MPa (5000 psi) and stirred, at which point only a small portion of the TBTF had dissolved. This solution was allowed to cool to 23 °C overnight at 34.5 MPa (5000 psi). The TBTF came out of solution as chunks of gels dispersed in CO_2. Gels of TBTF in toluene were recovered when the CO_2 was vented. Similar results were obtained using hexanes as co-solvent. These results are consistent with the prior reports [37, 38], which indicated that extremely high concentrations (60+ wt%) of pentane co-solvent were required for TBTF to dissolve in CO_2.

HAD2EH - A mixture of 2gr HAD2EH and 23gr toluene (8wt% HAD2EH) was heated to 40^{o}C while being stirred. The resultant solution was allowed to cool to ambient temperature and a clear rigid gel formed. This rigid gel was placed in the sample volume of the phase behavior cell in a 2:23:75 (HAD2EH : toluene : CO_2) wt% ratio. The high-pressure CO_2 acted as an anti-solvent at 34.5 MPa (5000 psi) and 23 °C, dissolving the toluene and leaving solid fibers and flakes of HAD2EH behind. The mixture was then heated to 75 °C at 34.5 MPa (5000 psi) and stirred overnight, at which point only a portion of the HAD2EH had dissolved. This mixture solution was allowed to cool to ~23 °C at 34.5 MPa (5000 psi). Large blobs of HAD2EH-gelled toluene formed. We then assessed a different means of mixing the components. A mixture of 2:23:75 HAD2EH : toluene : liquid CO_2 a wt% ratio was added to the cell, and then mixing and heating commenced. The high-pressure CO_2 acted mixed readily with the toluene, leaving clumps of HAD2EH powder behind. The mixture of CO_2 and HAD2EH was heated to ~75 °C at 34.5 MPa (5000 psi) while being stirred, at which point only a small portion of HAD2EH had dissolved, while the majority of the HAD2EH remained in slightly gelled clumps. This mixture was allowed to cool to ambient T overnight at 34.5 MPa and the HAD2EH came out of solution as blobs of toluene-rich gels dispersed in CO_2.

12HSA - A mixture of 2gr 12HSA and 23gr toluene (8wt% 12HSA) was heated to ~75 °C while stirring. The resultant solution as allowed to cool to 23 °C, and a single-phase, transparent, rigid gel formed. This gel was placed in the sample volume of the high-pressure phase behavior cell. Liquid CO_2 was then added such that a 2:23:75 (12HSA : toluene : CO_2) wt% ratio mixture was present. The high-pressure CO_2 acted as an anti-solvent at 34.5 MPa (5000 psi) and 23 °C, dissolving the toluene and leaving fibers and flakes of 12HSA behind. The mixture was heated to 75 °C at 41.4 MPa (6000 psi) with the stirrer at 2000 rpm. Only a small portion of the 12HSA dissolved. This mixture was allowed to cool to 23 °C at 34.5 MPa (5000 psi). The 12HSA precipitated in the form of blobs of toluene-rich gels dispersed in CO_2. A mass of HSA-gelled toluene was recovered when the CO_2 was vented.

We then assessed a different means of mixing the components. A mixture of 2:23:75 wt% 12HSA : toluene : CO_2 was introduced to the sample volume of the phase behavior cell. The CO_2 quickly acted as an anti-solvent at 34.5 MPa (5000 psi) and 23 °C, dissolving some the toluene and leaving clumps of 12HSA powder behind. The solution was then heated to 75 °C at 34.5 MPa (5000 psi) and stirred, at which point some of 12HSA dissolved, while some of the 12HSA remained suspended in the fluid as soft translucent gels. This mixture was allowed to cool to 22 °C overnight at 34.5 MPa (5000 psi). An opaque, light brown mass of CO_2-swollen gel blobs filled the entire sample volume. Upon subsequent slow expansion of the high-pressure mixture via lowering the position of the movable piston at the bottom of the sample volume, the flat bottom of this brown mass remained flat and stationary in the sample volume as clear CO_2 expanded into the volume under the gel and above the sliding piston. Upon removal of the CO_2, a soft monolith of a porous 12HSA : toluene foamed gel remained.

Following the lead of [39], a solution of 2gr 12HSA and 23gr ethanol (8wt% 12HSA) formed a transparent solution (not a gel) by heating the mixture gently to ~75 °C while stirring, thereby allowing the 12HSA to completely dissolve in ethanol. The solution was then cooled to 23 °C; it remained a low viscosity solution. This solution was then transferred to the sample volume of the windowed phase behavior cell along with liquid CO_2 in a 2:23:75 (12HSA : ethanol : CO_2) wt% ratio. The high-pressure CO_2 acted as an anti-solvent at 34.5 MPa (5000 psi) and 22 °C, dissolving the ethanol and leaving fibers and flakes of 12HSA behind. The mixture was then heated to ~75 °C at 41.4 MPa (6000 psi) and stirred, at which point only a small portion of the 12HSA dissolved. This mixture was allowed to cool to 22 °C at 34.5 MPa (5000 psi), and a significant amount of 12HSA precipitated as swollen white flakes.

Table 8: Relative viscosity results for small molecule direct thickeners

Thickener	Mw	T °C	P MPa	Thickener Conc. [wt%]	CO_2 Conc. [wt%]	Co-solvent	Co-solvent Conc [wt%]	Is thickener soluble?	Falling object	Relative visc. (±10%)
OG/XL	-	23	13.8	0.34	81	Hexane	18.66	no	B	n/a
EG	62	23	24.1	2	98	-	-	yes	C	1.0
EG	62	23	27.6	2	98	-	-	yes	C	1.0
AOT	445	25	20.7	1.5	78.5	Ethanol	20	yes	C	2.5
TBTF*	309	25	34.5	2	75	Toluene	23	no	-	-
HAD2EH*	331	25	34.5	2	75	Toluene	23	no	-	-
12HSA**	300	23	34.5	2	75	Toluene	23.00	no	-	-
12HSA	300	23	34.5	2	75	Ethanol	23.00	no	-	-

1.3.4 Indirect Thickeners

Unfortunately, we did not have any remaining PDMS polymer with pendent C_{30} groups, previously synthesized by GE Global Research, to assess. Because the Pitt-GE Global Research project funded by ARPA-E had expired, we were unable to obtain more of this novel stabilizer from the GE Global Research chemists.

PSM – When PSM and CO_2 were first combined, the polymeric components quickly precipitated to the bottom of the cell as the lower molecular solvent components dissolved in CO_2. After being mixed overnight (10 hours) at the same conditions reported by the researchers [40], an opaque, white, C/O waterless emulsion of mm-sized CO_2 droplets separated by continuous films of an oleic phase had filled the entire phase behavior sample with the exception of two very large (~5 mm diameter) droplets of clear CO_2 and several small blobs of undissolved polymer. (It is likely that with improved mixing, the mixture would have been more homogeneous throughout the entire sample volume.) The mixture was not a transparent single-phase CO_2-rich solution, therefore, the sample of PSM that we received was not a direct thickener as described by Al Yousef [40]. However, it could be considered as an indirect thickener that slowly established a waterless, C/O emulsion with a very high volume fraction (quality) of liquid CO_2. Although not thermodynamically stable, the emulsion was stable enough to persist without any noticeable collapse several hours after the cessation of mixing. Unfortunately, a small piece of undissolved polymer became lodged between our aluminum cylinder and the Pyrex wall of our windowed viscometer and we were unable to obtain falling cylinder apparent viscosity values during several attempts. However, such C/O waterless emulsions can exhibit high apparent viscosity, and a prior report of high viscosity of CO_2 that was "thickened" by PSM [40] may have been attributable to the high apparent viscosity of indirectly thickened CO_2 (a C/O emulsion) such as those we previously reported (Alzobaidi et al. 2019). Alternately, the sample of PSM that we received from the manufacturer may have differed significantly from that used by the authors of the 2019 study [40].

Table 9: Relative viscosity results for the indirect thickener

Thickener	Mw	T °C	P MPa	Thickener Conc. [wt%]	CO_2 Conc. [wt%]	Co-solvent	Co-solvent Conc. [wt%]	Is thickener soluble?	Falling object	Relative visc. (±10%)
PSM***	-	25	17.2	2	98	-	-	no	C	-

1.4 Conclusions

PolyFAST and PFA remain the only verifiable CO_2 thickeners that dissolve in neat CO_2 at conditions associated with EOR. PolyFAST is particularly effective, where high molecular weight versions that contain the proper proportion of styrene (21 mol%) are able to induce a 138-fold increase in CO_2 viscosity at 4wt%, while PFA addition at the same concentration resulted in only a 3-5-fold increase. However, it has been recently demonstrated that these fluoroacrylate-rich polymers are likely to adsorb significantly onto sandstone or carbonate rock [29]. Further, both materials are inherently expensive and there are concerns about the toxicity of hydrolysis degradation products associated with these polymers, particularly if they contain eight fluorinated carbons in the fluoroacrylate monomer. Although these environmental concerns can be mitigated by using fluoroacrylate monomers with short, fluorinated segments (e.g. $-C_6F_{13}$ and $-C_4F_9$), it remains unlikely that either polyFAST or PFA could be used in a large scale EOR or hydraulic fracturing operation.

High molecular weight PDMS is also a well substantiated CO_2 thickener, although a substantial amount of toluene co-solvent (e.g. 23 wt%) is required to attain dissolution at EOR conditions, as has been noted since the first reports on its evaluation in the early 1990s. [16, 35]. A 4-6-fold increase in CO_2 viscosity was realized using 2 wt% of PDMS (Mw 500,000) and toluene co-solvent. This degree of thickening is comparable to that attained with 4wt% PFA. Although we were not able to assess them in this study, it would not be surprising that recently reported variants of silicone oil would also have the potential to thicken CO_2 if a co-solvent was used for polymer dissolution.

High molecular weight PVAc (Mw 500,000) remains the most technically and economically viable oxygenated hydrocarbon-based polymer capable of thickening CO_2. However, like PDMS, a large amount of co-solvent (e.g. 23 wt% toluene) is required to permit PVAc to dissolve in CO_2 at EOR conditions. The addition of 2wt% PVAC and toluene resulted in a 70% increase in CO_2 viscosity.

Although PVEE and P1D have received a good deal of recent attention, our results are more in line with the earlier results of Heller and co-workers concerning the efficacy of low molecular weight oligomers [6]. Both PVEE and P1D appear to be very modest CO_2 thickeners. Further, no literature was found in which low molecular weight, non-associating polymers in dilute concentration were used to thicken any other fluid, including water or oil. Although no increase in viscosity was measured when PVEE was dissolved in CO_2 in the absence of a co-solvent, a 30% increase in CO_2 viscosity was achieved with PVEE when toluene was added. This suggests that a portion of the thickening may be attributable to the presence of the co-solvent and/or the ability of the co-solvent to cause the P1D to swell more significantly. No significant increase in viscosity was observed with the falling object viscometer for P1D, although this material did not require a co-solvent for dissolution in CO_2. These results, coupled with the absence of any literature verifying that dilute concentrations of oligomers or low molecular weight can thicken water or oil, suggest that CO_2 thickening using low molecular weight non-associating oligomers is unlikely to result in a significant degree of CO_2 thickening.

The ionic surfactant AOT was soluble in CO_2 only when a substantial amount of ethanol was introduced as a co-solvent. The resultant solution was 2.5 times more viscous than CO_2, in good agreement with the claims in the literature [41]. However, an 80% CO_2-20% ethanol solution at the conditions listed in Table 1 is 1.7 times more viscous than pure CO_2. Therefore, the AOT has apparently self-assembled into micelles that further increase relative viscosity.

The two low viscosity liquids (phosphate ester mixture; acidic trivalent ion solution) that are known to quickly thicken liquid propane or LPG at very low concentration apparently require a very substantial amount of alkane co-solvent to dissolve in CO_2. The 25% hexane – 75% CO_2 solution used in this work was incapable of keeping the crosslinked network in solution. It appears that a CO_2-alkane solution containing closer to 50% alkanes is required [36] to and thicken CO_2.

Ethylene glycol was soluble in CO_2; however, it did not yield a detectable viscosity increase. Hydroxyaluminum di-2-ethylhexanoate, tributyltin fluoride, and 12-hydroxystearic acid (12HSA) were insoluble in CO_2, even in the presence of 23 wt% co-solvent. The 12HSA-toluene-CO_2 mixture did form an opaque gel that filled the cell; upon the subsequent removal of CO_2 via depressurization at constant volume, a soft, monolithic, free-standing fibrous foam of 12HSA fibers laden with toluene remained in the cell.

The sample of PSM mixture that we received, described as a *"mixture of allyl ethers, acrylate, acrylic long carbon chain esters/benzenes, propylene carbonate/allyl ethyl carbonate, dimethyl carbonate, and white oil/silicon or oil/petroleum ether"* [40], was insoluble in CO_2. However, prolonged mixing with CO_2 led to the establishment of a coarse CO_2-in-oil emulsion of mm-sized CO_2 droplets that filled most of the sample volume (although undissolved solid was clearly observed). This undissolved material prevented the free fall of the cylinder and therefore the apparent viscosity of the CO_2-in-oil emulsions could not be determined. Based on our recent study of oil-soluble silicone-alkyl polymeric surfactants capable of quickly stabilizing CO_2-in-mineral oil waterless emulsions, this type of rarely reported waterless, high quality (i.e. volume fraction CO_2) emulsion that we observed by mixing PSM with CO_2 may indeed exhibit a high apparent viscosity. It has the potential to be an indirect CO_2 thickener that forms a completely waterless CO_2-in-oil emulsion.

With regard to novel, future research directions, there appear to be few promising avenues related to CO_2-polymer solutions given the profound amount of work that has been completed in this area. There is little chance that dilute concentrations of non-associating oligomers can thicken CO_2 (or any other fluid) in dilute concentration. However, there are many novel designs of lower molecular weight associating polymers containing two or more CO_2-phobic associating groups that can be explored, such as benzene-ring functionalized oligomers of CO_2-philic oligomers. With regard to small associating molecules, although phosphate esters with alkyl tails are soluble in CO_2, the crosslinked phosphate ester network is CO_2-insoluble. The design of phosphate esters with highly CO_2-philic tails (perhaps sugar acetates) has not been reported and could lead to a viscosity-enhancing CO_2-soluble crosslinked phosphate ester network. In our opinion, this is the most promising avenue for CO_2 thickener development. High apparent viscosity C/O emulsions can be stabilized (for many hours to a few days without mixing) with CO_2-soluble non-fluorous, completely, hydrophobic surfactants. However, this C/O emulsion must contain a high proportion of an oil that is not miscible with CO_2, therefore such emulsions would be of interest only as alternate fracturing fluids for highly water-sensitive unconventional formations in which C/W foams could not be used. There have been a few reports of stable nanoparticle dispersions in CO_2 and a single report of an apparent increase in CO_2 viscosity. However, future research in this area should begin with a thorough investigation of silica nanoparticles that are surface-functionalized with non-fluorous highly CO_2-philic ligands. If these nanoparticles can be dispersed in high-pressure $CO_{2,}$ the apparent viscosity of the dispersion should be measured and the ability of the dispersion to propagate through porous media should be verified.

2.0 Mixtures of CO_2 and Polyfluoroacrylate Based on Monomers Containing Only Six or Four Fluorinated Carbons - Phase Behavior and Solution Viscosity

Polyfluoroacrylate (PFA) $[CH_2CHCOO(CH_2)_n(CF_2)_{m-1}CF_3]_k$, Figure 1, is a hydrophobic, oil-phobic, homopolymer fluoropolymer.

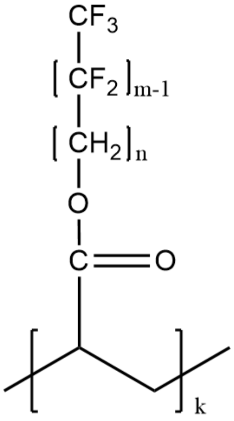

Figure 2: PFA, with n -CH_2- methylene units, (m-1) -CF_2- units, and m total fluorinated carbons in the side chain; there are k monomeric repeat units in the polymer

If PFA is based on a monomer with six or seven fluorinated carbon atoms, the polymer will be amorphous,[29, 42] whereas PFA synthesized from a monomer containing eight fluorinated carbons or greater is semi-crystalline [43, 44]. PFA is insoluble in conventional hydrocarbon solvents, but can readily dissolve in highly fluorinated liquid solvents such as nonafluorobutyl methyl ether ($H_3C\text{-}O\text{-}C_4F_9$), dihydrodecafluoropentane ($F_2HC\text{-}CFH\text{-}C_3F_7$), and hexafluoroisopropanol ($CF_3CHOHCF_3$) [29]. High molecular weight PFA is remarkable in that it exhibits extremely high solubility in liquid or supercritical CO_2, as first reported nearly three decades ago [45]. To date, there have been no reports of PFA with a molecular weight so high that it is CO_2-insoluble.

The fluoroacrylate monomer, small concentration of initiator, and PFA product each exhibit sufficient solubility in liquid or supercritical CO_2 to allow the free radical solution polymerization of fluoroacrylate to form PFA in liquid or supercritical CO_2 [45, 46]. PFA can also be synthesized via solution polymerization of fluoroacrylate in fluorinated liquid solvents or via bulk polymerization [29, 46, 47].

PFA remains the most CO_2-soluble high molecular weight homopolymer that has been identified in the literature [48]. Solubility data at polymer concentrations up to 16 wt% PFA in CO_2 have been reported [42]. There are several other high molecular weight homopolymers that can dissolve in CO_2 at a concentration of at least several weight percent, such as polydimethylsiloxane (PDMS), poly(vinyl acetate) (PVAc), poly((1-O-(vinyloxy) ethyl-2,3,4,6-tetra-O-acetyl-β-D-glucopyranoside), amorphous poly(lactic acid) (PLA), and poly(methyl acrylate) (PMA). However, these non-fluorous polymers require significantly higher pressures to attain dissolution in pure CO_2 than PFA [49], and can only dissolve at similar pressures to PFA with the addition of an organic co-solvent (e.g. 25wt% toluene – 75wt% CO_2) [48-51].

DeSimone's group was the first to report that PFA increases the viscosity of CO_2 by a factor of 2-7 in dilute concentrations (3-7 wt %) [11]. The ability to form a single-phase, thermodynamically stable solution of a polymer of molecular weight sufficient to significantly impact the viscosity of the CO_2-rich solution is referred to as "CO_2 thickening" or "direct thickening". Direct thickening of CO_2 is distinct from the "indirect thickening" or "apparent thickening" of CO_2 via the generation of high apparent viscosity, thermodynamically unstable, high-pressure, two-phase, CO_2-in-water foams or emulsions [52-56], or completely waterless CO_2-in-oil foams and emulsions that have a high apparent viscosity [4].

Most of the subsequent interest in fluoroacrylate-based CO_2 direct thickeners was focused on a high molecular weight fluoroacrylate$_{71\ mol\%}$-styrene$_{29mol\%}$ random copolymer (polyFAST) that yielded much greater viscosity increases than the PFA homopolymer of comparable molecular weight due to intermolecular associations between the pendent aromatic groups in polyFAST [12, 57].

Chemical engineering interests in CO_2-PFA solutions have ranged from the formation of powders and fibers via the rapid expansion of PFA-CO_2 solutions through nozzles [43], to the use of PFA as a stabilizing dispersant during the dispersion polymerization of methyl methacrylate (MMA) in CO_2 [58]. Potential petroleum engineering applications have included in-depth CO_2 mobility control [57] and near-wellbore CO_2 conformance control during CO_2 EOR [29].

There have been numerous reports related to the phase behavior of CO_2-PFA mixtures, which are summarized in Table 1. The m and n values of PFA (Figure 1, Table 1) correspond to the PFA chemical formula $-[CH_2CHCOO(CH_2)_n(CF_2)_{m-1}CF_3]_k-$. The cloud point pressure along an isotherm has been observed to drop significantly with PFA concentrations below ~0.5wt%, however at greater PFA concentrations, the cloud point pressure is relatively flat. Temperature, PFA concentration, and cloud point pressure results from the relatively flat portions of the cloud point loci, typically in the 0.5 - 16 wt% PFA in CO_2 range, of previously published isothermal pressure-composition (P-x) diagram are presented in the last three columns on the right. Data from studies that reported cloud points for a single PFA concentration, always greater than 0.5% PFA in CO_2, are also presented in the last three columns.

Table 10: Summary of PFA-CO_2 phase behavior studies reported in the literature, and the results of this work. The last three columns on the right correspond to examples of Px data. The chemical formula of PFA is $[CH_2CHCOO(CH_2)_n(CF_2)_{m-1}CF_3]_z$

Reference	Mw /10^6	Mn /10^6	m,n	Tg °C	Tm °C	Am or SC	T range studied in paper °C	Complete PFA conc. range studied in paper wt%	T Value for flat portion of Px curve °C	PFA conc. range where the cloud point is flat wt%	Corresponding approximate cloud point pressure range MPa
Shin et al. [46]	-	-	8,2	-	-	-	27-97	0.94 - 9.27	30	0.94-9.27	8.18 - 10.24
									35	0.94-9.27	8.96 - 11.75
									40	0.94-9.27	10.34 - 13.61
									45	0.94-9.27	11.85 - 15.16
									50	0.94-9.27	13.39 - 16.68
									55	0.94-9.27	14.63 - 17.92
									60	0.94-9.27	16.16 - 19.40
									65	0.94-9.27	17.54 - 20.44
									70	0.94-9.27	18.64 - 21.99
									75	0.94-9.27	19.75 - 22.88
									80	0.94-9.27	20.99 - 24.16
									85	0.94-9.27	22.47 - 25.29
									90	0.94-9.27	23.50 - 26.41
Blasig, Shi, Enick and Thies [43]	0.25	0.086	8,2	-	78	SC	25-100	0.01 – 6.0	25	0.5 - 6.0	11 – 12
									50	0.5 - 6.0	19 - 21
									70	0.5 - 6.0	25 - 26
									100	0.5 - 6.0	33 – 34
Mawson, Johnston, Combes and DeSimone [44]	-	-	8*,2	-23	88	SC	24-70	0.087 - 7.32	24	1.5 - 7.3	11 – 12
									30	1.5 - 7.3	12 - 13
									35	1.5 - 7.3	14 - 15
									40	1.5 - 7.3	16 - 17
									50	1.5 - 7.3	19 - 20
									60	1.5 - 7.3	22 - 23
									70	1.5 - 7.3	24 – 25
McHugh, Garach-Domech, Park, Li, Barbu, Graham and Tsibouklis [59]	-	-	8*,2	-	-	-	25-70	4	25	4	11.5
									30	4	13.5
									35	4	15.0
									40	4	17.0
									50	4	20.0
									60	4	23.0
									70	4	25.0
Luna-Bárcenas, Mawson, Takishima, DeSimone, Sanchez and Johnston [42]	1.2	-	7,1	-	-	Am ***	30-80	0.01 -16.0	30	0.5 – 16	12 – 14
									40	0.5 - 16	16 - 18
									50	0.5 - 16	19 - 21
									60	0.5 - 16	22 - 24
									70	0.5 - 16	25 - 26
									80	0.5 – 16	28 – 29

Table 10 (continued).

Hsiao, Maury, DeSimone, Mawson and Johnston [60]	1.0	-	7,1	-	-	-	25- 80	0.1 - 5.0	30	0.5 - 5.0	12 – 14
									40	0.5 - 5.0	16 - 18
									50	0.5 - 5.0	19 - 21
									55	0.5 - 5.0	21 - 22
									60	0.5 - 5.0	22 - 24
									65	0.5 - 5.0	23 - 25
									70	0.5 - 5.0	25 - 26
									80	0.5 - 5.0	27 – 29
McHugh, Garach-Domech, Park, Li, Barbu, Graham and Tsibouklis [59]	-	-	7,1	-	-	-	25-80	4	25	4	11.5
									30	4	13.5
									35	4	15.0
									40	4	17.0
									50	4	20.5
									60	4	24.0
									70	4	26.5
									80	4	29.0
Zaberi, Lee, Enick, Beckman, Cummings, Dailey and Vasilache [29]	0.60	0.25	6,2	6.0	No	Am	24	1 – 8	24	1 – 8	10
This work C_6F_{13} PFA3	0.201	0.0098	6,2	-9.9	No	Am	25-125	1 – 4	25	1 – 4	10
									50	1 - 4	19
									75	1 - 4	25 - 26
									100	1 - 4	32 - 33
									125	1 – 4	36 – 37
This work C_6F_{13} PFA1	1.25	0.061	6,2	-4.1	No	Am	25-125	1 – 4	25	1 – 4	10
									50	1 - 4	19
									75	1 - 4	26 - 27
									100	1 - 4	33 - 34
									125	1 – 4	37 – 38
This work C_6F_{13} PFA2	2.89**	0.31**	6,2	-2.8	No	Am	25	1 - 4	25	1 – 4	CO_2-insoluble to 70 MPa
This work C_4F_9 PFA1	0.823	0.039	4,2	-23.8	No	Am	25- 125	1 - 4	25	1 – 4	10
									50	1 - 4	19
									75	1 - 4	26 - 27
									100	1 - 4	33 - 34
									125	1 – 4	37 – 38
This work C_4F_9 PFA3	1.831	0.213	4,2	-23.1	no	Am	25-125	1 - 4	25	1 – 4	11
									50	1 - 4	20
									75	1 - 4	27
									100	1 – 4	33-34
									125	3 – 4	37-38

*Am = amorphous; SC = semi-crystalline; *Corresponding authors confirmed that there are errors in the PFA molecular drawings in these papers (with each having one extra CF_2 group), the names of the monomers and polymers in both papers are correct and the values of m reported in this table are based on the monomer names. **Some of the polymer remained undissolved in the solvent used for molecular weight analysis; the true molecular weight is suspected to be higher than 2.1 E6. *** Although DSC results were not provided in the paper, the PFA was described as amorphous.*

PFA is semi-crystalline when there are eight fluorinated carbons or more in the repeat unit, while PFAs based on monomers containing six or seven fluorinated carbons are amorphous. The glass transition temperature (T_g) of PFA is relatively low, -23 °C to 6.0 °C, depending upon structure. The weight-average molecular weight of PFA, (which is infrequently reported due to the paucity of analytical tools designed to operate with fluorinated solvents and fluoropolymer solutions) usually falls in the 100,000 – 1,200,000 range. Both the weight average and number average molecular weights have only been reported in several papers by our team [29, 43].

These literature results indicate that PFA is at least several wt% soluble in high-pressure CO_2 at pressures below 40 MPa at temperatures up to 100 °C. The solubility of PFA in CO_2 is not strongly affected by the number of fluorinated carbons for monomers containing 6-8 fluorocarbons or the number of methylene spacers (1 or 2). The phase behavior data that has been reported for the PFA-CO_2 mixture is cloud point data in the 0.5 – 16 wt% PFA concentration range for an isothermal pressure-composition, or P-x, diagram. The cloud point pressure curves often exhibit very little curvature at concentrations above ~0.5wt% PFA. A maximum in cloud point pressure along an isotherm is typically exhibited in the 1 - 8 wt% range [42-44, 46, 60]. As a result, some investigators select a single PFA concentration, such as 4 wt% [59] or 5 wt% [46], for PFA-in-CO_2 solubility studies rather than reporting P-x curves over a wider range of PFA concentration.

Although complete pressure-compositions diagrams have been presented for mixtures of CO_2 and small CO_2-philic compounds [61], none of the studies listed in Table 1 presented a complete P-x diagram (mixtures from 100% PFA to 100% CO_2) for the CO_2-PFA pseudo-binary mixture.

The cloud point locus of a PFA-CO_2 mixture increases very slightly with substantial increases in PFA molecular weight for the complete range of molecular weights that have been reported to date [42-44, 46]. The cloud point of PFA over the 1 - 10 wt% PFA concentration range at ~20 °C, 50 °C and 100 °C is roughly 100 bar, 200 bar and 330 bar, respectively [42-44]. No reports of the phase behavior of ultra-high molecular weight PFA in CO_2 (2-10 million Da) have been previously reported.

Table 1 shows that there have been four reports related to PFA with eight fluorinated carbons in the sidechain [43, 44, 46, 59], and three reports involving PFA with seven fluorocarbons in the monomer [42, 59, 60]. There is one report [29] involving PFA synthesized from a fluoroacrylate containing six fluorinated carbons. There have been no prior reports of PFA solubility in CO_2 based on four fluorinated carbons in the monomeric unit.

The Statistical Associating Fluid Theory (SAFT) has been used to correlate the cloud point pressures of PFA; this model yielded very modest changes in the cloud point pressure for PFA molecular weights of 100,000 and 1,000,000 [42].

Regarding the viscosity of PFA-CO_2 solutions, the first report of CO_2 thickening induced by PFA was reported by DeSimone’s group [11], which showed that 4-8 wt% PFA in CO_2 could induce 1.5 - 7.2-fold increases in solution viscosity, Table 2. Thereafter, several papers have been published reporting the viscosity of PFA-CO_2 solutions. For example, a dilute solution of PFA in CO_2 ($PFA_{1\%}$-CO_2) was assessed for mobility control during a lab-scale CO_2 enhanced oil recovery project [47]. Falling ball viscometer results indicated that this solution was about 3.8 times more viscous than pure CO_2 under the same conditions, while capillary viscometry of the same solution indicated that the solution was ~3.5 times as viscous as neat CO_2 at very low shear rates. The following table provides examples of PFA-CO_2 solution viscosity results found in the literature; in all cases viscosity was measured at pressures greater than the cloud point pressure of the solution at the temperature and pressure of interest to ensure that the solution remained in the single phase.

Table 11: Summary of PFA-CO_2 falling cylinder viscosity studies reported in the literature, and the results of this work

Reference	Mw ($x10^6$)	Mn ($x10^6$)	m, n	T range for PFA-CO_2 viscosity °C	PFA conc. range for CO_2 viscosity wt%	Example conditions				Relative viscosity $\mu_{(PFA-CO2)}/\mu_{CO2}$ at same T,P
						PFA conc wt%	T °C	P MPa	Shear rate s^{-1}	
McClain et al. (1996)	1.4	-	7,1	50	3.4-6.7	4.1*	50	24.0	-	1.5
						3.8*	50	36.0	-	3.0
						8.1*	50	24.0	-	3.3
						7.4*	50	36.0	-	7.2
Huang et al. (2000)	-	-	8,2	25	3-5	3	25	34.5	-	8.5
						4	25	34.5	-	15.3
						5	25	34.5		17.7
Zaberi (2019)	0.60	0.25	6,2	25	1	1	25	20.7	1200	3.8
						1	25	20.7	3600	3.3
						1	25	20.7	6300	1.9
This work C_6F_{13} PFA1	1.3	0.061	6, 2	25	1-5	1	25	20.7	8460	1.59
						1	25	27.6	5306	2.03
						2	25	20.7	6820	1.98
						2	25	27.6	6426	1.77
						3	25	13.8	4850	2.71
						3	25	20.7	4840	2.79
						3	25	27.6	3910	2.90
						3	25	34.5	2130	3.67
						3	25	41.4	2040	4.12
						4	25	20.7	3460	3.90
						4	25	27.6	2470	4.61
						5	25	20.7	1638	8.23
						5	25	27.6	1460	7.76
This work C_4F_9 PFA1	0.823	0.039	4,2	25	1-4	1	25	13.8	12200	1.07
						1	25	20.7	9370	1.44
						1	25	27.6	7200	1.58
						1	25	34.5	5500	1.41
						1	25	41.4	5100	1.65
						2	25	13.8	6900	1.91
						2	25	20.7	5100	2.65
						2	25	27.6	3400	3.34
						2	25	34.5	2300	3.42
						2	25	41.4	2300	3.65
						3	25	13.8	8350	1.57
						3	25	20.7	4780	2.82
						3	25	27.6	3140	3.62
						3	25	34.5	2210	3.53
						3	25	41.4	2660	3.17
						4	25	13.8	4630	2.84
						4	25	20.7	3200	4.21
						4	25	27.6	3222	5.40
						4	25	41.4	1340	6.25
						4	25	27.6	5169	3.97
						4	25	27.6	7118	1.20

Table 11 (continued).

This work C_4F_9 PFA3	1.831	0.213	4,2	25	4	2	25	13.8	3050	4.3
						2	25	20.7	2120	6.4
						2	25	27.6	1740	6.5
						2	25	34.5	1020	7.6
						2	25	41.4	780	10.8
						3	25	13.8	1380	9.51
						3	25	20.7	1040	13.0
						3	25	27.6	800	14.3
						3	25	34.5	630	12.3
						3	25	41.4	490	17.2
						4	25	13.8	1060	12.4
						4	25	20.7	555	24.3
						4	25	27.6	409	27.8
						4	25	34.5	321	24.3
						4	25	41.4	270	31.2
						4	50	27.6	1070	10.7
						4	50	34.5	580	17.5
						4	50	41.4	500	17.4
						4	75	34.5	1010	8.73
						4	75	41.4	630	8.90

*these wt% values were estimated based on the density of pure CO2 combined with the wt/v % values of 3.4 and 6.7 reported in (McClain et al, 1996)

Relative to neat CO_2 at the same conditions, the degree of CO_2-thickening can be represented by relative viscosity values greater than unity (relative viscosity is the ratio of the viscosity of the PFA-CO_2 solution to the viscosity of neat CO_2 at the same temperature and pressure). As shown in Table 2, relative viscosity values ranging from 1.2 to 7.2 have been reported in prior studies at PFA concentrations ranging from 1 – 7.4%. Therefore, PFA does *not* induce the several order-of-magnitude increases in viscosity at dilute concentrations, such as those observed using small, associating molecules (e.g. crosslinked phosphate esters, tributyltin fluoride) in liquid propane or hexane [10]. PFA-CO_2 solutions are shown to be shear-thinning in the few studies where the effects of shear rate are included [29, 57]. The efficacy of PFA as a thickener increases with increasing pressure, with this increase becoming less dramatic at very high-pressures [11]. This can be attributed to the increasing solvent strength of CO_2 with increasing CO_2 density as increased pressure in the single-phase region led to increases in CO_2 density that can cause the PFA coil to swell and become a more effective thickener.

All prior investigations of PFA-CO_2 solutions, Tables 1 and 2, were conducted with PFA that was based on a fluoroacrylate monomer with 6 to 8 fluorinated carbons (m = 6, 7 or 8). There have been no prior reports of C_4F_9-based PFA solutions in liquid or supercritical CO_2. At the present time, C_8F_{17}-based fluoroacrylates are not in use, C_6F_{13}-based fluoroacrylates dominate the fluoroacrylate co-polymer market, and C_4F_9-based fluoroacrylate monomers are not currently used in commercial products but are available for lab-scale studies [62].

C_4F_9-based fluoroacrylate monomers provide a distinct environmental and health advantage relative to the C_8F_{17}-based fluoroacrylate. Most living organisms cannot readily metabolize nor eliminate perfluoroacid ultimate degradation products of C_8F_{17}-based PFA that form when the polymer is subject to hydrolysis and subsequent oxidation. This results in prolonged elimination half-lives for perfluorooctanoic acid (PFOA). The data is sparse on the direct adverse effects of C_8F_{17} acids on humans, but various kinds of liver, endocrine, and neonatal disorders have been linked to PFOA accumulation in animal studies [63, 64]. The effect of using fluoroacrylate monomers with shorter fluoroalkyl segments is pronounced. The perfluoroacid ultimate degradation products of C_4F_9-based and C_6F_{13}-based PFA are comparable, and both are distinctly safer than the ultimate degradation product of the C_8F_{17}-based PFA. Consider the following table, which contains the acid degradation products associated with various types of PFA, namely perfluorooctanoic acid (PFOA), perfluorohexanoic acid (PFHxA) and perfluorobutanoic acid (PFBA). PFOA, PFHxA and PFBA have metabolic half-lives of 1000-8000 days, 14-49 days, and 3-5 days, in humans, respectively. Therefore, both C_4F_9- and C_6F_{13}-based PFA are considered to have short chain fluoroalkyl acidic degradation products with metabolic half-lives that are significantly less than that of the -C_8F_{17}-based PFA.

Table 12: Comparison of metabolic half-lives in perfluoroalkanoic acid (PFAA) illustrates the short metabolic half-lives of -C_4F_9-based and -C_6F_{13}-based PFAA degradation products PFBA and PFHxA, respectively, relative to the long metabolic half-lives of -C_8F_{17}-

Number of fluorinated carbons	PFAA Chemical	Humans: Metabolic half life (days)	Non-human Primates/monkeys: Metabolic half life (days)	Rats: Metabolic half life (days)	Reference
7	PFOA	~3000	20.1 - 32.6	-	Agency for Toxic Substances and Disease Registry [65] Review
7	PFOA	1000	14 - 42	0.13 - 5.0	Gannon, Johnson, Nabb, Serex, Buck and Loveless [66] review
5	PFHxA	14 - 49	0.083 - 0.21	-	Russell, Nilsson and Buck [67]
5	PFHxA	-	1	0.05 - 0.2	Gannon, Johnson, Nabb, Serex, Buck and Loveless [66] review
5	PFHxA	5.1	2.1	0.1 - 0.6	Luz, Anderson, Goodrum and Durda [68]
3	PFBA	3.0	1.68 - 1.71	0.04 - 0.4	Agency for Toxic Substances and Disease Registry [65] Review
3	PFBA	3 - 4	2	0.3	Gannon, Johnson, Nabb, Serex, Buck and Loveless [66] Review

The main objectives of this work are to establish the CO_2-solubility and CO_2-thickening capability of C_6F_{13}-based PFA, and to then compare these properties to those of C_4F_9-based PFA. Both C_6F_{13}-based and C_4F_9-based PFA degradation products are perfluorinated acids, PFHxA and PFBA respectively, that have significantly safer toxicological properties than those associated with PFOA, which is the degradation product of C_8F_{17}-based PFA. There have been no prior phase behavior or viscosity reports related to solutions of a C_4F_9-based PFA in CO_2, while there has been only one prior report at 25 °C related to the phase behavior and viscosity of a single sample of C_6F_{13}-based PFA in CO_2 [29].

2.1 Materials and Methods

2.1.1 Materials

Cylinders of liquid CO_2 with an eductor tube (99.9% CO_2, bone dry) were obtained from Matheson and used as received.

Cylinders of N_2 (99.9% N_2) were obtained from Matheson and used as received.

C_4F_9-based fluoroacrylate monomer (2-(perfluorobutyl)ethyl acrylate, 1H,1H,2H,2H nonafluorohexyl acrylate, 98%, Mw 318.14, 4-tert-butylcatechol (TBC) inhibitor) was obtained from TCI and passed through an inhibitor removal column prior to use.

C_6F_{13}-based fluoroacrylate monomer (2-(perfluorohexyl)ethyl acrylate, or 1H,1H,2H,2H tridecafluorooctyl acrylate, 99+%, Mw 418.15, b.p. 65 °C at 20 mm Hg, monomethyl ether hydroquinone (MEHQ) inhibitor) was obtained from Daikin America, Inc. and passed through an inhibitor removal column prior to use.

TBC and MEHQ inhibitor removal columns were obtained from Sigma Aldrich and used as received.

re-crystallized azobisisobutyronitrile (AIBN) initiator, was obtained from Sigma Aldrich and used as received in its re-crystallized state.

Hydromethoxynonafluorobutane ($C_4F_9OCH_3$), 3M™ Novec™ 7100 Engineered Fluid, was obtained from Sigma Aldrich and used as received.

Certified ACS methanol (99.8%) was obtained from Fisher Scientific and used as received.

2.1.2 Synthesis of PFA

The synthesis of the C_6F_{13}-based fluoroacrylate homopolymer is carried out via bulk polymerization using AIBN as an initiator in a manner previously described in great detail [29]. Different ratios of AIBN:monomer were used; a lower molecular weight PFA is typically obtained using a higher molar ratio of AIBN to monomer. The same procedure is followed for the C_4F_9-based fluoroacrylate monomer.

2.1.3 Characterization of PFA Samples

T_g values for PFA were measured using a Perkin Elmer Pyris 6 Differential Scanning Calorimeter. Mw and Mn was determined using Gel Permeation Chromatography (GPC) with hexafluoroisopropanol (HFIP) as the continuous phase. The polymer solubility in high-pressure CO_2 is determined via the previously detailed non-sampling procedure [10-12, 29, 44, 49, 50] that involves the slow, isothermal expansion of a transparent, colorless, high-pressure, single-phase solution of known composition until small droplets of PFA-rich liquid appear, causing the mixture to become cloudy. The pressure at this point was considered to be the cloud point. The cloud point was determined 5 times and the average value reported. All five measurements were within 0.5 MPa of the average value. The viscosity of the PFA-CO_2 solutions is determined using a previously aluminum cylinder viscometer, which has been previously presented in great detail [10, 12, 29, 57, 69]. The use of a falling cylinder allows one to estimate the single shear rate associated with the falling object [10, 70], as opposed to a falling ball that experiences a broad shear rate range [69].

Viscosity can be determined using the following expression

$$\mu = \frac{K*(\rho_c - \rho_l)}{Vc_t} \qquad \text{2-1}$$

μ is viscosity (mPa s), ρ_c is the object density (2.7 g/cm^3 for aluminum), ρ_l is fluid density (g/cm^3), Vc_t is cylinder terminal velocity (cm/s), and K is the characteristic constant for the viscometer (mPa cm^4 g^{-1}). There is an analytic solution for K for the falling cylinder case [29], however this theoretical value of K is extremely sensitive to tiny variations in the cylinder diameter and/or tube diameter. Therefore, the value of K for a close-clearance falling cylinder viscometer is usually determined by calibrating the apparatus with pure CO_2.

The shear rate for a Newtonian fluid along the cylindrical surface of a cylinder falling can only be calculated with a knowledge of the experimentally determined terminal velocity, Vc_t, as

$$\frac{dVz}{dr}\Big|_{r=rc} = Vc_t\left[\frac{-2r_c - (r_t{}^2 - r_c{}^2)\dfrac{1}{r_c \ln\left(\frac{r_c}{r_t}\right)}}{\ln\left(\frac{r_c}{r_t}\right)(r_t{}^2 + r_c{}^2) + (r_t{}^2 - r_c{}^2)} + \frac{1}{r_c \ln\left(\frac{r_c}{r_t}\right)}\right] \qquad \text{2-2}$$

where r_c is the cylinder diameter (cm) and r_t is the Pyrex tube inner diameter (cm).

Viscosity experiments were repeated 5 times, and the average value of relative viscosity (the ratio of viscosity of the PFA-CO_2 solution to the viscosity of CO_2 at the same temperature and pressure) is reported. All relative viscosity measurements were with 10% of the average value.

2.2 Results and Discussion

2.2.1 PFA Synthesis and Characterization

Tables 4 and 5 provide the glass transition temperature and molecular weight data for the four C_6F_{13}-based PFA samples and the two C_4F_9-based PFA samples, respectively. None of the PFA samples exhibited a melting point. Each PFA was amorphous, transparent, sticky, and elastic and characterized by a sub-ambient T_g.

The bulk polymerization method led to PFA exhibiting a broad temperature range between the onset T_g and midpoint T_g, and a high polydispersity index (PDI) value. This is probably the result of significant mass transfer resistances occurring during the polymerization, namely the monomer-PFA solutions becoming quite viscous during the 12-hour polymerization. PFA molecular weight increased with decreasing AIBN concentration.

Table 13: Four bulk-polymerized C_6F_{13}-based PFA samples

PFA #	Onset T_g (°C)	Midpoint T_g (°C)	Wt% AIBN	Mn (kDa)	Mw (kDa)	PDI
C_6F_{13} PFA3	-28.14	-9.90	0.010	9.82	201	20.5
C_6F_{13} PFA4	-21.58	-4.36	0.005	24.0	347	14.5
C_6F_{13} PFA1	-24.39	-4.14	0.002	61.7	1250	20.3
C_6F_{13} PFA2	-23.03	-2.79	0.001	313	2890	9.25

Table 14: Two bulk-polymerization C_4F_9-based PFA samples

PFA #	Onset Tg (°C)	Midpoint T_g (°C)	wt% AIBN	Mn (kDa)	Mw (kDa)	PDI
C_4F_9 PFA1	-31.3	-23.8	0.011	38.9	823	21.2
C_4F_9 PFA3	-32.4	-23.1	0.003	213	1831	8.59

2.2.2 Phase Behavior

The highest molecular weight C_6F_{13}-based PFA sample that was synthesized in this study, (C_6F_{13} PFA2, Mw 2.89 E6, Mn 3.13 E5, PDI 9.25), represents the highest molecular weight PFA that has yet been reported in the literature, Table 1. This PFA remained insoluble in CO_2 at 25 °C and pressures as high as to 62 MPa. Despite prolonged mixing (2 hr) at these conditions, it appeared that none of the transparent PFA sample has dissolved or even softened. This is the first report of a CO_2-insoluible PFA at 25 °C and pressures to 62 MPa, indicating that the unfavorable entropic effects of the extremely high molecular weight polymer can render the PFA CO_2-insoluble despite the highly favorable enthalpic interactions of the fluoroacrylate moiety and CO_2.

Figure 2 presents pressure-composition (Px) diagrams for CO_2 combined with either C_6F_{13} PFA1, C_6F_{13} PFA3, C_4F_9 PFA1, or C_4F_9 PFA3; these cloud point data are also listed in Table 1. These represent the lowest and highest molecular weight CO_2-soluble C_6F_{13}-based PFA samples, respectively, synthesized in this study. To the best of our knowledge, as shown in Table 1, this is the first time that the CO_2-solubility values of two PFA samples with the same monomeric unit but significantly different molecular weight have been experimentally compared in the same study. Similarly, as shown in Table 1, this is the first time that the CO_2-solubility of PFA homopolymers based on different monomeric units have been contrasted in the same study.

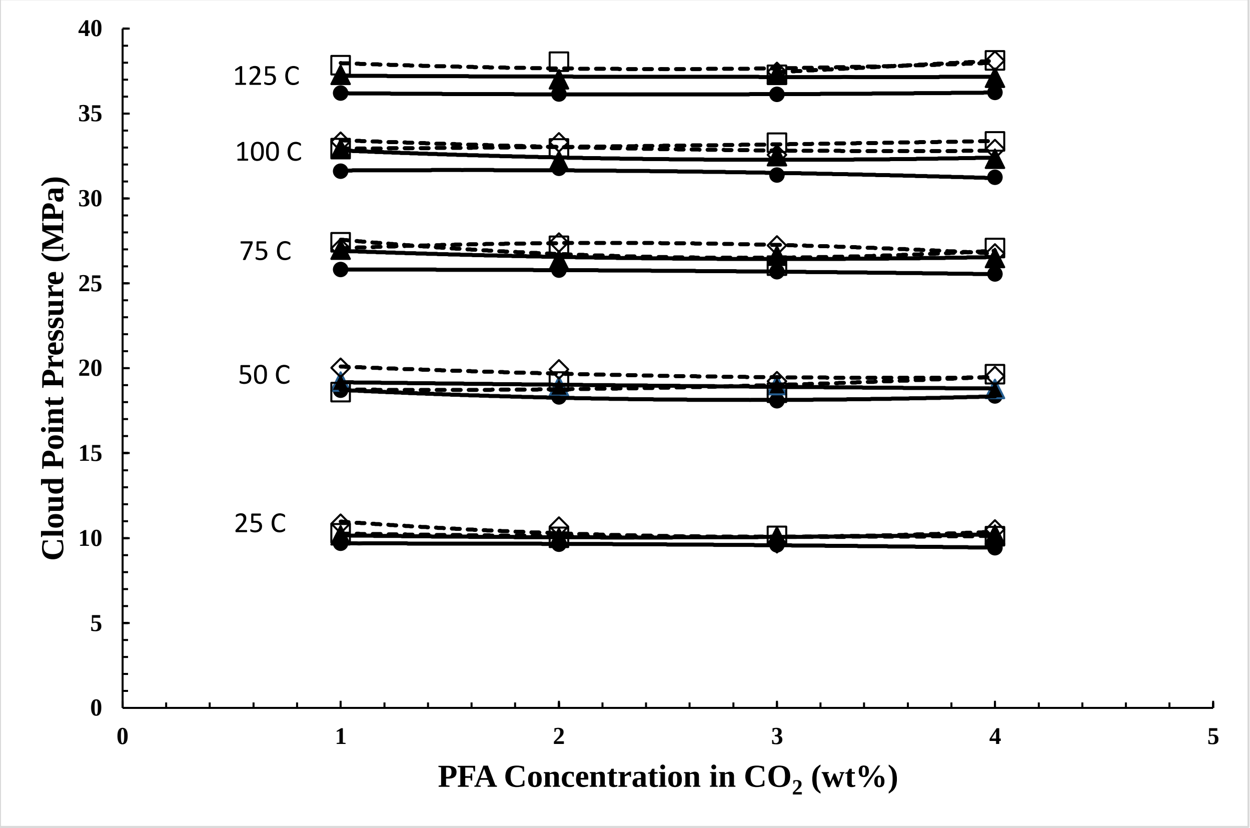

Figure 3: Cloud point data for mixtures of CO_2 and C_6F_{13} PFA1 (Mw 1.25 E6, filled circles), CO_2 and C_6F_{13} PFA3 (Mw 2.01 E5, filled triangles), CO_2 and C_4F_9 PFA1 (Mw 8.23 E5, open squares), CO_2 and C_4F_9 PFA3 (Mw 1.83 E6, open diamonds)

All four PFA samples were soluble in CO_2, exhibiting flat cloud point curves in the 1 – 4 wt% PFA range that increased with temperature in the 25 – 125 °C range. The cloud point pressures measured at 25, 50, 75 and 100 °C are consistent with previously reported cloud point data, in the literature, regardless of the number of fluorinated carbons in the monomer used in the prior studies, as summarized in Table 1. There is no discernible effect of PFA molecular weight on the cloud point pressure for either the C_4F_9-based PFA (M_w of 8.23E5 and 1.83 E6) or the C_6F_{13}-based PFA (M_w 2.01 E5 and 1.25 E6). However, in the 50 – 125 °C range, it appears that the C_4F_9-based PFA cloud point curves are slightly higher than those of the C_6F_{13}-based PFA. This infers that the C_4F_9-based PFA may be very slightly less soluble in CO_2 than the C_6F_{13}-based PFA, but this is a very modest difference of less than 1 MPa. In general, these results are favorable for those who may consider using either C_4F_9- or C_6F_{13}-based PFA in a process involving CO_2; the CO_2-solubility of PFA is very comparable, whether one uses a C_4F_9-based, C_6F_{13}-based, or C_8F_{17}-based fluoroacrylate monomer, as long as the average molecular weight (M_w) of the PFA is less than ~ 2 E6.

2.2.3 Relative Viscosity

As expected, increasing concentrations of PFA lead to an increase in solution viscosity. Consider Figure 3, which shows the effect of increasing C_6F_{13} PFA1 concentration on the CO_2-rich solution viscosity at 25 °C and 20.7 MPa (3000 psi), up to 5 wt%. These relative viscosity data are also presented in Table 2 along with the corresponding shear rate for each experiment. In all cases, the CO_2-PFA solution was in the single phase region.

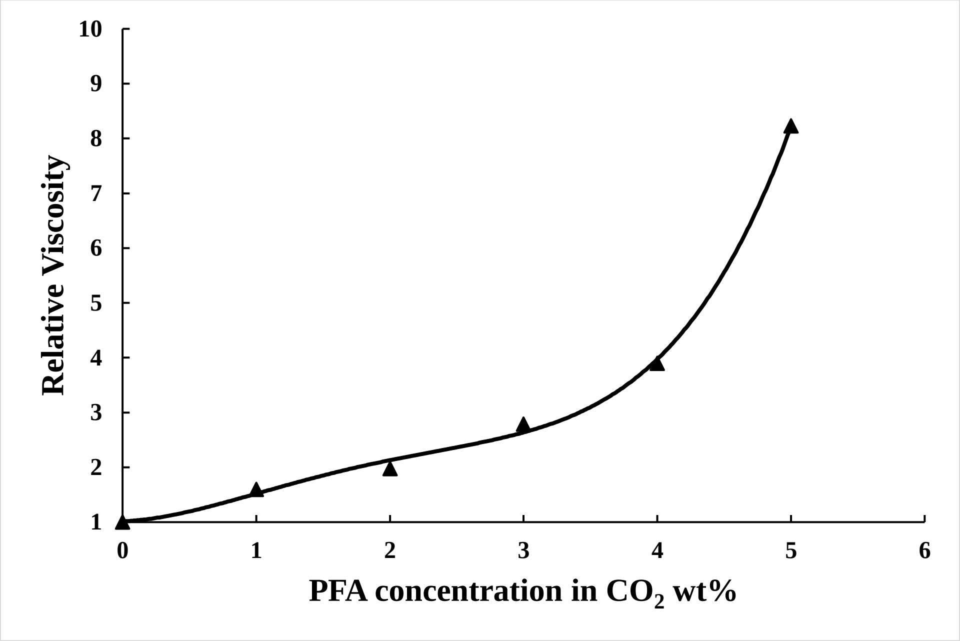

Figure 4: Relative viscosity results for CO_2-C_6F_{13} PFA1 (Mw 1.25E6) solutions as a function of PFA concentration at 25° C and 20.7 MPa

Increasing concentrations of the C_4F_9 PFA1 polymer also resulted in an increase of solutions viscosity, as shown in Figure 3 and Table 2. Further, as shown in Figure 4 and Table 2, the higher molecular weight sample of C_4F_9-based PFA provided a significantly greater thickening effect (at the same mass concentration in CO_2) as the lower molecular weight analog.

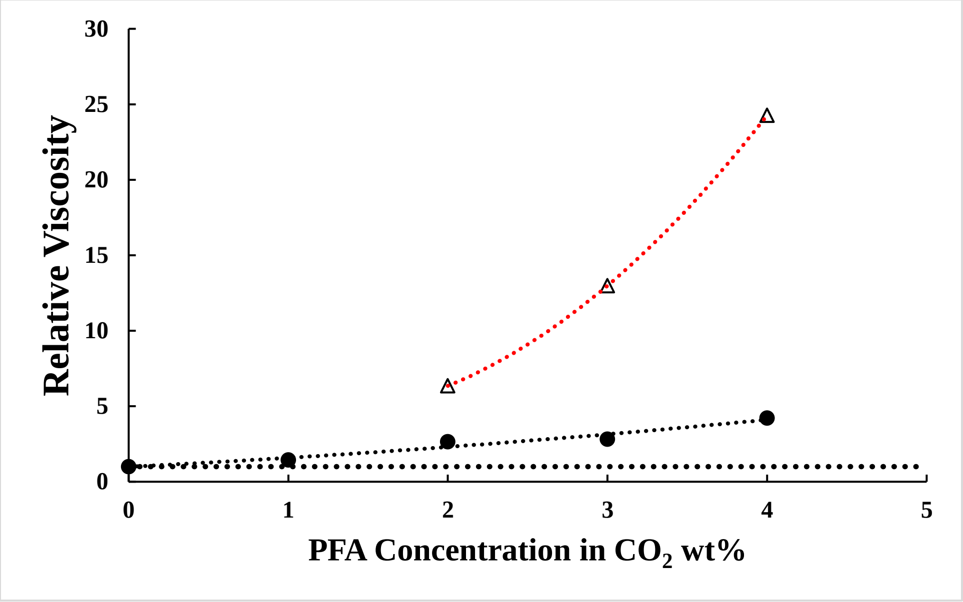

Figure 5: Relative viscosity results for CO_2-C_4F_9 PFA1 (Mw 8.23 E5) (filled circles, black dashed curve) and CO_2-C_4F9 PFA3 (Mw 1.83 E6) (open triangles, red dashed curve) solutions as a function of PFA concentration at 25 °C and 20.7 MPa.

As the temperature of a C_4F_9-based PFA-CO_2 solution was increased from 25 °C to 75 °C at constant pressure, which was maintained at a value (34.48 MPa or 41.38 MPa) great enough to ensure a single-phase solution, the ability of PFA to thicken CO_2 was diminished, Figure 5 and Table 2. Viscosity typically scales with temperature exponentially, so this linear decrease in log(viscosity) with increasing temperature was expected.

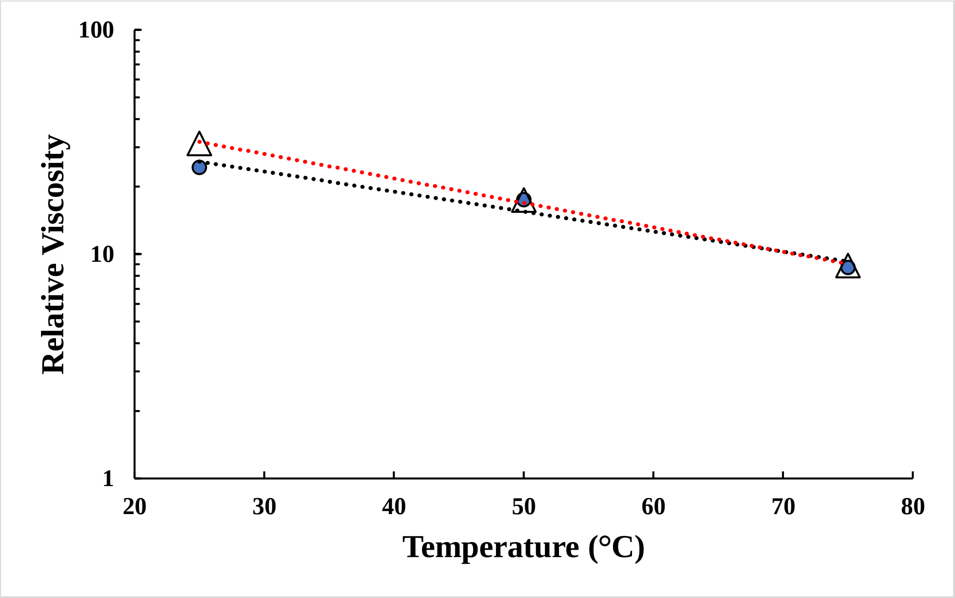

Figure 6: Effect of temperature on viscosity of C_4F_9 PFA3 – CO_2 solutions as a function of temperature at 41.40 MPa and 34.48 MPa. Filled circle with black dotted linear fit (R^2=0.955) data at 34.48 MPa, open triangles with red dotted linear fit (R^2=0.998) data

Increasing pressure for a C_4F_9-based PFA also led to increases in solution viscosity, as shown for a 3 wt% C_4F_9 PFA1 in CO_2 solution, Figure 6 and Table 2. This is probably due to the CO_2 gaining solvent strength with increasing pressure, which increases CO_2 density (e.g. pure CO_2 density is 0.865 and 1.009 g/ml at 25 °C and 13.8 MPa and 41.4 MPa, respectively)[71]. The increased solvent strength of CO_2 would cause the PFA polymer coils to swell to a greater degree, leading to an increase in solution viscosity. Similar pressure-induced effects were observed for the CO_2-C_6F_{13} PFA1 solutions as a function of pressure at 25 °C and 3 wt% C_6F_{13} PFA1, as shown in Table 2.

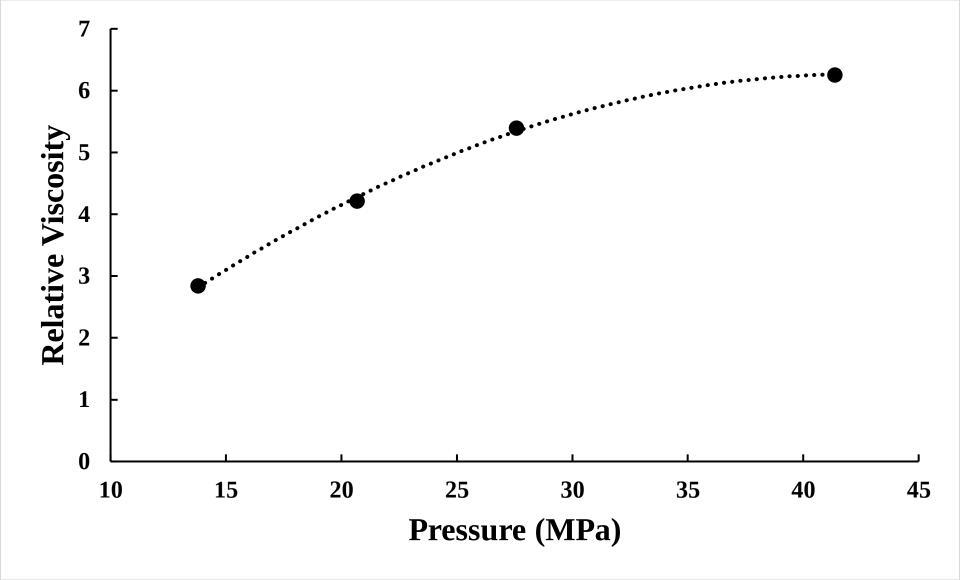

Figure 7: Relative viscosity results for CO_2-C_4F_9 PFA1 solutions as a function of pressure at 25 °C and 3 wt% C_4F_9 PFA1

The effect of shear rate on solution viscosity for the 96 wt% CO_2 – 4wt% C_4F_9 PFA1 sample at 25 °C and 27.6 MPa was assessed using three aluminum cylinders, each having a slightly different diameter (3.10083, 3.13690, and 3.16179 cm). The results are shown in Figure 7 and Table 2.

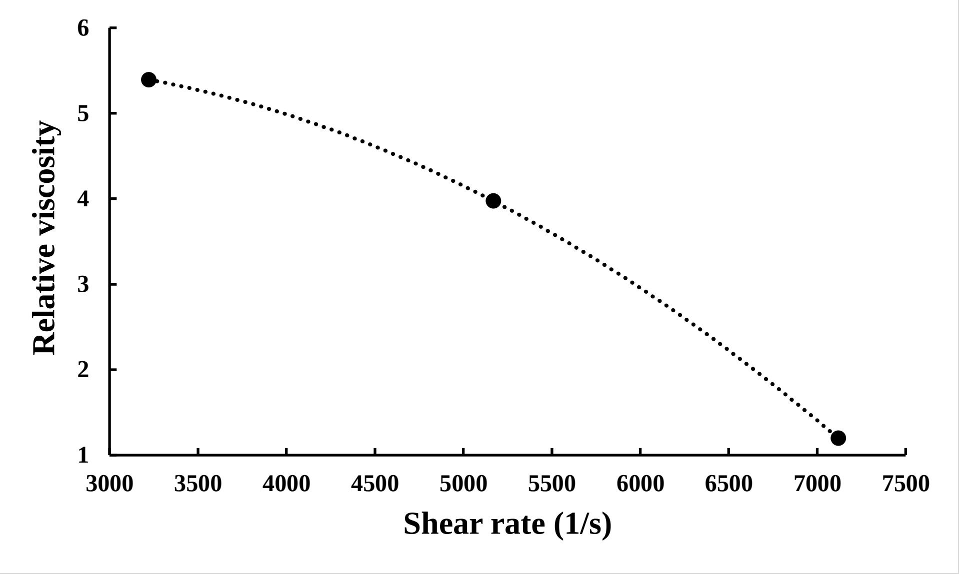

Figure 8: Relative viscosity results for CO_2-C_4F_9 PFA1 solutions as a function of shear rate at 25 °C, 4wt% C_4F_9 PFA1, and MPa

As expected, and in agreement with prior reports[29, 57], the solution is shear-thinning over this range of shear rate.

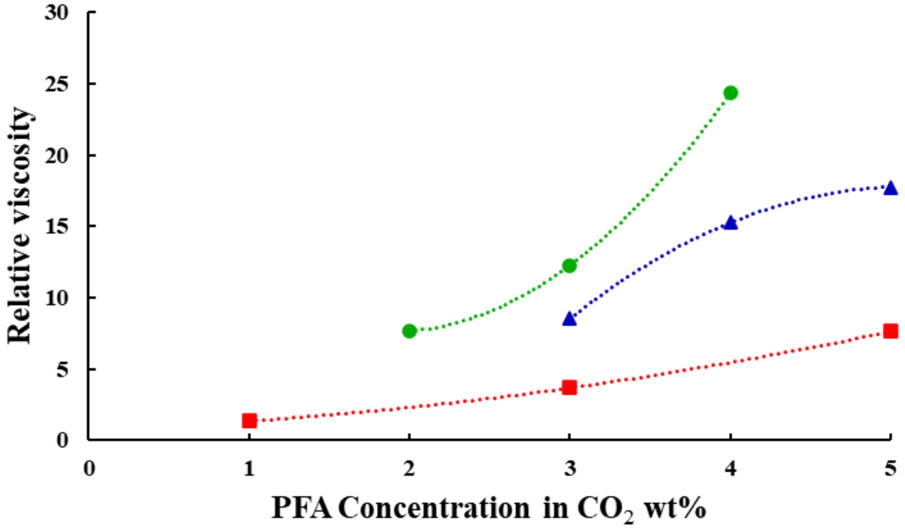

Figure 9: Comparison of relative viscosities of C_4F_9-based (green circles, M_w=1.81 E6, this work), C_6F_{13}-based (red squares, M_w=1.25E6 this work), and C_8F_{17}-based (blue triangles, Mw unknown, Huang et al., 2000) PFA in CO_2 solutions as a function of polymer concentration.

Figure 9 shows that the viscosity of C_4F_9-based and C_6F_{13}-based solutions of PFA in CO_2 are similar to each other and their C_8F_{17} analog. As expected, the higher molecular weight C_4F_9-based PFA solution displayed a greater viscosification effect than the -C_6F_{13} based PFA solution. The M_w of the C_8F_{17}-based PFA solution is unknown, but it is encouraging that it shows viscosification similar to the other samples.

2.3 Conclusions

The ultimate degradation product of C_8F_{17}-based PFA is PFOA, which is so bio-accumulative that the $CH_2CHCOO(CH_2)_2(CF_2)_7CF_3$ fluoroacrylate monomer is no longer used in commerce. It is also well known that PFA generated by the homopolymerization of $(CH_2CHCOO(CH_2)_2(CF_2)_7CF_3$ is remarkably CO_2-soluble. Because PFHxA and PFBA exhibit metabolic half-lives that are roughly two orders of magnitude less than that of PFOA, any PFA made from $CH_2CHCOO(CH_2)_2(CF_2)_5CF_3$ or $CH_2CHCOO(CH_2)_2(CF_2)_3CF_3$ will be far more benign than the homopolymers of $CH_2CHCOO(CH_2)_2(CF_2)_7CF_3$. However, prior to this study, there was only a single report of the CO_2-solubility and CO_2-thickening potential of the C_6F_{13}-based PFA, and no reports of a C_4F_9-based PFA. Therefore, our goal was to polymerize several samples of C_6F_{13}-based PFA and C_4F_9-based PFA, characterize the PFA, determine the CO_2-solubility of the PFA in terms of cloud point loci ai the 25 – 125 °C temperature range, and assess the CO_2-thickening capability of the PFA in terms of the ratio of the viscosity of a PFA-CO_2 solution to the viscosity of CO_2 at the same conditions. Further, the influences of PFA monomer type, concentration (wt%), pressure, temperature, and shear rate on PFA-CO_2 solution viscosity were determined.

Four samples of C_6F_{13}-based PFA (M_w of 2.01E5, 3.47E5, 1.25E6, and 2.89E6) were synthesized via bulk polymerization. Each C_6F_{13}-based PFA was amorphous, with a very low midpoint T_g that fell in the -10 to -3 °C range. Two samples of C_4F_9-based PFA (Mw of 823000, and 1821000) were also synthesized. Both were amorphous, with even lower midpoint glass transition temperatures of -24 and -23 °C, respectively.

One PFA sample (a C_6F_{13}-based PFA, Mw 2.89E6) was the highest molecular weight PFA yet to be reported vis-à-vis solubility studies in CO_2. Further, this was the only PFA sample that was very difficult to dissolve in hexafluoroisoproanol (the solvent used for molecular weight analysis) and it could not be dissolved in CO_2 despite prolonged mixing at 25 °C and 62 MPa. This appears to be the first report of CO_2-insoluble PFA; apparently the unfavorable entropic effects of the extremely high PFA molecular weight were more significant than the favorable enthalpic effects associated with the intermolecular interactions between the CO_2 and fluoroacrylate repeat unit. Therefore, this particular PFA was not used in any CO_2-solubility of CO_2-thickening study. It is recommended that future studies of PFA involved polymers with molecular weights of roughly 2E6 or less.

The cloud point pressure of the highest and lowest molecular weight samples of the C_6F_{13}- and C_4F_9-based PFA was determined in the 25 - 125 °C temperature range at PFA concentrations ranging between 1-4 wt% in CO_2. In general, the cloud point curves were not only similar to one another, but also comparable to previously reported results for C_8F_{17}-based PFA. The cloud point curves were relatively flat, displayed an increase to higher pressures with increasing temperature, displayed little dependence on PFA molecular weight for either C_6F_{13} PFA or C_4F_9 PFA, but exhibited a very modest shift to higher pressure values for C_4F_9 PFA at temperatures at or above 50 °C.

The CO_2-thickening capability of the PFA was determined at single-phase conditions for PFA-CO_2 mixtures. The CO_2-thickening of the C_6F_{13}-based and C_4F_9-based PFA were comparable to one another and similar to that previously reported for C_8F_{17}-based PFA. The greatest relative viscosity measured in this study was a 31-fold increase in CO_2 viscosity for the highest Mw C_4F_9-based PFA (Mw 1.89 E6) at 4 wt% in CO_2 at 25 °C and 41.4 MPa. As expected for solutions of non-associating high molecular weight polymers in solution, the relative viscosity (solution viscosity/CO_2 viscosity at the same conditions) decreased with increasing temperature, increasing shear rate, decreasing pressure, decreasing PFA concentration, and decreasing PFA molecular weight for the same PFA mass concentration.

In conclusion, PFA generated from the C_6F_{13}-based fluoroacrylate ($CH_2CHCOO(CH_2)_2(CF_2)_5CF_3$) or the C_4F_9-based fluoroacrylate ($CH_2CHCOO(CH_2)_2(CF_2)_3CF_3$) exhibits about the same CO_2-solubility and CO_2-thickening capability as PFA made with the C_8F_{17}-based monomer ($CH_2CHCOO(CH_2)_2(CF_2)_7CF_3$). Because the ultimate degradation products of the C_6F_{13}-based and C_4F_9-based PFA (PFHxA and PFBA, respectively) have significantly shorter metabolic half-lives than the C_8F_{17}-based PFA ultimate degradation product (PFOA), it is strongly recommended that any future studies of PFA homopolymers or fluoroacrylate copolymers for use in CO_2 be conducted with the C_6F_{13}-based or C_4F_9-based fluoroacrylate monomer. Although this certainly will promote environmental safety and improved worker health, all fluoroacrylate monomers (regardless of the number of fluorinated carbons in the pendent group) are inherently expensive.

3.0 Equilibrium and Flow-Through Cement Sealing Using Solutions of C_6F_{13}-Based Polyfluoroacrylates in CO_2

3.1 Introduction

Questions regarding safety and wellbore integrity have long plagued the petroleum industry worldwide. There are both real and perceived environmental impacts related to the unintended leakage of natural gas and/or oil that need to be addressed, which can impact everything from public policy to real estate prices [72]. For example, claims of methane leaking into groundwater due to the hydraulic fracturing (i.e. “fracking”) of wells [73] to the micro-seismic events associated with the subterranean disposal of produced water from fracturing operations into aquifers [74] have led many opponents to voice their concerns related to fossil energy production, while proponents tout the advantages of domestic abundance and “cleaner than coal” energy [75]. Both sides would likely agree, however, that improvements in wellbore integrity would enhance the health and safety of workers and community members and better protect the environment.

Reliable sources of significant amounts of data related to wellbore integrity are not readily available or frequently published, and there is no industry standard on what constitutes a compromised or leaking well. Further, discrepancies between reports on wellbore integrity may be related to studies focusing on conditions where problems are less likely to be found (e.g. newer wells) or more likely to be found (e.g. very old wells). This can lead to differences in the average likelihood of wellbore integrity problems of an order of magnitude, as shown in a meta-analysis of wellbore integrity studies [76]. Even in the US alone, the frequency of wellbore integrity issues ranges from 1.9% to 75%. Not surprisingly, the 75% result was related to 50 wells in a field that was discovered in 1921 with the failure criterion being the observation of gas bubble seeping to the surface, while the lowest percentage of well integrity failure of 1.9 – 4.3% in five separate reports corresponded to 10,806 wells drilled after 2005.

With such disparate standards associated with wellbore failure, it is not surprising that there is no agreed-upon metric for wellbore integrity problems. To complicate matters, data on some newly completed wells may not be available, while many older and abandoned wells may remain unreported or un-assessed. Further, there may be no incentive for operators to publish accurate counts of their problematic wells with problems, regardless of how “problem” is defined. Therefore, only a rough order-of-magnitude appreciation of the number of actual wellbore integrity issues remains available. Although there is a great degree of uncertainty in how many wells have troublesome integrity problems, it is known that there are roughly two million wells in the US alone [77]. Even if only a very small fraction of these wells has wellbore integrity problems, a significant number of wellbores may need remediation.

A conceptual illustration of the common wellbore integrity problems is found in Figure 1, which is based on similar images and information found in two references [78, 79]

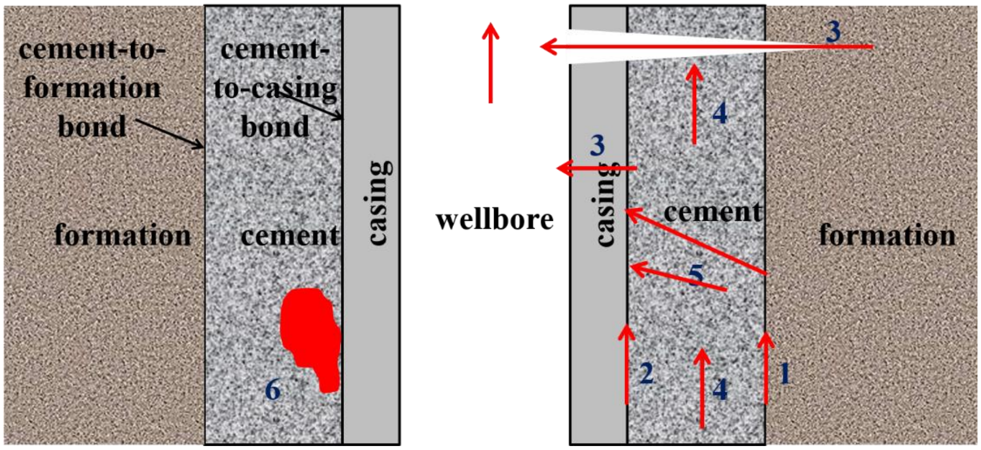

Figure 10: Cement Defects That Can Lead to Wellbore Integrity Issues. (1) Gaps between the formation and the cement; (2) the micro-annulus between the cement and outside of the casing; (3) fractures passing through the wall of the casing into the wellbore

3.1.1 Wellbore Integrity Remediation Techniques

3.1.1.1 Cement Squeeze

The most commonly used method of sealing wellbores, either for retirement or to fix breaches, is the cement pour or cement squeeze [79]. A cement squeeze is the most common remedial method used to restore wellbore integrity, especially for voids and cracks that are significant in size. Fresh cement has a density of roughly 1.9 g/ml and contains particles in the 1 – 100 micron size range [80]. The rheology of cement slurries is highly dependent on temperature, water/cement ratio and the type of admixture used, but in general they exhibit Bingham plastic viscosities of 10 – 100 mPa s at 23 ^{o}C [81-84]. Cement squeezes are well suited for large voids, but are unable to flow into micro-channels due to particle bridging and filter cake formation. A commonly used product is a Portland cement slurry, which is formulated by mixing 72.5% wt% Portland cement with 27.5 wt% water. It is a logical selection because the annular space between the outside of the wellbore tubing and the rock formation through which the well was drilled is initially filled with cement. It is an appropriate selection for filling large volumes due its compatibility with hardened cement in the annulus and its reasonable viscosity for pumping (hundreds of mPa s) when first prepared with water. Cement is also commonly used to close the annular or microannular fractures that often appear between the metal casing and the adjacent layer of cement. However, cement pours have difficulty flowing into cracks with gap widths of the same size or smaller than the particles in the slurry, with sizes ranging up to ~ 100 microns [80]

3.1.1.2 Resin Squeeze

The resin squeeze typically exhibits a viscosity of several hundred to several thousand mPa-s. Epoxies are generally low molecular weight monomers or oligomers that are reacted with hardeners or cross-linkers [85]. For example, the Halliburton product offered for wellbore integrity solutions, WellLock ®, is made of a mixture of epoxides and functional amines. Bisphenol A-based resins are commonly used in wellbore remediation [86]. Epoxy resins allow for the structural integrity of a solid adhesive with low viscosity injection liquids. Because epoxies in these settings are typically engineered on-site for each circumstance, the exact physical and rheological properties of a resin product can vary according to the needs of the wellbore integrity problem [87, 88]. This allows for injections of two liquid reactants, which are more viscous than cement pours but do not have any solid particles that may aggregate in microfractures. As a result, resin squeezes are often used in cracks that are too small or complex for a cement squeeze [86, 87]. The use of additives to increase the chemical or thermal resistance, physical properties, or bonding strength of epoxy resin is also practiced. For example, Genedy (2014) synthesized nanocomposites composed of the epoxy combined with materials such as nanoclay and carbon nanotubes have been used in conjunction with epoxy. It was noted, however, that it is challenging to maintain the low viscosity of the injection solutions while having introduced enough nanomaterial to improve the performance of the sealant.

3.1.1.3 Aqueous Emulsions of Polymerizing Hydrocarbons

A relatively new technology for sealing cracks is the use of an emulsion of hydrocarbon-based droplets that can polymerize and crosslink, such as the products from Seal-Tite. This formulation “activates” and solidifies in the presence of large pressure drops that occur at crack entrances. Although the composition of this is proprietary, the product literature makes it apparent that Seal-Tite is a 100-500 mPa s aqueous suspension of droplets containing monomers, oligomers, polymers, initiators and cross-linking agents [89-93]. Apparently, the emulsion droplets cannot enter small cracks, therefore they accumulate and congeal at the entrance to such cracks. Given the appropriate time, temperature and amount of these aggregated droplets, polymerization and crosslinking can occur that seals the crack entrance. This strategy is advantageous because the suspension can maintain a reasonably low viscosity of several hundred mPa s as it travels long distances, and then form the required solid seal only at the crack entrance. Once the crack entrance is sealed, the excess emulsion can be removed without damaging the polymerized, crosslinked barrier at the crack entrance. (In contrast, cement and epoxy products will completely harden everywhere that they remain.) Seal-Tite is not asserted to be effective for small cracks in cement that leak natural gas and do not necessarily have a large pressure drop, especially if the cracks are small and the well itself is deep.

3.1.1.4 The Novel High-Pressure Polyfluoroacrylate-CO_2 (PFA-CO_2) Solution Sealant

In this study, the fluid used to improve wellbore integrity is a single-phase, thermodynamically stable solution of a dilute concentration (~ several weight percent) of high molecular weight polyfluoroacrylate (Mw 1E5 – 2E6) dissolved in high-pressure CO_2. As shown in the previous section, PFA, including their ability to dissolve in CO_2 and thicken CO_2, are similar regardless of the length of the fluorocarbon segment in the monomer. However, the ultimate degradation products associated with the C_6F_{13} and C_4F_9-based PFA are more environmentally benign than PFA based on the fluoroacrylate monomer containing the C_8F_{17} segment [65-68] (Lemaire et al. 2021). In this study, the C_6F_{13}-based fluoroacrylate was used.

PFA has long been known to be highly CO_2-soluble at elevated pressure without the need for the introduction of a co-solvent such as toluene or hexanes [11]. Enick and co-workers [29, 47] initially assessed a dilute solution (1 wt%) of PFA in CO_2 ($PFA_{1\%}$-CO_2) as a mobility control fluid for CO_2 enhanced oil recovery (EOR). Because falling ball viscometer results indicated that this solution was almost four times as viscous as pure CO_2, it was expected that the pressure drop associated with displacing ($PFA_{1\%}$-CO_2) through these confined sandstone and carbonate cores would increase by a factor of four compared to pure CO_2. However, dramatic (e.g. 100 – 1000-fold) increases in pressure drop resulted, indicating that the permeability of the cores was being reduced by PFA adsorption and deposition of PFA across pore throats. A qualitative understanding of the fate of the PFA was realized in that some PFA adsorbed onto rock surfaces, some PFA formed bridges across pore throats, and some PFA passed through the core [29, 47], however, our team was not able to quantify the equilibrium adsorption of PFA on either sandstone or carbonate rock. Our prior study (Zaberi et al., 2020) concluded that these dramatic permeability reductions were highly undesirable for mobility control. However, it was shown that when PFA-CO_2 solutions were injected into mechanically isolated watered-out thief zones, the adsorption of PFA, and the resultant dramatic decreases in thief zone permeability, could improve near-wellbore conformance control.

In this study, we attempt to exploit the adsorption of PFA in another petroleum engineering application; the reduction of the apparent permeability, and possibly the complete closure, of cracks in cement for improved wellbore integrity. As shown in Table 1, the ($PFA_{1\%}$-CO_2) solution is several orders of magnitude less viscous than cement, resin or aqueous emulsions Therefore the ($PFA_{1\%}$-CO_2) solutions could more readily access and flow more deeply into the smallest cracks; the subsequent PFA adsorption and wettability alteration could greatly restrict the flow of gas, oil or brine through the cracks. In addition to adsorption, additional PFA could be deposited within the cracks if the PFA-CO_2 solution is not displaced from the crack by high-pressure CO_2 immediately prior to depressurization; in this case the reduction of pressure below the cloud point of the PFA-CO_2 solution (~10 MPa at 25 °C) would cause PFA to come out of solution and precipitate within the crack.

Table 15: Select Physical Properties of Wellbore Integrity Agents

Material	**Viscosity @ 25 C (mPa s)**	**Available solids free?**	**Reference**
Portland cement (72% solids)	100-200	No	Shahriar and Nehdi [94]
Epoxy resin precursors	500-5000	Yes	Perez, Melo, Blanc, Roncete and Jones [86]
Seal-Tite	100-500	Yes	Rusch and Romano [91]
1% C_6PFA in CO_2 @ 13.8 MPa	0.9-1.1	Yes	Zaberi, Lee, Enick, Beckman, Cummings, Dailey and Vasilache [29]

A PFA-CO_2 solution is intended to be another tool for wellbore integrity remediation; it is *not* intended to replace cement, epoxy resins or aqueous emulsions of polymerizing droplets. In fact, a PFA-CO_2 solution would obviously be inappropriate for filling large voids in cement because the adsorption of PFA onto cement surfaces would result in only a thin polymer film. Therefore, the PFA-CO_2 solution is best suited for sealing smaller aperture cracks that provide undesirable leakage pathways for natural gas or oil but may be difficult to seal with relatively high viscosity media such as cement, epoxy, or aqueous emulsions.

3.1.2 Adsorption From a High-Pressure CO_2 Solution onto Solid Surfaces

There have been reports of adsorption of relatively low molecule weight, well-defined compounds from a high-pressure, CO_2-rich solution onto a solid surface, primarily for separation and purification (as opposed to modification of the solid surface). Perhaps the most notable example is the adsorption of caffeine, $C_2H_{10}N_4O_2$, (which had been extracted with liquid or supercritical CO_2 from green coffee beans or black tea) from the CO_2 solution onto activated carbon [95]. Other examples of adsorption of compounds dissolved in CO_2 onto surfaces include the adsorption of tocopherol acetate, Vitamin D3 and α-tocopherol onto Silica Zeofree 5170 [95], α-tocopherol and δ-tocopherol onto the stationary phases of unmodified silica [96], artemisinin onto silica gel [97], and hexafluoroacetylacetonate ($Pd(hfac)_2$) onto the internal surfaces of mesoporous silica [98]. A literature review has summarized the results of dozens of studies of the preparation of supported metal nanostructures in which the sequential steps of the preparation include dissolving a metal complex in supercritical CO_2 or a CO_2-rich mixture, adsorption of the metal complex onto the nanoporous solid, and the conversion of the adsorbed metal complex to the desired metal species [99].

The proposed PFA-CO_2 solution involves the high-pressure adsorption of a polydisperse polymer - rather than a monodisperse, well-defined, low molecular weight compound - onto a solid surface. There have been numerous studies related to the adsorption of polymers onto mineral surfaces, but these used water or brine as the solvent, not liquid or supercritical CO_2. For example, the equilibrium adsorption of a partially hydrolyzed polyacrylamide (PAM) dissolved in brine (50 °C, TDS 10,000 ppm, pH 8) onto particles derived from a crushed reservoir core was well represented by a Langmuir isotherm and exhibited a plateau of about 4.5 mg polymer per gram rock at aqueous phase polymer concentrations of ~ 0.2 wt% [100]. Even more recently, a study of dynamic polymer adsorption was conducted using aqueous PAM solutions flowing through sandstone obtained from a formation outcrop [101] exhibited Type IV adsorption behavior [102]. A limitation of these static adsorption results is that the chemical composition of portions of the surface area of crushed rock particles differs from the composition of the surface area of a consolidated porous medium used in dynamic tests. Further, the consolidated medium used in dynamic testing is more representative of the medium that the polymer solution will actually be transported through in the field test [103].

Polymer adsorption is not the only mechanism by which polymer can be “lost” as the aqueous polymer solutions passes through a porous and permeable rock during dynamic testing. Additional polymer retention occurs when the polymer molecules in aqueous solution become mechanically entrapped in the consolidated sandstone or limestone rock. Mechanical entrapment can be caused by one of more of the following: hydrodynamic retention, trapping within dead-end pores, straining and bridging [103]. Both adsorption and mechanical entrapment of PFA was observed as PFA-CO_2 solutions flowed through sandstone and carbonate cores, although the quantitative levels of adsorption and entrapment could not be quantified [29].

Despite the numerous reports of polymer adsorption from an aqueous solution at low pressure, to the best of our knowledge, there have no prior reports of adsorption isotherms for polymers from a high-pressure liquid or supercritical CO_2-rich solution. Unfortunately, we were not successful in measuring PFA adsorption onto cement at high-pressure. Our strategy was to determine decreases in PFA concentration in high-pressure CO_2 from a specified initial value (caused by adsorption) by measuring decreases in the PFA-CO_2 viscosity with a falling object viscometer. However, the particles interfered with the fall of the close clearance ball or cylinder.

Further, in the few cases where particles did not present problems, the changes in PFA concentration were too small to induce significant changes in PFA-CO_2 fluid viscosity. As a result, we are unable to perform the PFA material balance that could have quantified the equilibrium concentration of PFA in CO_2 and the amount of PFA adsorption onto cement at elevated pressure.

The ability to reduce the apparent permeability of dry, cracked Portland cement with PFA-CO_2 solutions is examined. In four cases the PFA-CO_2 solution is continuously displaced through a confined split or cracked Portland cement sample and the increase in pressure drop at constant flow rate (or the decrease in flow rate at constant pressure drop) is monitored. In five cases, the split cement sample is bound together with tape, confined in a core holder for an initial measurement of apparent permeability using water, removed from the core holder, dried under vacuum, immersed in a high-pressure PFA-CO_2 solution for 24 hours, depressurized, and then re-confined in a core holder for another apparent permeability measurement with water.

3.2 Materials and Methods

3.2.1 Materials

At Pitt, cylinders of liquid CO_2 (99.9% CO_2, bone dry) with an eductor tube were obtained from Matheson. At NETL, CO_2 (99.99%) was obtained from Praxair. At SINTEF, CO_2 (99.7%) was obtained from AGA A.S.

PFA was bulk polymerized following the technique described previously. The properties of the samples used at the NETL, SCAL and SINTEF facilities are provided in Table 2. The chemical structure of PFA is shown in Figure 2 along with several images that display “sticky” and “stretchy” characteristics.

Table 16: Three bulk-polymerizaed C_6F_{13}-based PFA samples

PFA #	Onset T_g (°C)	Midpoint T_g (°C)	Wt% AIBN	Mn (kDa)	Mw (kDa)	PDI
C_6F_{13} SINTEF	-21.58	-4.36	0.005	24.0	347	14.5
C_6F_{13} SCAL	n/a	n/a	0.004	250	600	2.4
C_6F_{13} NETL	-24.39	-4.14	0.002	61.7	1250	20.3

Figure 11: PFA structure and physical appearance

The cloud point pressure of these PFA polymer samples at 25 °C is about 10 MPa in the 1-4wt% PFA in CO_2 concentration range.

n-Decane (99%) was obtained from Sigma Aldrich and used as received.

3.2.2 Methods

3.2.2.1 Model cracked cement

At NETL, solid cylinders of Class H Portland cement was mixed at a 38% water content. Cement was immediately poured into 2.54 cm ID Buna-N rubber sleeves and allowed to cure at room temperature for a period of at least 28 days. After curing for a month, the cores were cut to approximately 7.62 cm length by trimming the ends. The cores were then halved along the length to form two half cylinders. The cylinders were then mated to their original orientation to alleviate any deviation in the lengthwise cut. These cement cylinders were impermeable to high-pressure CO_2. Therefore, model cracks were generated by sawing each Portland cement cylinder in half through its axis. Then the symmetric halves were placed together and held in place by wrapping tape around the cylindrical cement surface. This resulted in a flat, rectangular crack that extends through the cement from one circular end to the other. The tape, which was unaffected by immersion in CO_2-rich fluids, retained the cement halves together, thereby allowing the sample to be shipped from NETL to Pitt for immersion in PGFA-CO_2 solutions.)

At SINTEF, Portland G cement was used to prepare the cement slurry. The cement was mixed with water with a ratio of 2. The mixture was pre-sheared at 4000 rpm for 15 seconds, followed by a continuous mixing at a motor speed of 12000 rpm for 35 seconds. The pre-mixed cement slurry was then prepared into the final cement sample using two half-cylinder moulds with a diameter of 1.27 cm and 8 cm length. The sample was left to harden in an oven at 40°C for 48 hours. During the unmoulding process, each piece broke radially into smaller pieces (five in total). The sample surfaces were not polished or treated any further.

At SCAL, two 15.24 cm long, 5,08 cm diameter cement plugs were formed using a slurry of Class H cement and distilled water (38% H_2O slurry). The plugs were allowed to cure in a pressure vessel at reservoir conditions for approximately 15 hours. The ends of the plugs were trimmed with a diamond saw blade to provide parallel faces (forming a right cylinder). Each plug was sliced in half along its length using a diamond wire. One plug was rebuilt by turning the top half of the cylinder 180° from its original orientation and closed with no proppant or spacers. The second plug had 100 mesh proppant evenly distributed along the face of the “crack,” leaving a larger gap between the halves than the first plug.

3.2.2.2 Quantifying the Conductivity of the Model Crack Using Darcy’s Law

A convenient measure of the ability of the crack cement to allow fluid to pass through the crack is a pseudo-absolute permeability-based Darcy’s law. We realize that the single crack in the cement cylinder does not constitute a porous medium. However, each of the Darcy’s law parameters required for this pseudo-absolute permeability measurement can be easily measured or determined for the single fluid that is saturating and flowing through the crack (flow rate, pressure drop, cylinder diameter and length, fluid viscosity). Further the ability of the PFA treatment to reduce or seal the conductivity of the cracked cement can be readily assessed by comparing the pseudo-permeability values of the cracked cement before and after exposure to the high-pressure PFA-CO_2 solution. For example, for measurements done on a cracked cement sample before and after treatment with PFA, one could determine the absolute pseudo-permeability of the sample using the same fluid at the same temperature, outlet pressure, and pressure drop by measuring the corresponding flow rate.

3.2.2.3 Initial CO_2 Pseudo-Permeability of the Crack, Introduction of PFA-CO_2 Solution, and Measurement of Reduced Pseudo-Permeability

NETL- Two apparatuses were used for permeability. For the first apparatus, the cracked cement sample is placed within an X-ray transparent, carbon fiber, Hassler-Style core holder (38 °C, 34.5 MPa) inside of a Toshiba® Aquilion TSX-101A/R medical computed tomography (CT) scanner and subjected to at least 3.4 MPa of overburden pressure that forces all the subsequently injected fluid to flow through the crack (rather than flowing around the cement). The system was configured to facilitate injection of pure CO_2 or PFA-CO_2 solutions, Figure 4. The pure CO_2, constant flow rate injection configuration was used to measure the initial crack pseudo-permeability prior to injecting PFA-CO_2 solutions. Subsequently, the injection fluid could be switched to a PFA-CO_2 solution by directing CO_2 into a windowed, agitated 600 ml high-pressure vessel (Parr) that had previously filled with a mixture of PFA and CO_2 and stirred at a pressure of 20.7 MPa, which is significantly above the cloud point (10 MPa), until a single-phase solution formed. The PFA-CO_2 effluent of the vessel was directed into the cement crack. This results in a small amount of dilution of the PFA in CO_2 during the experiment that can be quantified with the following expression:

$$\mathrm{C}_{\mathrm{PFA,effluent}} = C_{PFA,initial}e^{-V_{CO_2}/V_{mixer}} \qquad 3\text{-}1$$

where $C_{PFA,effluent}$ is the concentration of PFA in the CO_2-rich solution leaving the mixing vessel, $C_{PFA,initial}$ is the concentration of PFA in the CO_2-rich solution originally in the mixing vessel, V_{CO2} is the volume of CO_2 displaced into the mixer from the pump, and V_{mixer} is the volume of the mixing vessel. The flow displacement (FD) pump and pressure displacement (PD) pump were both Teledyne ISCO model 500 HP syringe pumps. Two differential pressure (dP) regulators, both Rosemount model 3051 CD, with ranges of 0-0.062 MPa & 0-2.07 MPa, respectively, were used to measure the pressure drop across the core. Reduction in permeability was monitored by measuring the increase in pressure drop that occurred as the PFA adsorbed within the crack. As will be noted in the Results section, deposition of PFA within the tubing and interior of the receiving PD pump was problematic during cleanup, therefore the apparatus shown in Figure Z was only used for one experiment (CEM0).

Attempts to image PFA deposition with the CT scanner were made during the CEM0 experiment. Although there is a significant density difference between PFA (1.6 gr/ml), CO_2-PFA solutions (~0.7-0.9 gr/ml) and cement (3.15 gr/ml), the PFA films were expected to be very thin and possibly undetectable with the medical CT. The general rule of thumb is that one needs at least 3 voxels to have certainty in the detection of a substance. In the medical CT scanner, the resolution was about 100 microns, therefore layer of PFA of PFA less than 300 microns (0.3 mm) in thickness will probably not be reliably detectable. However, even 3 voxels may not be sufficient; in cases where the attenuation of the substance is closer to air than the bulk of pixels, beam hardening effects can mask the substance.

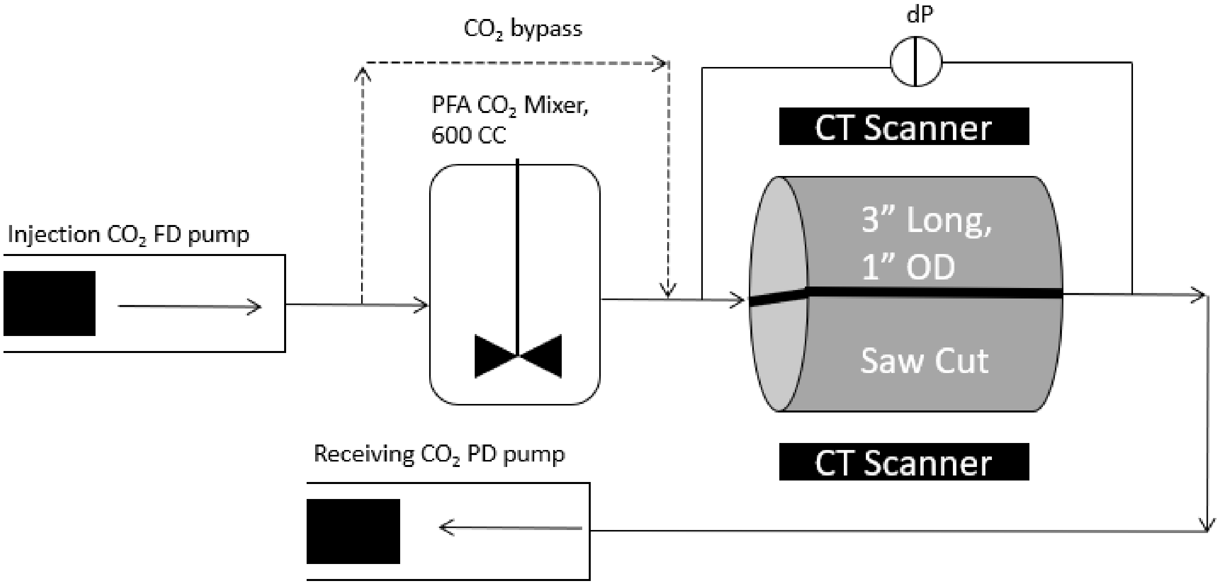

Figure 12: NETL high-pressure apparatus for CT imaging and determination of apparent permeability of cracked cement; CO2 or PFA-CO2 as flowing fluids during pseudo-permeability tests

For all other NETL permeability experiments (CNTR, CEM2, CEM5, CEM7, CEM8, and CEM9), initial pseudo-permeability was measured using a DCI bench-top permeameter using water. A backpressure regulator was used to maintain 0.69 MPa effluent pressure, while water was injected through the split cement and a differential pressure was measured. Radial confining pressure was maintained at 4.14 MPa. The integrated DCI software automatically calculated permeability based on sample dimensions and pressure data.

After permeability was determined, the split cement, which remained wrapped around its cylindrical surface with tape, was removed from the core holder and thoroughly dried under vacuum prior to the subsequent immersion of the dry, split cement sample in high-pressure solutions of polyfluoroacrylate (PFA) in CO_2, which were performed at the University of Pittsburgh. These immersion tests involved the introduction of the split cement sample, PFA and CO_2 into a windowed, agitated, tiltable, rock-able, invertible, variable-volume phase behavior cell

(Schlumberger 180 °C, 69 MPa) with a sample volume large enough (3.175 cm diameter, up to 15 cm length) to accommodate the split cement sample. The phase behavior cell is housed within an air bath (CSZ, -20 to 180 °C) and temperature was maintained at 25 °C. The pressure was adjusted to a value well above the cloud point pressure of 10 MPa at 25 °C for solutions containing 1-4wt% PFA in CO_2 (C_6F_{13} PFA1 from Table 13) and the split cement remained immersed in quiescent PFA-CO_2 solution for 24 hours. The CO_2 was then slowly vented from the sample volume over a one-hour period.

After verifying that the tape retained its integrity, the PFA-treated split cement was then returned to NETL for determination of pseudo-permeability to water using the DCI bench-top permeameter. This technique, which was used for CEM2, CEM5, CEM7, CEM8, and CEM9 samples by the NETL-Pitt team, is illustrated in Figure 5.

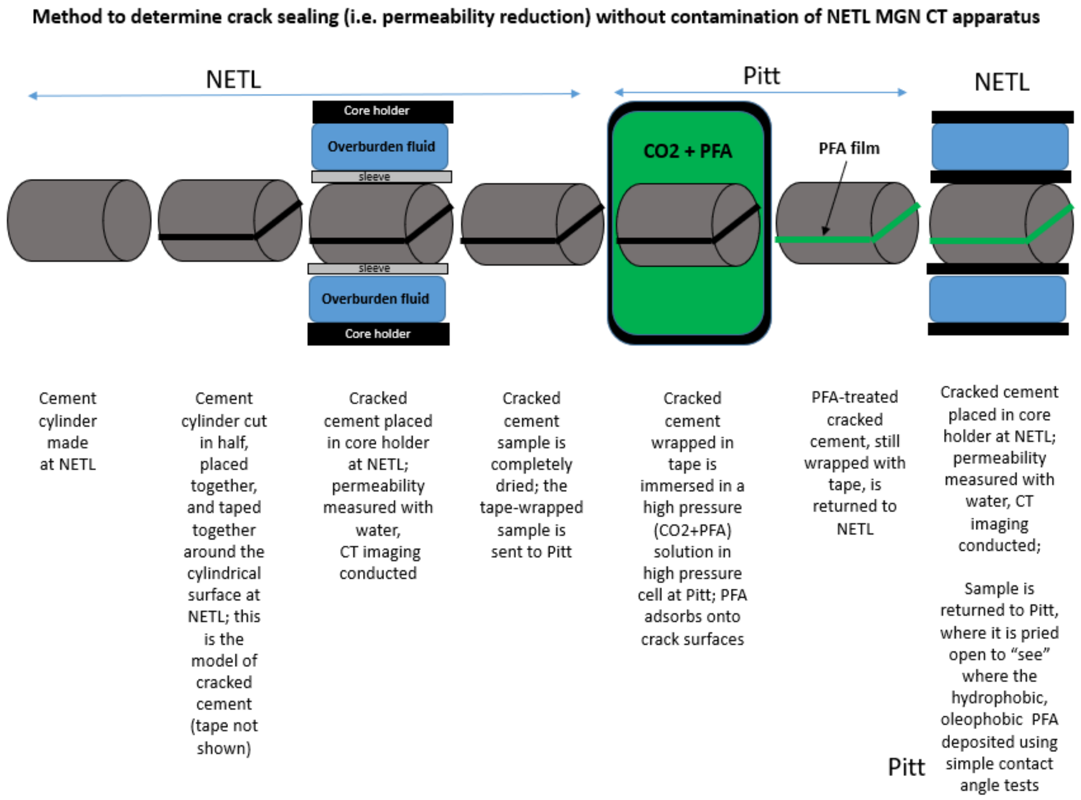

Figure 13: Multiple-step assessment of new sealant for closing cracks; this strategy prevented the flow of PFA-CO_2 solutions in the high-pressure CT imaging/permeability equipment at NETL downstream of the sample.

Because of the extensive time requirement to complete a single treatment and analysis of a split cement sample using this multiple-step approach that involved two shipments per sample, we were only able to study cracks in cement (i.e. cracks bounded only by cement surfaces). Further, we were only able to apply the PFA-CO_2 solution to dry cracked cement samples (i.e. cracks were not saturated with brine or oil prior to immersion in PFA-CO_2). We were *not* able to study microannular cracks at the steel-cement interface or cracks at cement-shale interfaces.

SINTEF- A cross-section of the core holder setup is depicted in Figure 6. The cement sample parts were placed in between two 3D-printed end pieces. Both end pieces had two ports, one for the process and one for the differential pressure across the sample. The cement sample, together with the end pieces, was set inside a shrinking tube to hold all components together. 1/16-inch 316 stainless steel tubing was used as lines, two on the top and two on the bottom (one for process and one for differential pressure) and one additional for confinement. The lines were passed through a Swagelok® 2.54 cm to 1.27 cm reducing union, and they were fixed in place by filling all the inner space with epoxy resin. Once the resin was cured, a sleeve of polyurethane was made around the core, from the end to the resin, enclosing all the lines. After the sleeve was cured, the part was inserted into an aluminium (Al 6082 T6) tube with an internal diameter of 21 mm and 200 mm in length. The confinement space was filled with paraffin oil.

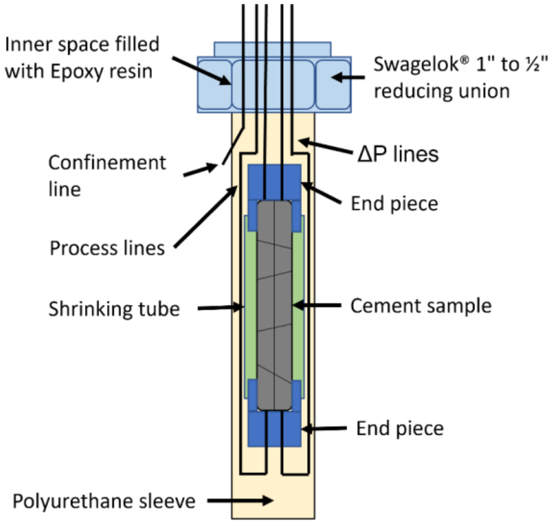

Figure 14: Cross-section of the core (i.e. split cement sample) holder setup.

The SINTEF cracked cement flooding apparatus is shown in Figure 7. The core holder and the bottle containing the PFA/CO_2 solution (C_6F_{13} PFA4 from Table 13) were placed inside a temperature-controlled air bath (i.e. cabinet). A 2.54 cm stainless steel pipe with a length of 200 mm followed by a fine regulated manually operated valve was used to maintain a constant effluent pressure. The apparatus was designed to initially allow the introduction of CO_2 into the crack (for initial crack pseudo-permeability determination) and all of the high-pressure tubing. The injectant can be instantaneously switched to a PFA-CO_2 solution of known composition. This PFA-CO_2 solution, which was initially isolated from the rest of the high-pressure tubing and cracked cement, was prepared in a variable-volume vessel into which known amounts of PFA and CO_2 were added to the sample side of the sliding piston with an O-ring around its perimeter. The PFA/CO_2 mixture was then compressed to a pressure of 15 MPa, which was significantly greater than the cloud point pressure of 10 MPa. Mixing was achieved by rocking the cell for 30 minutes to $\pm 45^o$ from horizontal every 10 seconds with a stainless steel mixing ball within the sample volume labelled as “PFA + CO_2” in Figure Y. (The conditions associated with this non-windowed, SINTEF apparatus were replicated in the windowed variable-volume cylindrical vessel at Pitt to ensure the mixing would be sufficient to yield a single-phase solution.) The volumetric injection rate of constant-composition PFA-CO_2 solution was maintained (at the same value as the CO_2 injection) by injecting distilled water into the water side of the sliding piston within the variable-volume vessel using a high-pressure PD pump (VP-series, Vindum Engineering). The confinement/overburden pressure was 22 MPa, and the experiment was done at 25 °C and an effluent pressure of ~15 MPa.

Initially, the CO_2 displacement pump (DP) was used to force liquid CO_2 through the cracked cement sample at a constant rate until a steady state pressure drop ($P_{in} – P_{out}$) was attained ($0 < t < 13$ min), which allowed for the calculation of the cracked cement pseudo-permeability (13 min $< t <$ 93 min). The injectant was then switched to the PFA/CO_2 solution (93 min $< t <$ 280 min) and stopped when P_{in} came within 2 MPa of the overburden pressure.

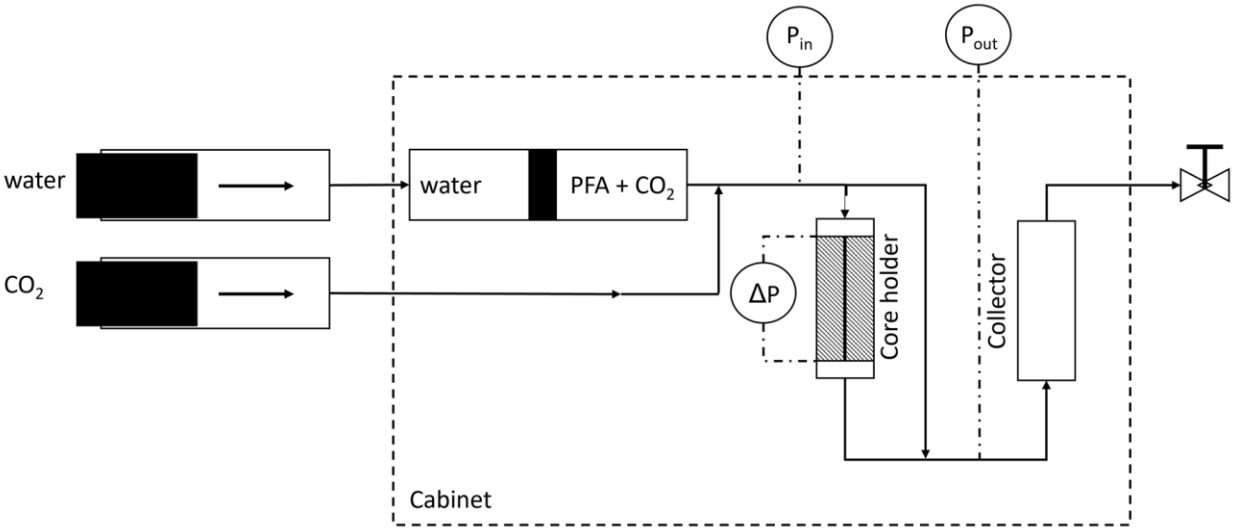

Figure 15: SINTEF high-pressure apparatus for CT imaging and determination of apparent permeability of cracked cement; CO_2 or PFA-CO_2 as flowing fluids during pseudo-permeability tests

SCAL- The apparatus used at SCAL, Figure 8, was similar in configuration to that used at NETL, Figure 5. The CO_2 source bottle was plumbed to the inlet port of the delivery positive displacement pump (Ruska). The outlet of the CO_2 PD Pump was directed to the 600 ml windowed, agitated CO_2-PFA mixer (Parr), where a magnetically driven shaft with an impeller mixed the CO_2 and PFA at a pressure well above the cloud point pressure. A bypass route around the mixer was also plumbed, so that either pure CO_2 or the CO_2/PFA mixture (C_6F_{13} PFA from Zaberi) [29] could be injected into the cracked cement. From the mixer (and the bypass), the high-pressure fluid was directed to a core holder where the cracked cement cylinder was retained. A small amount of dilution of the PFA/CO_2 mixture occurred during this experiment (Equation 3-1). A differential pressure transducer (Yokogawa) measured the pressure drop across the inlet and outlet faces of the cement plug. A vacuum pump (Hitachi) was used to remove as much air from the system as possible before injecting CO_2. The outlet of the core holder was fed to a receiving PD, which ran at an equal volumetric rate but opposite direction of the delivery PD.

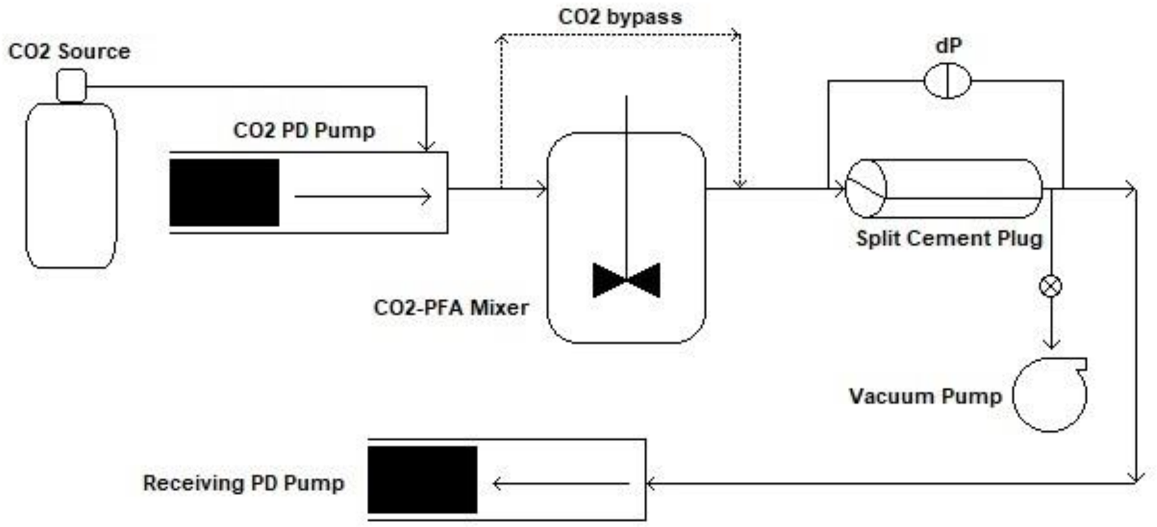

Figure 16: SCAL high-pressure apparatus for determination of apparent permeability of cracked cement; CO_2 or PFA-CO_2 as flowing fluids during pseudo-permeability tests

3.2.2.4 Contact Angles and Detecting the Location of the PFA Films on the Crack Surfaces

Small disks of Portland cement from NETL (2.54 cm in diameter and 1 cm thick) were used to assess the hydrophobicity and oleophobicity of bare cement and PFA-coated cement. Two samples were bare cement. Two cement samples were immersed in a 5wt% PFA in hydrofluoroether solution for an hour, followed by air drying, rendering a PFA-coated cement surface. Two cement samples were immersed in a 4wt% PFA-96% CO_2 solution at 25^oC and 20.7 MPa for 24 hours, which was also expected to yield PFA-coated cement.

Small drops of distilled water or decane were then placed at multiple positions on the surface of the six horizontal samples. Images of the droplets and measurements of the contact angle through the liquid droplet were taken using the sessile drop method at ambient conditions in air using an optical tensiometer (Attension Theta). A microsyringe was used to place a drop of either decane or deionized water on the cement sample. The contact angle was measured at the water-air-cement or decane-air-cement contact point in the liquid zone. A contact angle of 0^o reflected that the surface was completely wet by the liquid, contact angles of $\sim 90^o$ implied that the surface was of intermediate wettability, and contact angles greater than 90^o indicated that the surface was not conducive to being wet by the liquid. A comparison of the liquid-air-cement and liquid-air-PFA treated cement provided an easily discernible contrast between bare cement and PFA-coated cement.

To determine where the PFA had deposited on the cement surfaces that bound the model crack, the cement halves were gently pried apart at the end of the post-PFA treatment pseudo-permeability experiment. For the CNTR, CEM2, CEM5, CEM7, CEM8, CEM9 experiments at NETL that used water as the fluid for permeability measurements, the cement half-cylinders were then thoroughly dried. A simple technique based on our droplet results was used to determine if a particular location on the cement surface was bare or coated with a film of PFA. Many small drops of oil (e.g. decane) were placed on the cement surface. As will be shown in the Results section, the oil spreads out quickly and completely on bare cement, whereas the oil will bead up slightly on PFA-coated cement. Therefore, in regions of the surface where the oil droplets do not spread out (i.e. the oil droplets form beads of oil), the cement can be considered as PFA-coated, while regions of cement surface where the oil spreads can be considered bare cement without any polymer.

Water was also considered for this test. However, (as will be shown in the Results) although water beads up dramatically on PFA-coated cement, water beads up to a lesser extent on bare cement. It was easier to visually distinguish bare cement from PFA-coated cement using oil droplets rather than water droplets.

3.3 Results

3.3.1 PFA-Induced Wettability Changes

Figure 9 presents a series of images of droplets of decane (top row) or water (bottom row) that have been placed on disks of bare Portland cement (left column), disks of Portland cement coated with PFA via immersion in a 5%PFA-in-hydrofluoroether liquid solution and drying (center column), and the bottom semi-circular end of a cement Portland cement half-cylinder that was immersed in a PFA-CO_2 solution in a vertical for 24 hours at 25 °C and 20.7 MPa prior to the CO_2 being vented from the vessel. The PFA-in-hydrofluoroether treated samples had a visibly thicker layer of PFA compared to the PFA-CO_2 immersed surfaces. The decane drop was immediately absorbed into the bare cement; therefore, the decane-air-bare cement contact angle was estimated as ~0^o. However, when the oil droplet was placed on PFA-coated cement, the contact angle increased to 40-57^o. The contact angle for water-air-bare cement was system was 40-60^o. However, when the water was placed on PFA-coated Portland cement, the contact angle increased to 96-

108°. Therefore the PFA on the cement made the cement more hydrophobic (the contact angle increased from 40-60° to 96-108°) and more oil-phobic (the contact angle increased from 0° to 40-57°). This PFA-induced enhancement of oil-phobicity and hydrophobicity is similar to that previously reported [29] for drops of oil and water on sandstone and carbonate rock, except that those bare porous media readily absorbed both oil and water droplets prior to PFA treatment.

Figure 17: Typical examples of liquid water or decane droplets on Portland cement at 25 °C in air; blue scale bar = 0.5 mm. Ranges of contact angles for many drops are presented parenthetically.

Top left: Decane on bare cement, contact angle of 0° (oil drop immediately absorbed into cement)

Top center:Decane on PFA (from hydrofluoroether solution)-coated cement, contact angle 57° (43-57°)

Top right:Decane on PFA (from 4wt% solution in CO_2)-coated cement, contact angle 47° (40-55°)

Bottom left: Water on bare cement, contact angle of 60° (ranged from 40-60°)

Bottom center:Water on PFA (from hydrofluoroether solution)-coated cement, contact angle 108°

Bottom right:Water on PFA (from 4wt% solution in CO_2)-coated cement, contact angle 100° (96-100°)

3.3.2 Crack Sealing

A complete set of crack sealing experiments at ~25 °C for this project is presented in the Table 2. All PFA-CO_2 solutions used in the nine experiments involving PFA-CO_2 solutions were prepared at single-phase conditions (i.e. at pressures above the cloud point pressure of the PFA-CO_2 mixture).

Four of the experiments (SCAL SPLIT, SCAL SPSND, SINTEF 1, CEM0) involved the continuous flow of PFA-CO_2 into the cracked cement sample at elevated pressure; no depressurization of the PFA-CO_2 solution occurred during these experiments. Therefore, reductions in permeability are attributed solely to PFA adsorption. No PFA precipitation occurred during data collection because the pressure was always maintained well above the cloud point pressure of the PFA-CO_2 solution.

All five cracked cement immersions (CEM2, CEM 5, CEM7, CEM8, CEM9) in high-pressure PFA-CO_2 solutions lasted 24 hours, followed by a one-hour depressurization of the PFA-CO_2 solution. This allowed for the deposition of PFA onto cement surfaces by adsorption at high-pressure followed by the precipitation of PFA from the PFA-CO_2 solution within the crack during depressurization.

The average values of PFA concentration are given for the continuous flow tests conducted at SCAL and NETL designated as CPMF or CFMP. The values of permeability are apparent permeability based on Darcy's law using the circular cross-section of the cracked cement cylinder and the properties of pure CO_2. The split cement samples CEM2, CEM5, CEM7, CEM8, CEM9, and CNTR were thoroughly dried after water was used for pre-PFA permeability test; then the cracked cement samples were immersed in a PFA-CO_2 solutions. The CO_2 viscosity at crack outlet conditions was 0.0963 mPa-s at 25 °C, 20.8 MPa, and 0.0861 mPa-s at 25 °C, 15.1 MPa [71].

SCAL- The first SCAL model crack SPLIT exhibited the initial lowest apparent permeability to CO_2, 81 nD, of any of the samples tested. This crack was quickly rendered impermeable, as indicated by the injection rate attaining a value of 0 during the constant pressure drop injection of a small amount (2 ml) of the 1% PFA in CO_2 solution.

In the subsequent SCAL test, designated as SPSND, a small amount of same was placed between the cement halves to enhance the initial apparent permeability to 89 µD. A 92% reduction in apparent permeability was attained after constant flow rate injection of 150 ml of a PFA-CO_2 solution with an average composition of 0.89% PFA. The solution was ~2 times as viscous as pure CO_2. The 12-fold reduction in permeability is much greater than what would have been expected from pure viscosity effects. Even greater reductions in apparent permeability could have occurred, but the test had to be terminated because the difference between the pore pressure on the inlet side of the split cement and overburden pressure was approaching the minimum acceptable value.

One would expect that the cracked cement sample with the lowest apparent permeability (in the nD or µD range) would be associated with cracks having the smallest gap size range. The thin films of PFA that adsorb in these cracks would have a much greater chance to significantly reduce the apparent permeability than in cracks that have much wider crack apertures and higher initial apparent permeability. Therefore, it is not surprising that the only experiment in which the apparent permeability was reduced to zero was for the cracked cement with the smallest initial apparent permeability of only 81 nD (SCAL SPLIT). Further, an excellent result of 92% reduction in apparent permeability was obtained in the sample with a permeability of only 89 µD (SCAN SPLSND).

Table 17: Summary of experiments at SCAL in which the apparent permeability of cracked cement was reduced via the application of high-pressure PFA-CO_2 solutions

Sample	**Mode of applying PFA-CO_2 to crack**	**P confine**	**PFA**	**Flow Rate of PFA-CO_2 solution**	**Perm Loss**	**Vol of PFA-CO_2 soln. inj.**	**Mass of PFA inj.**	**Crack surface area (top + bottom)**	**PFA/cm^2 injected**
		MPa gauge	wt%	ml/min	**%**	ml	g	in^2/cm^2	gm/cm^2
SPLIT	CPMF	41.4	0.99	0.008-0	**100**	2	0.0184	24/154.8	1.19E-4
SPSND	CFMP	34.5	0.89	0.25	**92**#	150	1.223	24/154.8	7.90E-3

SINTEF- The sole experiment conducted at SINTEF utilized a constant flow rate injection of an CO_2-rich solution containing 4% PFA. The injection rate was varied several times during this experiment. Ultimately this injection of 57 ml of the PFA-CO_2 solution reduced the initial apparent permeability of the cracked cement, 3.67 mD, by about 96%. This PFA solution is ~8 times more viscous than pure CO_2. Once again, the ~25-fold permeability loss is much greater than what would be expected from viscosity effects alone. As was the case for the second SCAL test, SPSND, even greater reductions could have occurred, but the test was terminated as the difference between the pore pressure on the inlet side of the split cement and overburden pressure was approaching the minimum acceptable value.

Table 18: Summary of experiments at SINTEF in which the apparent permeability of cracked cement was reduced via the application of high-pressure PFA-CO_2 solutions

Mode of applying PFA-CO_2 to crack	**PFA**	**Flow Rate of PFA-CO_2 solution**	**Post PFA perm**	**Perm Loss**	**Vol of PFA-CO_2 soln. inj.**	**Mass of PFA inj.**	**Crack surface area (top + bottom)**	**PFA/cm^2 injected**
	wt%	ml/min	fluid	**%**	ml	g	in^2/cm^2	gm/cm^2
CFMP	4.00	0.5, 0.4,0.1	PFA-CO_2	**96**	57	2.070	5.11/33.0	6.08E-2

Table 19: Summary of experiments at NETL in which the apparent permeability of cracked cement was reduced via the application of high-pressure PFA-CO_2 solutions

Sample	**Pre-PFA Perm**	**Mode of applying PFA-CO_2 to crack**	**PFA**	**Flow Rate of PFA-CO_2 solution**	**loss in perm**	**Vol of PFA-CO_2 soln. inj.**	**Mass of PFA inj.**	**Crack surface area (top + bottom)**	**PFA/cm^2 injected**
			wt%	ml/min	**%**	ml	g	in^2/cm^2	gm/cm^2
CEM0	CO_2	CFMP	0.39	2.00	**50**	266	4.894	6/38.7	3.16E-2
CEM7	water	IMM	1.00	0	**29**			6/38.7	
CEM2	water	IMM	4.00	0	**93**			6/38.7	
CEM5	water	IMM	3.00	0	**22**			6/38.7	
CEM8	water	IMM	1.00	0	**48**			6/38.7	
CEM9	water	IMM	2.00	0	**60**			6/38.7	
CNTR	water	IMM	0.00	0	**0**			6/38.7	
CEM3	water	CRACK	4.0	0	n/a			6/38.7	
CEM4	water	CRACK	2.0	0	n/a			6/38.7	

A control test was performed, CNTR, using no polymer to verify that the immersion of the split cement sample in CO_2 and subsequent hour-long depressurization was not altering the apparent permeability of the sample. There was no detectable change in the 70 mD apparent permeability of CNTR due to pressurization, soaking/immersion in liquid CO_2, and slow depressurization of the CO_2.

A modest 50% reduction in permeability was attained in the CEM0 run, which was conducted in the CT imaging apparatus, Figure 4. The initial apparent permeability of CEM0, 3.80 mD, was very similar to that of SINTEF 1. This experiment used a relatively low concentration of PFA, averaging only 0.39%, in CO_2. Further, due to safety-related prohibitions on overnight high-pressure experiments at NETL, a very high injection rate of 2.0 ml/min was used. Because we did not have the opportunity to assess the kinetics of adsorption, it is not clear whether the low PFA concentration, the high injection rate, or both contributed to the relatively low apparent permeability reduction.

Further, our attempts to image PFA film formation during the CEM0 run using CT-imaging were unsuccessful. Beam hardening effects induced a distinct, several mm-wide lightening of all cement surfaces, including the crack, that would have obscured the detection of films. (CT images taken at ambient conditions after PFA-treatment of several other runs found in Table 2, including SCAL SPLIT and several CEM runs from NETL, were also unable to provide evidence of PFA films.)

One sample, CNTR, was soaked in pure CO_2 for 24 hours as a control. No permeability decrease was detected. Five samples, CEM2, CEM5, CEM7, CEM8, and CEM9 were successfully PFA-treated using the procedure illustrated in Figure 5 that involved measuring the initial apparent permeability of the sample to water at NETL, immersing the dried sample in PFA-CO_2 at Pitt, and returning the sample to NETL to measure the reduction in permeability. It appears that, as one would expect, higher concentrations of PFA yield more significant reductions in permeability. For example, the 4%PFA in CO_2 solution used in CEM2 caused a 93% loss in apparent permeability, which was comparable to the 96% reduction that occurred in the SINTEF 1 experiment that also used a 4%PFA concentration in CO_2. The relatively low 1%PFA concentration in CO_2 used for CEM7 and CEM8, which had initial apparent permeability values of 9.04 mD and 50.1 mD, respectively, yielded relatively low reductions in apparent permeability of 29% and 48%, respectively. In that both SCAL experiments attained 100% and 92% reductions for very low permeability cracks, it appears that PFA concentrations of ~1wt% in CO_2 are insufficient to seal or reduce the apparent permeability of cracks with initial apparent permeability in the 1-100 mD range. Improved performance was realized for CEM9, where a 60% reduction of the initial apparent permeability of a 70 mD sample was attained using a 2%PFA in CO_2 solution.

CEM5 had unexpectedly poor performance. Even though the PFA concentration was 3% in CO_2, the initial apparent permeability of 24.7 mD was reduced by only 22%. This represents a less significant reduction in permeability than was attained in the CEM0 experiment that attained a 50% reduction in apparent permeability using a CO_2-rich solution contain only 0.39% PFA. Upon unwrapping of the cement cylinder after the post permeability measurements, CEM5 fell apart into multiple pieces, indicating that there were most likely other cracks that formed at some point, possibly contributing to the low change in permeability.

Two CEM experiments, CEM3 and CEM4, actually yielded an *increase* in apparent permeability subsequent to PFA treatment. It was determined that cracks in the cement formed during depressurization of the PFA-CO_2 solution that was too rapid (~10-15 minutes) that provided additional flow paths for CO_2 to pass through the sample. Hour-long depressurization was used for each successful CEM test, and CT imaging and visual inspection indicated that no new cracks formed during those tests (CEM0, CEM2, CEM5, CEM7, CEM8, CEM9, CNTR).

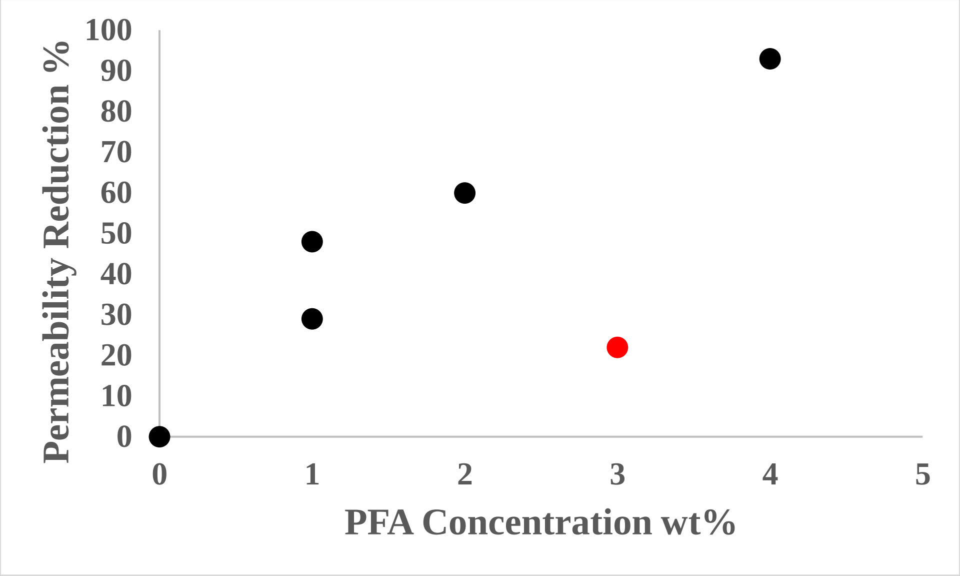

Figure 18: Permeability reduction as a function of PFA concentration in NETL tested cement cores
***Red point is CEM5, which broke apart upon unwrapping**

3.3.3 Detecting the Location of PFA Films of Split-Apart Samples

Figure 19 presents an example of a cement core that was immersed in a CO_2-PFA solution and was later unwrapped and split open to observe any PFA adsorption (CEM2). Qualitatively, the cement cores, even when unwrapped, took some force to be pried apart and as the cement pieces were separating, a clear, sticky elastic solid could be seen stretching and then breaking. During the deposition of decane, none of the drops in any of the cement samples spread out over any of the split halves of cement, meaning that at least some layer of PFA was present all throughout the crack.

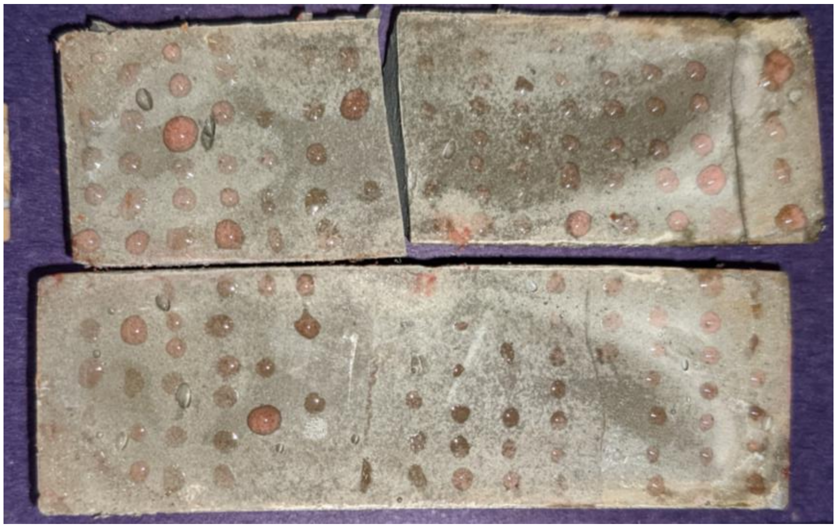

Figure 19: Typical post-PFA treatment cement with red dyed decane droplets

3.4 Conclusions

Because PFA is sticky, hydrophobic and oleophobic, it was hypothesized that the deposition of the PFA on cement surfaces could reduce the crack aperture and induce dramatic changes in wettability that could dramatically reduce the apparent permeability of the crack or, in the best case, completely seal the crack. These PFA-CO_2 solutions are most effective in sealing very low permeability, dry (i.e. no oil or brine present) cement cracks. For example, at the SCAL facility, a model cracked cement, made by sawing a 6” long, 2 inch diameter Portland cement cylinder in half along its axis, had an apparent permeability of only 81 nD (where permeability is a pseudo-permeability based on Darcy’s Law). The crack was completely sealed after only 2 ml of a 1wt% PFA-in-CO_2 solution was displaced into the crack. In another example, the injection of 150 ml of PFA-CO_2 solution with an average PFA concentration of 0.89% resulted in a 92% reduction of the apparent permeability of a split 6” by 2” cement sample from 89 μD to 7.32 μD.

At the SINTEF laboratory, the injection of 150 ml of PFA-CO_2 solution with a constant PFA concentration of 4.0% resulted in the 92% of the apparent permeability cement sample from 3.67 mD to 147 μD.

Regarding experiments conducted at Pitt and NETL, apparent permeability reduction was also attained via the immersion of the cracked cement in a PFA-CO_2 solution. In the best case, the apparent permeability of a split cement sample was reduced from 9.47 mD to 0.68 mD after a 24 hour immersion in a 4wt% PFA-in-CO_2 solution; a 93% reduction in permeability.

In five other tests in which split cement samples with an original permeability of 3.8 – 70 mD were immersed in 0.4-3wt% PFA-in-CO_2 solutions, 22-60% reductions in apparent permeability occurred. In general, higher PFA concentrations yielded improved performance. It appears that PFA concentrations of at least ~4% in CO_2 are required for cracked cement samples with an initial apparent permeability in the mD range.

Because PFA is a sticky polymer, all samples had to be pried apart to inspect the flat crack surfaces of each cement half after the permeability testing was complete. Small drops of decane, which quickly spreads on bare cement, beaded up at all locations on all cement surfaces. This indicated that PFA, which is an oleophobic polymer on which decane exhibits a contact angle of 40-57^o, had coated the entire interior flat cement surfaces that bounded the crack.

Two samples exhibited a huge increase in apparent permeability. These undesirable increases were attributable to cracks developing during depressurization (CEM3 and CEM4).

4.0 Future Directions

For future researchers looking to continue this work, I would suggest a few things regarding both the polymerization and specifically cement sealing. On the side of polymerization, looking into even fluoroacrylate monomers with even shorter fluoroalkyl moieties (such as the C_2F_5-, CF_3- and CH_2F-) to determine if PFA made from these monomers maintain the same carbon solubility and CO_2-thickening potential as the ones tested in this study. I would also suggest doing solution polymerization to try to reduce the PDI of the polyfluoroacrylate samples while not attaining excessively high molecular weights. (Unfortunately, a PFA sample that was solution-polymerized by adding a volume of hydrofluoroether to an equivalent volume of monomer had such a high molecular weight that it was unable to dissolve in the fluorinated solvent used by Daikin for their molecular weight analysis). More experiments could also be performed that would more precisely determine the molecular weight of that leads to insolubility of CO_2 in PFA, as we saw in one sample.

For cement sealing, doing more flow-through experiments (i.e. continuous experiments at high-pressure) to expand on the preliminary tests already done would go a long way to further substantiate PFA's usage as a wellbore integrity agent. Additionally, adding other wellbore conditions like initially filling the cracks with brine or oil will increase the robustness of the research done here.

On a more fundamental level, developing a method for determining PFA adsorption on cement particles or mineral particles (e.g. $CaCO_3$) in high-pressure CO_2 environments will allow one to quantify the amount of PFA deposition onto surfaces that could be attributed solely to high-pressure adsorption (excluding PFA precipitation during depressurization). Such a procedure would probably require a dedicated analytical tool capable of measuring the PFA contribution in a high-pressure CO_2 solution exiting a packed bed of a known amount of particles with of known specific surface area.

Rather than continuing to study only cracks bound by cement surfaces, one could investigate the ability of PFA-CO_2 solutions to seal or reduce the apparent permeability of steel-cement cracks that represent micro annular cracks. Preliminary studies of this system have been conducted at SINTEF using PFA generated during this study.

5.0 Bibliography

[1] J. Lee, Small Molecule Associative CO2 Thickeners for Improved Mobility Control, in: Chemical and Petroleum Engineering, University of Pittsburgh, 2016.

[2] R. Enick, D. Olsen, Mobility and Conformance Control for Carbon Dioxide Enhanced Oil Recover (CO2-EOR) via Thickeners, Foams, and Gels - A detailed Literature Review of 40 years of Research, (2011).

[3] J. Lee, S. Cummings, A. Dhuwe, R. Enick, E. Beckman, R. Perry, M. O'Brien, M. Doherty, Development of Small Molecule CO2 Thickeners for EOR and Fracturing, SPE 169039, in: S.o.P. Engineers (Ed.) SPE Improved Oil Recovery Symposium, Richardson, TX, 2014.

[4] S. Alzobaidi, J. Lee, S. Jiries, C. Da, J. Harris, K. Keene, G. Rodriguez, E. Beckman, R. Perry, K.P. Johnston, R. Enick, Carbon dioxide-in-oil emulsions stabilized with silicone-alkyl surfactants for waterless hydraulic fracturing, J Colloid Interface Sci, 526 (2018) 253-267. 10.1016/j.jcis.2018.04.056

[5] A. Gandomkar, M. Sharif, Nano composites performance as direct thickeners for gas based enhanced oil recovery, a new approach, Journal of Petroleum Science and Engineering, 194 (2020). 10.1016/j.petrol.2020.107491

[6] J.P. Heller, D.K. Dandge, R.J. Card, L.G. Donaruma, Direct Thickeners for Mobility Control of CO2 Floods, Society of Petroleum Engineers Journal, 25 (1985) 679-686. 10.2118/11789-pa

[7] B. Li, D. Shi, Q. Lv, H. Bai, C. Zheng, J. Xu, Experimental study on rheological properties of thickened CO2 in liquid and supercritical state, Petroleum Science and Technology, 36 (2018) 1913-1919.

[8] P. Lemaire, A. Alenzi, J. Lee, E. Beckman, R. Enick, Thickening CO2 with Direct Thickeners, CO2-in-Oil Emulsions, or Nanoparticle Dispersions: Literature Review and Experimental Validation, Energy & Fuels, 35 (2021) 8510−8540. https://doi.org/10.1021/acs.energyfuels.1c00314

[9] M. Hansch, M. Ranft, A. Dhuwe, R. Enick, Thickening compressed liquid and supercritical propane with bisurea DMHUT N,N'-(4-methyl-1,3-phenylene)bis[N-(1,5-dimethylhexyl)urea] for

enhanced oil recovery or waterless hydraulic fracturing, The Journal of Supercritical Fluids, 145 (2019) 85-92. 10.1016/j.supflu.2018.12.008

[10] A. Dhuwe, J. Lee, S. Cummings, E. Beckman, R. Enick, Small associative molecule thickeners for ethane, propane and butane, The Journal of Supercritical Fluids, 114 (2016) 9-17. https://doi.org/10.1016/j.supflu.2016.03.019

[11] J.B. McClain, D. Londondo, J.R. Combes, T.J. Romack, D.A. Canelas, D.E. Betts, G.D. Wignall, E.T. Samulski, J.M. Desimone, Solution Properties of a CO2-Soluble Fluoropolymer via Small Angle Neutron Scattering, Journal of the American Chemical Society, 118 (1996) 917-918. https://doi.org/10.1021/ja952750s

[12] Z. Huang, C. Shi, J. Xu, S. Kilic, R.M. Enick, E.J. Beckman, Enhancement of the Viscosity of Carbon Dioxide Using Styrene/Fluoroacrylate Copolymers, Macromolecules, 33 (2000) 5437-5442. https://doi.org/10.1021/ma992043+

[13] W. Sun, B. Sun, Y. Li, H. Fan, Y. Gao, H. Sun, G. Li, Microcosmic understanding on thickening capability of copolymers in supercritical carbon dioxide: the key role of π–π stacking, RSC advances, 7 (2017) 34567-34573.

[14] S. Kilic, R.M. Enick, E.J. Beckman, Fluoroacrylate-aromatic acrylate copolymers for viscosity enhancement of carbon dioxide, The Journal of Supercritical Fluids, 146 (2019) 38-46. https://doi.org/10.1016/j.supflu.2019.01.001

[15] W. Sun, B. Sun, Y. Li, X. Huang, H. Fan, X. Zhao, H. Sun, W. Sun, Thickening Supercritical CO2 with π-Stacked Co-Polymers: Molecular Insights into the Role of Intermolecular Interaction, Polymers, 10 (2018) 268.

[16] J.H. Bae, C.A. Irani, A Laboratory Investigation of Viscosified CO2 Process, SPE 20467, SPE Advanced Technology Series, 1 (1993) 166-171. https://doi.org/10.2118/20467-PA

[17] J. Lee, S. Cummings, E. Beckman, R. Enick, W. Burgess, M. Doherty, M. O'Brien, R. Perry, The solubility of low molecular weight polydimethyl siloxane in dense CO2 and its use as a CO2-philic segment, J Supercrit Fluid, 119 (2017) 17-25.

[18] A. Gandomkar, F. Torabi, M. Riazi, CO2 Mobility Control by Small Molecule Thickeners during Secondary and Tertiary Enhanced Oil Recovery, The Canadian Journal of Chemical Engineering, (2020) 1-11.

[19] Y. Wang, L. Hong, D. Tapriyal, I.C. Kim, I.-H. Paik, J.M. Crosthwaite, A.D. Hamilton, M.C. Thies, E.J. Beckman, R.M. Enick, Design and evaluation of nonfluorous CO2-soluble oligomers and polymers, The Journal of Physical Chemistry B, 113 (2009) 14971-14980.

[20] J. Stevens, Fracturing with a mixture of carbon dioxide and alcohol, in, US, 1989.

[21] J. Zhang, H. Liu, X. Lv, R. Zhang, B. Yu, Improve the performance of CO2-based fracturing fluid by introducing both amphiphilic copolymer and nano-composite fiber, SPE 176221, in: SPE/IATMI Asia Pacific Oil & Gas Conference and Exhibition, OnePetro, 2015.

[22] Z. Song, Supercritical carbon dioxide based fracturing system and application thereof, in, CN, 2014.

[23] Z. Jian, X. Bo, Z. Guoxiang, H. Wenhao, Y. Guang, J. Tieya, J. Shuo, Z. Zhiguo, A new thickener for CO2 Anhydrous fracturing fluid, MATEC Web of Conferences, 31 (2015).

[24] Y. Lu, W. Cui, J. Xu, Y. Duan, A New Liquid CO2 Based gel fracturing fluid with cylinder micelles structure, in: SPE Asia Pacific Hydraulic Fracturing Conference, Beijing, China, 2016.

[25] L. Jin, Y. Zheng, Quasi-dry CO2 fracturing - A new breakthough of liquid CO2 fracturing, in: Unconventional Resources Technology Conference, Denver, CO, 2019.

[26] Q. Yang, S. Meng, T. Fu, M. Li, S. Chen, 5 YEARS OF CO2 WATERLESS FRACTURING IN JILIN OILFIELD–WHAT WE HAVE LEARNED, in: International Conference on Applied Energy, Vasteras, Sweden, 2019.

[27] S. Meng, H. Liu, J. Xu, Y. Duan, Q. Yang, Z. Yao, Optimisation and Performance Evaluation of Liquid CO 2 Fracturing Fluid Formulation System, SPE 182284, in: SPE Asia Pacific Oil & Gas Conference and Exhibition, Society of Petroleum Engineers, 2016.

[28] X. Luo, S. Wang, Z. Wang, Z. Jing, M. Lv, Z. Zhai, T. Han, Experimental investigation on rheological properties and friction performance of thickened CO2 fracturing fluid, Journal of Petroleum Science and Engineering, 133 (2015) 410-420.

[29] H.A. Zaberi, J.J. Lee, R.M. Enick, E.J. Beckman, S.D. Cummings, C. Dailey, M. Vasilache, An experimental feasibility study on the use of CO_2-soluble polyfluoroacrylates for CO_2 mobility and conformance control applications, Journal of Petroleum Science and Engineering, 184 (2020) 106556. https://doi.org/10.1016/j.petrol.2019.106556

[30] R. Taylor, G. Funkhouser, R. Dusterhoff, R. Lestz, CO2 miscible optimized hydrocarbon blends and methods of using CO2 miscible optimized hydrocarbon blends, in: WIPO (Ed.), 2005.

[31] A. Dhuwe, A. Klara, J. Sullivan, J. Lee, S. Cummings, E. Beckman, R. Enick, R. Perry, Assessment of solubility and viscosity of ultra-high molecular weight polymeric thickeners in ethane, propane and butane for miscible EOR, Journal of Petroleum Science and Engineering, 145 (2016) 266-278. 10.1016/j.petrol.2016.05.018

[32] M.D. Doherty, J.J. Lee, A. Dhuwe, M.J. O'Brien, R.J. Perry, E.J. Beckman, R.M. Enick, Small Molecule Cyclic Amide and Urea Based Thickeners for Organic and sc-CO2/Organic Solutions, Energy & Fuels, 30 (2016) 5601-5610. 10.1021/acs.energyfuels.6b00859

[33] R. Enick, L. Hong, M.C. Thies, CO2 + β-D-Maltose Octaacetate system exhibits a global phase behavior of CO2-philic solids taht melt in dense CO2-rich fluids, J Supercrit Fluid, 34 (2005) 11-16.

[34] J.H. Bae, Viscosified CO2 Process: Chemical Transport and Other Issues, SPE 28950, in: SPE International Symposium on Oilfield Chemistry, San Antonio, TX, 1995.

[35] T.V. Harris, C.A. Irani, W.R. Pretzer, Enhanced Oil Recovery Using CO2 Flooding, in, US, 1990.

[36] R.S. Taylor, G. McIntosh, R. Litun, D. Munn, B. Bennion, M. Piwowar, G. Fyten, R. Romanson, O. Hoch, Montney fracturing-fluid considerations, in: Canadian International Petroleum Conference, Petroleum Society of Canada, 2009.

[37] A. Iezzi, P. Bendale, R.M. Enick, M. Turberg, J. Brady, 'Gel' formation in carbon dioxide-semifluorinated alkane mixtures and phase equilibria of a carbon dioxide-perfluorinated alkane mixture, Fluid Phase Equilibr, 52 (1989) 307-317. 10.1016/0378-3812(89)80337-1

[38] A. Iezzi, R. Enick, J. Brady, The direct viscosity enhancement of carbon dioxide, Supercritical Fluid Science and Technology, ACS Symposium Series 406, (1987) 122-139.

[39] P. Gullipalli, J.S. Tsau, J.P. Heller, Gelling Behavior of 12-hydroxystearic acid in organic fluids and dense CO2, SPE 28979, in: SPE International Symposium on Oilfield Chemistry, San Antonio, TX, 1995.

[40] Z. Al Yousef, O. Swaie, A. Alabdulwahab, S. Kokal, Direct Thickening of Supercritical carbon dioxide using CO2-soluble polymer, SPE 197185, in: Abu Dhabi International Petroleum Exhibition & Conference, Abu Dhabi, UAE, 2019. https://doi.org/10.2118/197185-MS

[41] C. Zhang, Z. Li, S. Li, Q. Lv, P. Wang, J. Liu, J. Liu, Enhancing sodium bis (2-ethylhexyl) sulfosuccinate injectivity for CO2 foam formation in low-permeability cores: dissolving in CO2 with ethanol, Energy & Fuels, 32 (2018) 5846-5856.

[42] G. Luna-Bárcenas, S. Mawson, S. Takishima, J.M. DeSimone, I.C. Sanchez, K.P. Johnston, Phase behavior of poly(1,1-dihydroperfluorooctylacrylate) in supercritical carbon dioxide, Fluid Phase Equilibr, 146 (1998) 325-337. https://doi.org/10.1016/s0378-3812(98)00215-5

[43] A. Blasig, C. Shi, R.M. Enick, M.C. Thies, Effect of Concentration and Degree of Saturation on RESS of a CO_2-Soluble Fluoropolymer, Ind Eng Chem Res, 41 (2002) 4976-4983. https://doi.org/10.1021/ie0201819

[44] S. Mawson, K.P. Johnston, J.R. Combes, J.M. DeSimone, Formation of Poly(1,1,2,2-tetrahydroperfluorodecyl acrylate) Submicron Fibers and Particles from Supercritical Carbon Dioxide Solutions, Macromolecules, 28 (2002) 3182-3191. https://doi.org/10.1021/ma00113a021

[45] J.M. Desimone, Z. Guan, C.S. Elsbernd, Synthesis of fluoropolymers in supercritical carbon dioxide, Science, 257 (1992) 945-947. https://doi.org/10.1126/science.257.5072.945

[46] J. Shin, Y.-W. Lee, H. Kim, W. Bae, High-Pressure Phase Behavior of Carbon Dioxide + Heptadecafluorodecyl Acrylate + Poly(heptadecafluorodecyl acrylate) System, Journal of Chemical & Engineering Data, 51 (2006) 1571-1575. https://doi.org/10.1021/je060066v

[47] R.M. Enick, J.J. Lee, S.D. Cummings, H.A. Zaberi, E.J. Beckman, C. Dailey, M. Vasilache, Fluoroacrylate Polymers as CO_2-soluble Conformance Control Agents, in: SPE Improved Oil Recovery Conference, Society of Petroleum Engineers, Tulsa, Oklahoma, USA, 2018. https://doi.org/10.2118/190176-MS

[48] Z. Shen, M.A. McHugh, J. Xu, J. Belardi, A. Mesiano, S. Bane, C. Karanikas, E. Beckman, R.M. Enick, CO_2-Solubility of oligomers and polymers that contain the carbonyl group, Polymer, 44 (2003) 1491-1498. https://doi.org/10.1016/S0032-3861(03)00020-X

[49] D. Tapriyal, Y. Wang, R. Enick, J. Johnson, J. Crosthwaite, M. Thies, I. Paik, A. Hamilton, Poly (vinyl acetate), poly ((1-O-(vinyloxy) ethyl-2, 3, 4, 6-tetra-O-acetyl-β-d-glucopyranoside) and amorphous poly (lactic acid) are the most CO_2-soluble oxygenated hydrocarbon-based

polymers, The Journal of Supercritical Fluids, 46 (2008) 252-257. https://doi.org/10.1016/j.supflu.2008.05.001

[50] M.L. O'Neill, Q. Cao, M. Fang, K.P. Johnston, S.P. Wilkinson, C.D. Smith, J.L. Kerschner, S.H. Jureller, Solubility of homopolymers and copolymers in carbon dioxide, Ind Eng Chem Res, 37 (1998) 3067-3079. https://doi.org/10.1021/ie980010x

[51] F. Rindfleisch, T.P. DiNoia, M.A. McHugh, Solubility of polymers and copolymers in supercritical CO_2, The Journal of Physical Chemistry, 100 (1996) 15581-15587. https://doi.org/10.1021/jp9615823

[52] S.S. Adkins, X. Chen, I. Chan, E. Torino, Q.P. Nguyen, A.W. Sanders, K.P. Johnston, Morphology and stability of CO_2-in-water foams with nonionic hydrocarbon surfactants, Langmuir, 26 (2010) 5335-5348. https://doi.org/10.1021/la903663v

[53] V.V. Dhanuka, J.L. Dickson, W. Ryoo, K.P. Johnston, High internal phase CO_2-in-water emulsions stabilized with a branched nonionic hydrocarbon surfactant, J Colloid Interface Sci, 298 (2006) 406-418. https://doi.org/10.1016/j.jcis.2005.11.057

[54] W.J. McLendon, P. Koronaios, R.M. Enick, G. Biesmans, L. Salazar, A. Miller, Y. Soong, T. McLendon, V. Romanov, D. Crandall, Assessment of CO_2-soluble non-ionic surfactants for mobility reduction using mobility measurements and CT imaging, Journal of Petroleum Science and Engineering, 119 (2014) 196-209. https://doi.org/10.1016/j.petrol.2014.05.010

[55] D. Xing, B. Wei, W.J. McLendon, R.M. Enick, S. McNulty, K. Trickett, A. Mohamed, S. Cummings, J. Eastoe, S. Rogers, D. Crandall, B. Tennant, T. McLendon, V. Romanov, Y. Soong, CO_2-Soluble, Nonionic, Water Soluble Surfactants That Stabilize CO_2-in-Brine Foams, SPE Journal, 17 (2012) 1172-1185. https://doi.org/10.2118/129907-PA

[56] S. Takishima, M.L. O'Neil, K.P. Johnston, Solubility of block copolymer surfactants in compressed CO_2 using a lattice fluid hydrogen-bonding model, Ind Eng Chem Res, 36 (1997) 2821-2833. https://doi.org/10.1021/ie960702q

[57] J.H. Xu, A. Wlaschin, R.M. Enick, Thickening carbon dioxide with the fluoroacrylate-styrene copolymer, Spe Journal, 8 (2003) 85-91. https://doi.org/10.2118/84949-Pa

[58] J.M. Desimone, E.E. Maury, Y.Z. Menceloglu, J.B. McClain, T.J. Romack, J.R. Combes, Dispersion polymerizations in supercritical carbon dioxide, Science, 265 (1994) 356-359. https://doi.org/10.1126/science.265.5170.356

[59] M.A. McHugh, A. Garach-Domech, I.-H. Park, D. Li, E. Barbu, P. Graham, J. Tsibouklis, Impact of Fluorination and Side-Chain Length on Poly(methylpropenoxyalkylsiloxane) and Poly(alkyl methacrylate) Solubility in Supercritical Carbon Dioxide, Macromolecules, 35 (2002) 6479-6482. https://doi.org/10.1021/ma012169i

[60] Y.-L. Hsiao, E.E. Maury, J.M. DeSimone, S. Mawson, K.P. Johnston, Dispersion Polymerization of Methyl Methacrylate Stabilized with Poly(1,1-dihydroperfluorooctyl acrylate) in Supercritical Carbon Dioxide, Macromolecules, 28 (2002) 8159-8166. https://doi.org/10.1021/ma00128a028

[61] L. Hong, M.C. Thies, R.M. Enick, Global phase behavior for CO_2-philic solids: the CO_2+ β-d-maltose octaacetate system, The Journal of supercritical fluids, 34 (2005) 11-16. https://doi.org/10.1016/j.supflu.2004.10.003

[62] American Chemistry Council, C6 Fluorotelomers Provide Critical Protection for Textiles, in, 2021.

[63] C. Lau, J.R. Thibodeaux, R.G. Hanson, M.G. Narotsky, J.M. Rogers, A.B. Lindstrom, M.J. Strynar, Effects of perfluorooctanoic acid exposure during pregnancy in the mouse, Toxicol Sci, 90 (2006) 510-518. https://doi.org/10.1093/toxsci/kfj105

[64] K. Steenland, T. Fletcher, D.A. Savitz, Epidemiologic evidence on the health effects of perfluorooctanoic acid (PFOA), Environ Health Perspect, 118 (2010) 1100-1108. https://doi.org/10.1289/ehp.0901827

[65] Agency for Toxic Substances and Disease Registry, Toxicological Profile for Perfloroalkyls (Draft For Public Comment), (2018).

[66] S.A. Gannon, T. Johnson, D.L. Nabb, T.L. Serex, R.C. Buck, S.E. Loveless, Absorption, distribution, metabolism, and excretion of [1-14C]-perfluorohexanoate ([14C]-PFHx) in rats and mice, Toxicology, 283 (2011) 55-62. https://doi.org/10.1016/j.tox.2011.02.004

[67] M.H. Russell, H. Nilsson, R.C. Buck, Elimination kinetics of perfluorohexanoic acid in humans and comparison with mouse, rat and monkey, Chemosphere, 93 (2013) 2419-2425. https://doi.org/10.1016/j.chemosphere.2013.08.060

[68] A.L. Luz, J.K. Anderson, P. Goodrum, J. Durda, Perfluorohexanoic acid toxicity, part I: Development of a chronic human health toxicity value for use in risk assessment, Regulatory Toxicology and Pharmacology, 103 (2019) 41-55. https://doi.org/10.1016/j.yrtph.2019.01.019

[69] A. Dhuwe, J. Sullivan, J. Lee, S. Cummings, A. Klara, E. Beckman, R. Enick, R. Perry, Close-clearance high-pressure falling ball viscometer assesent of ultra-high molecular weigh polymeric thickeners for ethane, propane, and butaone, Journal of Petroleum Science and Engineering, 145 (2016) 266-278. https://doi.org/10.1016/j.petrol.2016.05.018

[70] J. Heller, J. Taber, Development of Mobility Control Methods to Improve Oil Recovery by CO_2–2nd Annual Report, Contract No. DOE/MC/I0689-II, US DOE, (1982).

[71] E.W. Lemmon, M.O. McLinden, D.G. Friend, Thermophysical Properties of Fluid Systems, in: P.J. Lindstrom, W.G. Mallard (Eds.) NIST Chemistry WebBook, NIST Standard Reference Database Number 69, National Institute of Standards and Technology, Gaithersburg, MD, 2020. https://doi.org/10.18434/T4D303

[72] R. Throupe, R. Simons, X. Mao, A Review of Hydro "Fracking" and Its Potential Effects on Real Estate, Journal of Real Estate Literature, 21 (2013) 205-232. https://doi.org/10.5555/reli.21.2.k3t42212626j4783

[73] D.C. Holzman, Methane found in well water near fracking sites, Environ Health Perspect, 119 (2011) A289. https://doi.org/10.1289/ehp.119-a289

[74] W.L. Ellsworth, Injection-induced earthquakes, Science, 341 (2013) 1225942. https://doi.org/10.1126/science.1225942

[75] B.K. Sovacool, Cornucopia or curse? Reviewing the costs and benefits of shale gas hydraulic fracturing (fracking), Renew Sust Energ Rev, 37 (2014) 249-264. 10.1016/j.rser.2014.04.068

[76] R.J. Davies, S. Almond, R.S. Ward, R.B. Jackson, C. Adams, F. Worrall, L.G. Herringshaw, J.G. Gluyas, M.A. Whitehead, Oil and Gas wells and their integrity: Implications for shale and unconventional resource exploitation, Marine and Petroleum Geology, 56 (2014) 239-254. https://doi.org/10.1016/j.marpetgeo.2014.03.001

[77] M. Kelso, 1.7 Million Wells in the U.S.: a 2015 Update, in, FracTracker Alliance, 2015.

[78] B. Carey, Wellbore Integrity and CO2 Sequestration, in: Los Alamos National Laboratory, Los Alamos, NM USA, 2010.

[79] C. Teodoriu, C. Kosinowski, M. Amani, J. Schubert, A. Shadravan, Wellbore Integrity and Cement Failure at HPHT Conditions, International Journal of Engineering and Applied Sciences, 2 (2013). https://doi.org/10.1.1.687.4004

[80] C.F. Ferraris, V.A. Hackley, A.I. Avilés, Measurement of particle size distribution in Portland cement powder: analysis of ASTM round robin studies, Cement, concrete and aggregates, 26 (2004) 1-11. https://doi.org/10.1520/CCA11920

[81] A. Shahriar, Investigation on Rheology of Oil Well Cement Slurries, in: Civil and Environmental Engineering, University of Western Ontario, 2011.

[82] G.I. Abbas, S., S. Kumar, K.R. Memon, S.A. Khalwar, Characteristics of Oil Well Cement Slurry using Hydroxypropylmethylcellulose, Journal of Applied Sciences, 14 (2014) 1154-1160. https://doi.org/10.3923/jas.2014.1154.1160

[83] K.R. Memon, M.T. Shuker, M.K. Memon, A.A. Lashari, G. Abbas, Durability and Rheological Evaluation of Cement Slurries from Atmospheric to High Thermal Condition, Journal of Applied Sciences, 14 (2014) 1204-1209.

[84] W.E. Odiete, E.T. Iyagba, Modeling the flow behavior of cement slurry with temperature, International Journal of Concrete Structures and Materials, (2015).

[85] Halliburton, WellLock Resin Laboratory Results, in, Halliburton, https://www.halliburton.com/en-US/ps/cementing/cementing-solutions/resins/welllock-resin.html?contentType=Data%20Sheets&index=0&comp=C#, 2019.

[86] M.V. Perez, J. Melo, R. Blanc, A. Roncete, P. Jones, Epoxy Resin Helps Restore Well Integrity in Offshore Well: Case History, Offshore Technology Conference, (2017). https://doi.org/10.4043/28124-MS

[87] C. Beharie, S. Francis, K.H. Ovestad, Resin: An Alternative Barrier Solution Material, Society of Petroleum Engineers, (2015). https://doi.org/10.2118/173852-MS

[88] M. Alkhamis, A. Imqam, M. Milad, Evaluation of an Ultra-High Performance Epoxy Resin Sealant for Wellbore Integrity Applications, in: SPE Symposium: Decommissioning and Abandonment, Society of Petroleum Engineers, Kuala Lumpur, Malaysia, 2019. https://doi.org/10.2118/199184-MS

[89] D.W. Rusch, B.C. Ellis, Use of Pressure Activated Sealants to Cure Sources of Casing Pressure, in: SPE Western Regional Meeting, Society of Petroleum Engineers, Anchorage, AK, 1999. https://doi.org/10.2118/55996-MS

[90] M. Mendoza, J. Hernandez, D.W. Rusch, Leak-Sealant In Hydraulic Systems Minimizes Maintenence Costs In Offshore Wells, in: 2000 SPE International Petroleum Conference and Exhibition, Society of Petroleum Engineers, Mexico City, Mexico, 2000.

[91] D.W. Rusch, M. Romano, Internal Repair of Pipeline Leaks Using Pressure-Activated Sealant, in: SPE Eastern Regional Meeting, Society of Petroleum Engineers, Charleston, WV, 2004.

[92] D.W. Rusch, M.T. Slezak, Annulus Communications Eliminated using PressureActivated Sealant in: Spring 2015 Conference, Solution Mining Research Institute, Syracuse, NY, 2005.

[93] R.W. Chivvas, J.Y. Julian, D.N. Cary, Pressure-Activated Sealant Economically Repairs Casing Leaks on Prudhoe Bay Wells, in: 2009 SPE Western Regional Meeting, Society of Petroleum Engineers, San Jose, CA, 2009. https://doi.org/10.2118/120978-MS

[94] A. Shahriar, M. Nehdi, Rheological Properties of oil well cement slurries, Construction Materials, 165 (2010) 25-44. https://doi.org/10.1680/coma.2012.165.1.25

[95] G. Brunner, M. Johannsen, New aspects on adsorption from supercritical fluid phases, The Journal of supercritical fluids, 38 (2006) 181-200.

[96] M. Lübbert, G. Brunner, M. Johannsen, Adsorption equilibria of α-and δ-tocopherol from supercritical mixtures of carbon dioxide and 2-propanol onto silica by means of perturbation chromatography, The Journal of supercritical fluids, 42 (2007) 180-188.

[97] H. Xing, B. Su, Q. Ren, Y. Yang, Adsorption equilibria of artemisinin from supercritical carbon dioxide on silica gel, The Journal of Supercritical Fluids, 49 (2009) 189-195.

[98] M.J. Tenorio, A. Cabanas, C. Pando, J.A.R. Renuncio, Solubility of Pd (hfac) 2 and Ni (hfac) 2· 2H2O in supercritical carbon dioxide pure and modified with ethanol, The Journal of Supercritical Fluids, 70 (2012) 106-111.

[99] S.E. Bozbağ, C. Erkey, Supercritical deposition: Current status and perspectives for the preparation of supported metal nanostructures, The Journal of Supercritical Fluids, 96 (2015) 298-312.

[100] Y. Al-Wahaibi, A.-A. Al-Hashmi, S. Joshi, N. Mosavat, S. Rudyk, S. Al-Khamisi, T. Al-Kharusi, H. Al-Sulaimani, Mechanistic study of surfactant/polymer adsorption and its effect on

surface morphology and wettability, in: SPE Oil and Gas India Conference and Exhibition, OnePetro, 2017.

[101] V.H. Ferreira, R.B. Moreno, Polyacrylamide adsorption and readsorption in sandstone porous media, SPE journal, 25 (2020) 497-514.

[102] S. Brunauer, L.S. Deming, W.E. Deming, E. Teller, On a theory of the van der Waals adsorption of gases, Journal of the American Chemical society, 62 (1940) 1723-1732.

[103] R.N.N. Manichand, R.S.S. Seright, Field vs. Laboratory Polymer-Retention Values for a Polymer Flood in the Tambaredjo Field, SPE Reservoir Evaluation & Engineering, 17 (2014) 314-325. 10.2118/169027-pa